Investigation into the coupled 1D and 3D numerical modeling of an air-cooled heat exchanger configuration

OC Koekemoer

orcid.org/0000-0002-4780-2911

Dissertation submitted in partial fulfilment of the requirements for the degree *Master of Engineering in Mechanical Engineering*

at the North-West University

Supervisor:	Prof CG du Toit
Co-supervisor:	Dr JH Kruger

Graduation: October 2018

Student number: 21650020

Abstract

(Keywords: Air-Cooled Heat exchangers, one dimensional, 1-D, three dimensional, 3-D, coupled 1-D/3-D modelling, Computational Fluid Dynamics, CFD, duct flow, Numerical modelling)

One dimensional (1-D) systems CFD can be used to simplify the analyses of thermal-fluid problems with complex geometries as it has the capability to provide quick solutions on fluid dynamics such as pressure changes, temperature fluctuations and flow rates. Three-dimensional (3-D) component CFD is generally used to model more complex geometries, due to its ability to provide detailed information on fluid dynamics whether it be flow regimes, chemical reactions or multiple phase changes. Existing analytical models and experimental methods for the analysis of Air-Cooled Heat Exchangers (ACHE) are limited in their applicability and a full 3-D CFD analysis thereof can be very resource intensive. This study proposes the use of a coupled 1-D/3-D modelling approach to address these issues.

The coupled 1-D/3-D modelling approach, utilizing Ansys® Fluent and Flownex® SE, was used to set up different air-cooled heat exchanger test configurations which were then compared with equivalent full 3-D CFD models simulated using Star-CCM+. The coupling procedure, between Flownex and Ansys Fluent was achieved through the continuous exchange of flow boundary conditions to ensure mass, momentum and energy was conserved through the single combined flow domain. The Flownex and Fluent networks are explicitly coupled by transferring temperature and heat flux between the two networks.

For all the ACHE configuration test cases, the temperature of the water exiting the pipe network, the number of iterations, solution time and model size are the main attributes examined. These results will be compared with the relevant verification test case having the same input specifications and set up. This comparison of results between the two different solution approaches will form the basis on which the coupled 1-D/3-D modelling approach is tested.

Acknowledgements

First of all, I would like to thank the Lord for sustaining me and being my support through every large (and small) endeavour I have ever decided to take up in my life. Specifically, during the completion of this report.

I would also like to extend my gratitude towards my study leaders, Prof. C.G. du Toit and Dr J-H. Kruger, who were very generous with their time and knowledge and assisted me in each step to complete this thesis.

I would also like to acknowledge my family and all my friends for remaining interested in my progress and what I was doing. Your support and the fact that you all remained positive, even at times when I found it difficult, was of a great help.

Table of Contents

List of Figures

List of Tables

Nomenclature

Abbreviations	
1-D	One dimensional
3-D	Three-dimensional
ACHE	Air-Cooled Heat Exchanger
CFD	Computational Fluid Dynamics
CV	Control Volume
EDF	Empirical Duct Flow
FVM	Finite Volume Method
HX	Heat Exchanger
LMTD	Log Mean Temperature Difference
SCFD	Systems Computational Fluid Dynamics
SE	Simulation Environment
TEMA	Tubular Exchanger Manufacturers Association

Variables	
A	Area, m^2
C	Constant
E	East
h	Convective heat transfer coefficient, W/m^2K
i	Unit vector
j	Unit vector
k	Thermal conductivity W/mK; turbulent kinetic energy m^2/s^2; or unit vector
N	North
P	Nodal Point, Generation of Turbulent kinetic energy
R	heat transfer resistance (m^2K/W)
S	Source term; modulus of the mean strain rate tensor or South
T	Temperature, °C or K
u	x-component of velocity, m/s
UA	Overall all heat transfer coefficient, W/K
V	Volume; domain Volume m^3
v	y-component of velocity, m/s
$\bar{v}$	Unit vector
W	West
w	z-component of velocity, m/s
x	Coordinate
y	Coordinate
z	Coordinate

Greek Symbols	
Γ	Diffusion coefficient
ε	Epsilon, Turbulent energy dissipation rate, m^2/s^3
μ	Viscosity, kg/ms
η	Efficiency
ρ	Density, kg/m^3
σ	Turbulent Prandtl number or ratio
Φ	Energy dissipation term
φ	Variable

Subscripts	
b	Buoyancy
c	Convection term
d	Diffusion term
E	Energy
e	Exit
ε	Dissipation
f	Control volume face number
i	Inlet
k	Mean velocity gradient, turbulent kinetic energy
M	Momentum
p	Primary, control volume
s	Source term, secondary, surface
φ	Physical quantity
V	Domain volume
x, y, z	coordinate

Chapter 1: Introduction

Overview

The focus of Chapter 1 is to provide the reader with some context and background for the research. The terms of reference, research problem and research objectives are explained up front. The steps taken to verify the results of the coupled 1-D/3-D numerical modelling approach is briefly explained. This chapter concludes with the limitations and exclusions associated with this study and a summary of the chapter outline of this report.

1.1 Background

In any refrigeration or power generating cycle, heat has to be discharged. This is true for power plants, refrigeration and air-conditioning systems and process industries. A large variety of heat exchangers are available to accomplish the necessary heat rejection. The two most widely used coolants for heat rejection are water and air, which are used either separately or in combination to improve heat transfer (Kröger, 1998).

Typical heat rejection systems found widely in industry are spray-type cooling towers and air-cooled heat exchangers. Since atmospheric air is the more readily available of the two, it seems the logical choice to use. However, due to its high specific heat capacity, the use of water is preferred. Water is a limited resource, this means that thermal and chemical pollution of water, diminishing water resources and industries located in arid parts of the world; all contribute to the increased use of air-cooled heat exchangers instead of wet-cooled systems (Guyer & Bartz, 1991).

A major problem associated with air-cooled heat exchangers is the system's inherent sensitivity to atmospheric conditions. During windy conditions, the performance may drastically reduce due to recirculation, caused by the inflow of part of the buoyant plume back into the heat exchanger intake, as shown in **Figure 1**. Distorted inlet flow conditions reduce the flow through the heat exchanger and in the case of chemical plants, this may lead to insufficient condensing or cooling of process fluids.

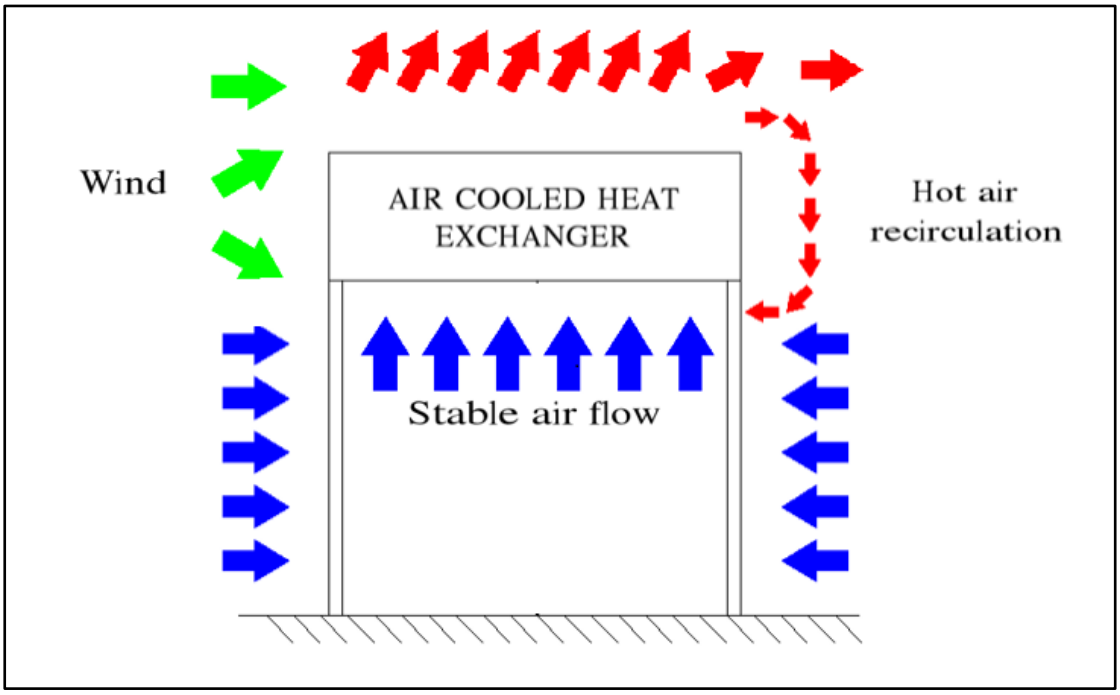

Figure 1: Hot air recirculation and wind effects on the performance of Air-Cooled Heat Exchanger

Adapted from source: (Calgavin, 2017)**.**

Existing analytical models and experimental methods for the analysis of air-cooled heat exchangers are limited in their applicability. The use of one-dimensional theoretical and analytical point models cannot resolve the spatial variation of temperature and velocity in three dimensions (Versteeg & Malalasekera, 2007). Important issues concerning external flow conditions i.e. recirculation and wind effects etc. may be neglected when using one-dimensional analytical models and may lead to inaccurate air-cooled heat exchanger performance predictions.

The quality of experimental results, on the other hand, are very much dependent on the measuring equipment's accuracy level and the proper location of measuring probes. Experimental investigations are limited by the atmospheric conditions present during the measuring period, not to mention that experimental investigations are both time consuming and costly. Therefore, it is not possible to investigate the influence of atmospheric conditions on the performance of air-cooled heat exchangers if these conditions were not present during measurements.

The use of Computational Fluid Dynamics (CFD) has been identified as a useful tool to investigate air-cooled heat exchangers that are characteristically difficult and expensive to investigate experimentally (Meyer, 2005). However, detailed 3-D CFD analysis of an air-cooled heat exchanger and the effects of various conditions on the performance thereof may be very resource intensive (time and computational power).

1.2 Problem Statement

As the need for air-cooled heat exchangers increases, the importance of ensuring accurate and predictable cooling performance becomes crucial to the efficient operation of a system and/or plant. As mentioned above detailed 3-D CFD analyses of an air-cooled heat exchanger can be resource intensive, therefore the need arises to investigate the effectiveness of 1-D/3-D coupling. The use of a coupled 1-D/3-D numerical modelling approach can aid in reducing the resources needed when simulating an air-cooled heat exchanger configuration whilst still providing accurate performance predictions.

1.3 Research aims and objectives

The main objective of this study is to investigate the feasibility of using an integrated systems CFD analysis or coupled 1-D/3-D numerical modelling approach, as an alternative to the more traditional detailed three-dimensional CFD analysis to obtain realistic performance predictions for an air-cooled heat exchanger configuration. Within the air-cooled heat exchanger configurations, the internal/duct flow is modelled using a 1-D network code, Flownex. The area of the simulation that would greatly benefit from the increased detail of CFD, the external/air flow field surrounding the tube or tube bundles, is modelled using the general mixed physics 3-D solver, Fluent.

1.4 Limitations of this study

The limitations of the study are as follow:

- Due to the complex nature of the problem, many simplifications have been made in order to create a computationally feasible numerical model.
- Due to resource constraints, this study does not allow for a large-scale investigation or case study analysis in using a coupled 1-D/3-D numerical modelling process.
- The 1-D/3-D modelling approach is not intended to help alleviate the problems inherent to air-cooled heat exchangers e.g. inlet flow distortion and hot plume recirculation, but instead help in reducing the model size and computational resources needed when simulating an air-cooled heat exchanger configuration.
- The different air-cooled heat exchanger configuration test cases are not intended to be a rigorous analysis of air-cooled heat exchangers, therefore not all phenomena surrounding these configurations will be analysed.
- A bare tube configuration is used within the air-cooled heat exchanger configurations test cases, since the focus of this study is to investigate the feasibility of using a coupled 1-D/3-D numerical modelling approach and not on the overall heat transfer capabilities of an air-cooled heat exchanger.

1.5 Verification of the Coupled 1D/3D modelling approach

By utilizing 1-D networks and 3-D meshes for fluid flow, the coupled 1-D/3-D numerical modelling approach will provide an integrated solution for the coupled flow and heat transfer problem. The coupled 1-D/3-D numerical modelling approach will be verified, for different air-cooled heat exchanger configurations, by comparing flow and temperature distributions in conjunction with model size, computation time, number of iterations, etc. to that of a full three-dimensional CFD analysis. Details regarding the solution algorithm, instruments applied and the information transfer between the 1-D and 3-D solver are discussed in **Chapter 4.**

1.6 Structure of the dissertation

The outline of the rest of the dissertation is summarised as follows:

Chapter 2: Literature Survey

Following the introductory chapter, a chapter discussing Air-Cooled Heat Exchangers and coupled 1-D/ 3-D CFD will follow. Within the literature survey, a summary will be provided so the reader can obtain the relevant background knowledge in order to position this study within research contexts. Basic concepts and definitions will be explored in detail. The literature survey contains the necessary theoretical content to ground the discussions in theory and also highlight previous research and studies on the same or similar topic.

Chapter 3: Theoretical Background

This chapter starts with the basic numerical modelling principles and elaborates the detail measures and applications of each, to solve the specific research problem at hand.

Chapter 4: Methodology

This chapter describes the methodology followed in order to achieve the required objectives of this study, reasons for using this methodology and the research instruments.

Chapter 5: Results

This chapter discusses the results obtained and verification of these results.

Chapter 6: Discussion, Conclusions and Recommendations

The report concludes with this chapter, devoted to discussing the results found in *Chapter 5* and how it relates to the background theory. The conclusion provides an answer to the research question. It also includes recommendations on the issues identified and proposes possibilities for future research.

Chapter 2: Literature Survey

Overview

This chapter is dedicated to Air-Cooled Heat Exchangers (ACHE) and coupled 1D/3D CFD. Within this chapter, a summary will be provided so that the reader can obtain the relevant background theory to position this study within context of existing research. Basic concepts, principles and definitions will also be explored further. The literature survey contains the necessary theoretical content to ground the discussions in theory and highlight previous research and studies on the same or similar topic.

2.1 Introduction

This research study was initially formulated with the idea of simulating an entire air-cooled heat exchanger with all included phenomena and challenges associated, but was later reduced to investigate whether the use of a coupled 1-D/3-D numerical modelling approach could serve as an efficient alternative to a full 3-D CFD analysis. A great deal of research has been done on various aspects of air-cooled heat exchanger design and analysis. This includes analytical, experimental and numerical work, however, due to the complex nature surrounding the analysis and modelling of an air-cooled heat exchanger the scope of this research study had to be adjusted to what is shown in the research aims, whilst keeping the limitations discussed in section **1.4** in mind.

A coupled 1-D/3-D numerical model, where the (internal) flow inside the pipes/ducts is modelled using a 1-D approach and the (external) flow around the pipes is modelled using a 3-D approach, is required to address the problems as stated for this research study. Previous research and studies with the same or similar problem statement will lend better understanding to the coupling strategies applied when coupling a 1-D duct flow solver to a 3-D general-purpose CFD solver.

2.2 Air-Cooled Heat Exchangers

In a typical air-cooled heat exchanger, ambient air is moved through one or more externally finned tube bundles, containing the process fluid, which has to be cooled or condensed. Heat transfer takes place between the air and the process fluid via the tube walls and fins. Fins significantly increase the effective heat transfer area, thus increasing the overall heat transfer capacity.

Ambient air may either be drawn or forced through the air-cooled heat exchanger by means of a fan. The former configuration depicted in **Figure 2** is referred to as an induced draft system while the latter, shown in **Figure 3**, is referred to as a forced draft system.

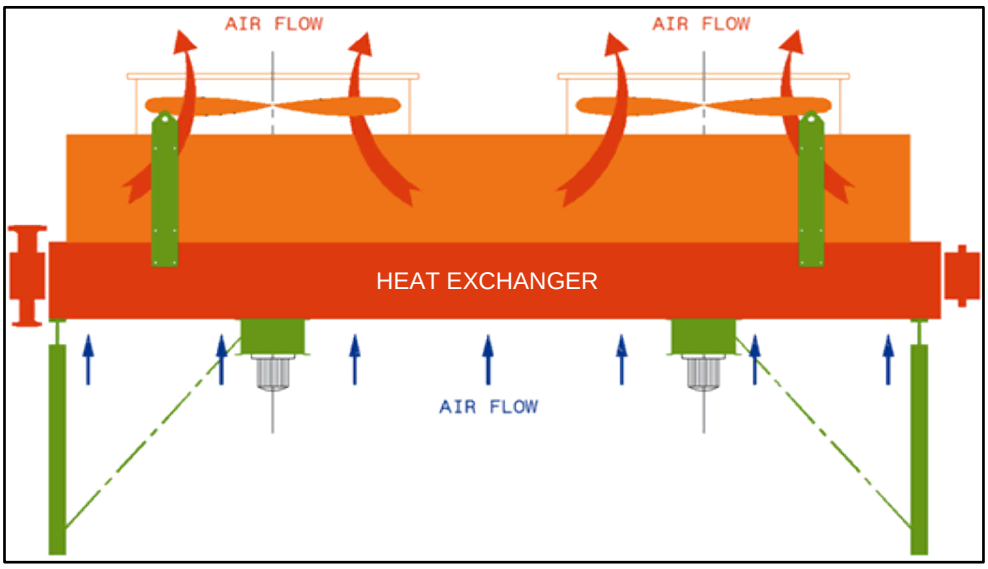

Figure 2: Induced draft air-cooled heat exchanger configuration

Source: (GEA Rainey Corporation, 2007)

Depending on the installation site and the type of application, there are advantages and disadvantages to both air-cooled heat exchanger configurations. Induced draft air-cooled heat exchangers (**Figure 2**) offer better distribution of airflow across the tube bundles and are less prone to hot air recirculation. Forced draft units, however have an electrical power advantage over induced draft units as the fans move the air before it is heated when passing through the tube bundles (Rohsenow, 1973).

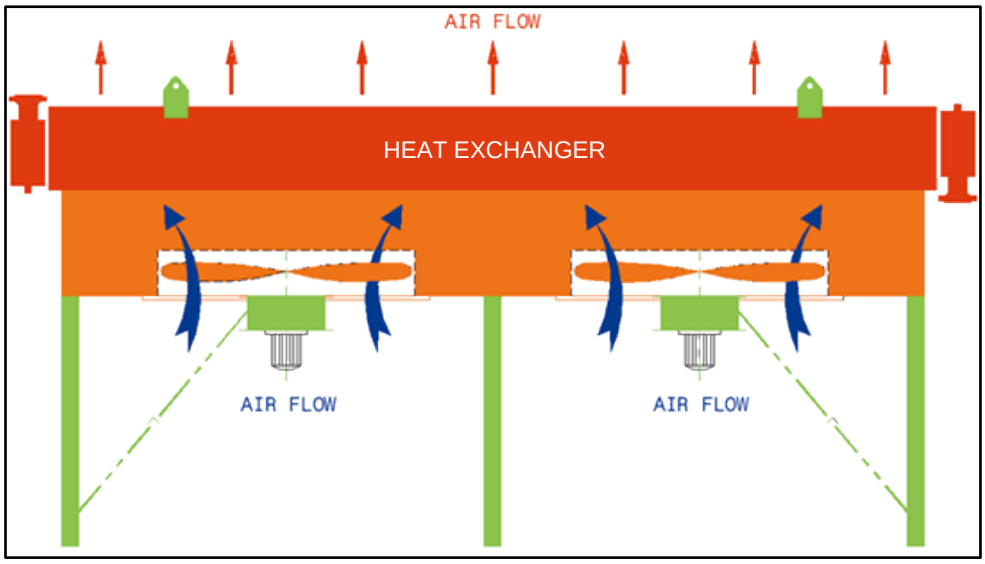

Figure 3: Forced draft air-cooled heat exchanger configuration

Source: (GEA Rainey Corporation, 2007)

In industry, the use of a forced draft configuration is recommended over an induced draft configuration. This is mainly due to the power savings achieved in forced draft units, since it significantly reduces overall operational costs.

The components and working principles of a forced draft air-cooled heat exchanger are shown in **Figure 4**.

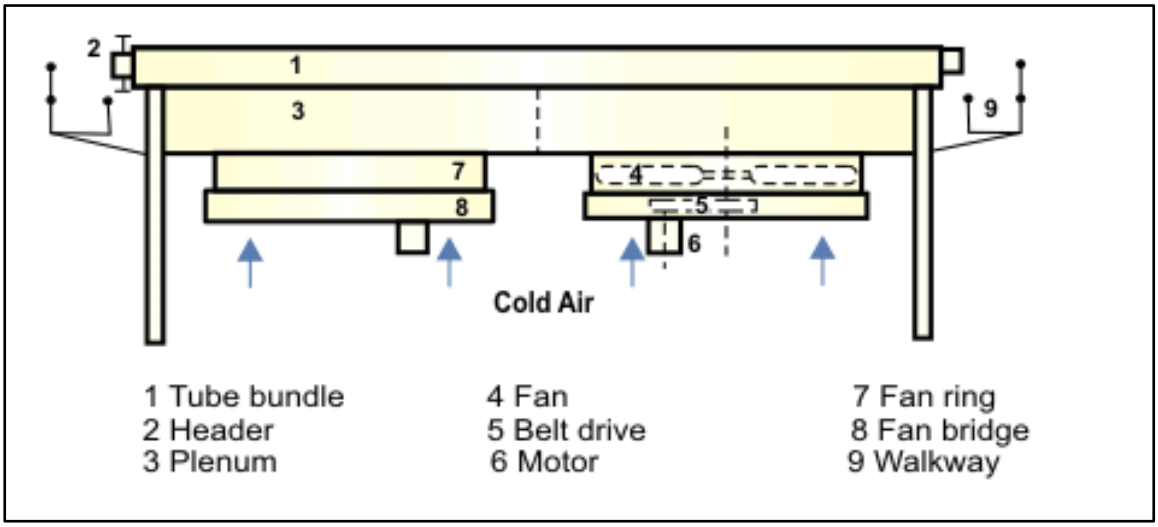

Figure 4: Components of a typical forced draft air-cooled heat exchanger

Source: (Amercool, 2003)

Figure 5 shows the typical layout of a forced draft air-cooled heat exchanger. Hot process fluid that needs to be cooled is pumped through an inlet header box, which distributes the fluid into the finned tubes. The water flows through the tubes and into a secondary header box chamber before exiting through an outlet or before being redirected for a second pass. At the same time, cooling air is forced over the finned tube bundle by means of a fan.

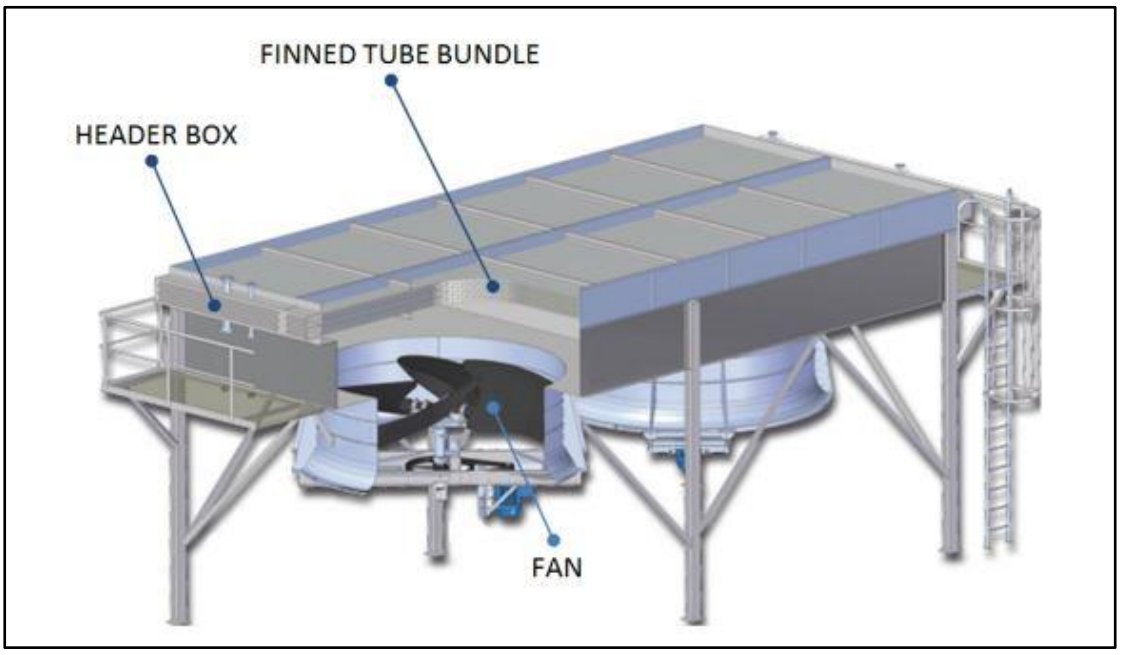

Figure 5: Typical Forced Draft Air-cooled Heat exchanger Configuration

Adapted from Source: (TUBETECH, n.d.)

The tubes are the basic component of an air-cooled heat exchanger, providing the heat transfer surface between the process fluid flowing through the inside of the tubes and the other fluid (air) flowing across the outside of the tubes. (Summers, 2011). Standard heat exchanger tube diameters range from 19.05 [mm] to 50 [mm] (Heaslip, 2008).

In an air-cooled heat exchanger, the tubes are installed in a specific pattern, of which the most common configuration/layout is triangular although a square pattern is also used. In addition, the tubes are spaced at equal intervals – the tube pitch is defined as the distance from tube centre to tube centre. The Tubular Exchanger Manufacturers Association (TEMA) requires that the ratio of tube pitch to the outer diameter or tube size be greater than 1.25 (Tubular Exchanger Manufactures Association, 2007).

Square layouts are at either 45° or 90°, while triangular layouts are either 30° or 60° as shown in **Figure 6**. Triangular layouts give a higher heat transfer coefficient and pressure drop than square layouts, which is particularly useful for heating and cooling of single-phase fluids and for condensation of fluids in gaseous phase (Heaslip, 2008).

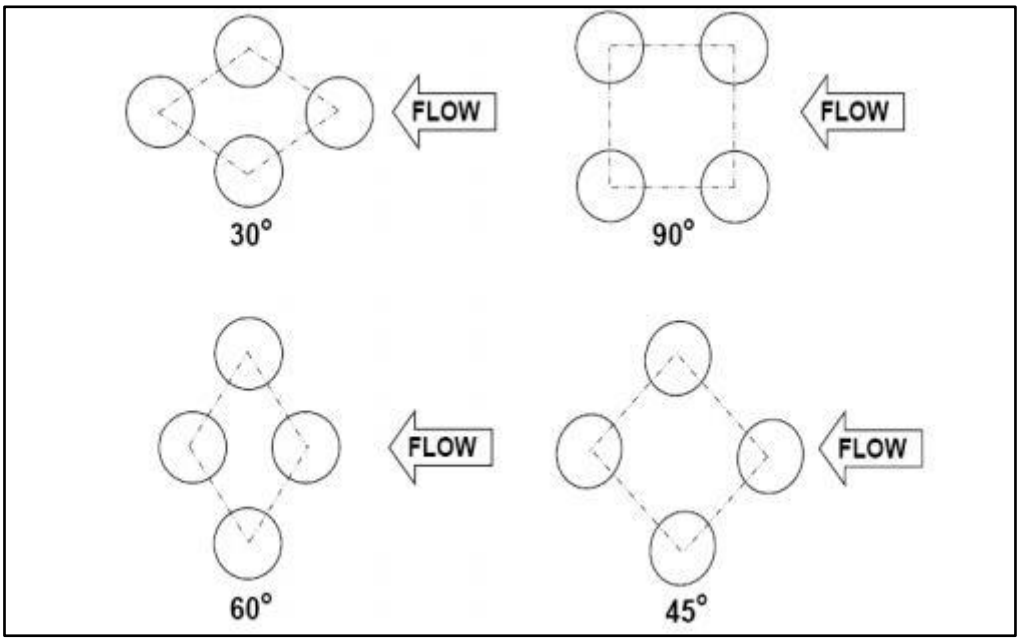

Figure 6: Tube layouts

Source: (Heaslip, 2008)

2.3 Coupled 1-D/3-D Computational Fluid Dynamics

One dimensional (1-D) systems CFD can be used to simplify the analyses of thermal-fluid problems with complex geometries as it has the capability to provide quick solutions on fluid dynamics such as pressure changes, temperature fluctuations and flow rates. Three-dimensional (3-D) component CFD is generally used to model more complex geometries, due to its ability to provide detailed information on fluid dynamics whether it be flow regimes, chemical reactions or multiple phase changes. Throughout the years, 1-D and 3-D CFD software solutions have been successfully used in the modelling of thermal-fluid systems in various industries. These include, but are not limited to the oil, gas, automotive, power and energy industries. Both 1-D and 3-D CFD assist in the understanding of fluid flow and results in improved system design and performance prediction. (Mentor Graphics, 2012).

In industry, various liquid cooled applications use a combination of ducted and non-ducted flows. The shell and tube heat exchanger configuration is probably the best known example of such an application (De Henau & Ahmed, 2005). Shell and tube heat exchangers are versatile heat exchangers used in power plants, refrigeration and air-conditioning systems or process industries. These units are usually made of several tubes connected to end heads and immersed in cooling fluid.

For the end heads, as well as the shell side volume (fluid volume surrounding the tubes), a 3-D CFD solver is recommended to simulate the pressure loss levels and heat transfer. The use of a 1-D solver, on the other hand, is better suited when analysing the tube flow, and is also preferable to reduce the size of the numerical model. The same solution strategy can be applied to Air-Cooled Heat Exchangers (ACHE) as they share similar heat transfer relationships to that of shell and tube heat exchangers (Amercool, 2003).

De Henau & Ahmed (2005) developed a method that couples a 1-D Empirical Duct Flow (EDF) flow solver to a general purpose 3-D solver. The coupling procedure between the different solvers was achieved through the continuous exchange of flow boundary conditions to ensure mass, momentum and energy were conserved through the single combined flow domain. In the framework of the EDF/CFD coupling however, it is limited to incompressible, steady state applications.

The EDF and CFD models are coupled at the fluid interface between the duct and the 3-D fluid domain. The coupling of the fluid domains is done by a sequence of boundary condition transfers from one domain to the other. Two types of boundary conditions are possible on the fluid interface. The first is to obtain the total pressure on the interface from the 3-D solver solution and applying it as a total pressure boundary condition on the 1-D solver. In return, a mass flow rate computed from the 1-D solver is imposed as a boundary condition on the 3-D solver. The second is to evaluate the fluid properties (mass flow rate or temperature) of the 3-D CFD solver solution and impose it on the 1-D solver. At the same interface, the 1-D solver returns a pressure to the 3-D solver and this pressure is used as a uniform pressure boundary condition on the 1-D duct flow solver interface

Provided that proper boundary conditions are defined in the consistent manner as described above, the coupled shell and tube heat exchanger calculation has been demonstrated to converge well in the applications that were examined. It is evident from the results (De Henau & Ahmed, 2005) that the velocity and pressures at discrete locations in the inlet and outlet sections of the shell and tube heat exchanger do not differ more than 2% when the EDF/CFD and full 3-D CFD methods are compared. Simulation results were compared to that of the Bell-Delaware correlation for heat exchangers and found to be within 10% of the values obtained from this correlation. This validation demonstrates an efficient and simplified approach to modelling 1-D and 3-D fluid flow. Using the 1-D EDF/3-D CFD approach, unnecessary use of 3-D elements is reduced in areas where one dimensional flow is dominant. This resulted in a 30% decrease of model size and a reduction in solution time of about 25 % (De Henau & Ahmed, 2005).

Wang, et al. (2015) and Park, et al. (2013) applied the same solution strategy as mentioned above to different transient model cases.

A complete numerical study of an engine cooling system was done by Masjuki (2011). This study consists of two sections, a coolant side and an air side. The coolant side, was modelled using a 1-D solver. The air side modelling, however, was conducted by using a 3-D CFD solver as the geometry effect towards cooling air flow needed to be examined in detail. Several options to define the coupling conditions between the two (1-D and 3-D) models exist. As the continuity of all quantities cannot be satisfied simultaneously, a choice has to be made on the coupling conditions being used. This includes: mean pressure, heat flux or mean velocity. Flowmaster and StarCD were used as the 1-D and 3-D solvers respectively.

Wang, et al. (2008) investigated the overall flow- and temperature flow field distribution for a thermal power plant in northern China. Special emphasis was placed on the air flow field surrounding the air-cooled heat exchangers, as the effect of hot plume recirculation was investigated on the entire plant, consisting over several different air-cooled heat exchangers.

Wang, et al. (2008) proposed the use of a realizable k-ε turbulence model, as it provides superior performance for flows involving rotation, recirculation and boundary layers subjected to strong adverse pressure gradients. From Ansys (2010) it is evident that the finite volume method is best suited to solve the governing equations on fluid flow and heat transfer as the buoyancy of air can be taken into account when simulating an air-cooled heat exchanger.

To predict the thermo-fluid performance of an air-cooled power generating unit Hu, (2014) presented a study in which the multi-scale system regarding the flow and heat transfer of such units could be modelled separately by two different sub-domains which were inter-linked by coupling the interfaces. The solution obtained for the air-side flow and heat transfer were linked as boundary conditions. The results indicated a 7.75% difference in thermo-flow characteristics relative to a multi-grid CFD. The resources and calculation time were significantly reduced by using this modelling strategy that also resulted in a solution within an acceptable range of accuracy.

Galindo, et al. (2011) describes the coupling methodology between an in-house 1-D code and the general 3-D CFD code Fluent by means of the Method of Characteristics. The Method of Characteristics is a technique implemented to solve partial differential equations. Mentor Graphics (2012) provides a coupled general-purpose 1-D/3-D CFD simulation software called FloEFD™. Reports indicate that simulation time can be reduced by as much as 65-75% in comparison to traditional CFD tools.

2.4 Summary

Various applications and coupling strategies associated with coupled 1-D/3-D modelling approaches have been discussed. From the research it is evident that the use of a coupled 1-D/3-D numerical modelling approach can reduce computational time and model size. In most cases this procedure is done on a systems level only.

Chapter 3: Theoretical Background

Overview

Chapter 3 will provide the reader with the necessary theoretical background to understand the issues and concepts surrounding coupled 1-D/3-D numerical modelling, different coupling strategies applicable to the scope of the research and the strategic alignment between the two. This chapter will also provide the background on all issues and initiatives, from planning right through to implementation.

3.1 Introduction

By utilizing both 1-D and 3-D solution approaches, the coupled 1-D/3-D numerical modelling approach will provide an integrated solution for the coupled flow and heat transfer problem as depicted in different air-cooled heat exchanger simulation test cases. For that reason, it is important to look at the different solution strategies accompanying this coupled 1-D/3-D modelling approach. The 3-D CFD solver (Fluent) used to model the (external) flow around the pipes makes use of a CFD approach while the1-D solver (Flownex) used to model the (internal) flow inside the pipe/ducts uses a so-called Systems-CFD (SCFD) approach.

3.1.1 Computational Fluid Dynamics (CFD)

Finite volume Computational Fluid Dynamics (CFD) entails the solution of the differential equations for the conservation of mass, momentum and energy on a per unit volume basis. A typical two-dimensional control volume used in the CFD approach is shown in **Figure 7**. Fluid properties such as temperature, pressure and velocity are assumed to vary little over the control volume and these properties, as a whole, can be represented by the average value situated at the nodal point P within the control volume (Versteeg & Malalasekera, 2007).

For the control volume the conservation of mass and energy is typically written around the nodal point P and the conservation of momentum is written for the flows over the boundaries at the control volume interfaces (Rousseau, 2014).

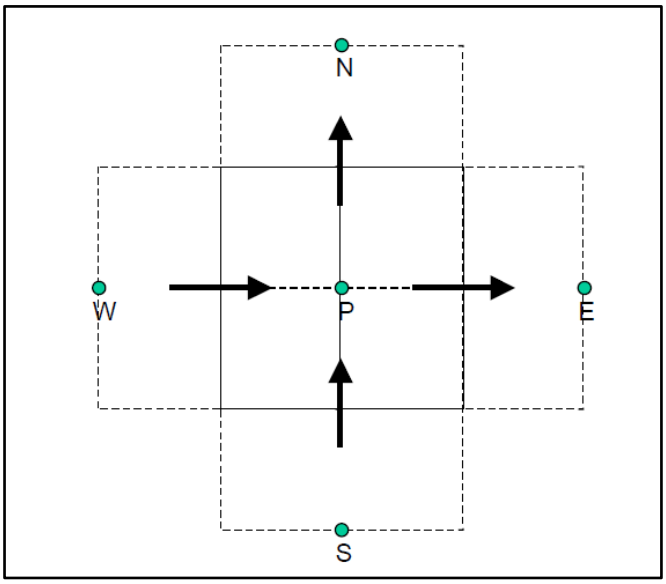

Figure 7: Typical control volume for a CFD approach

Source: (Rousseau, 2014)

3.1.2 Systems Computational Fluid Dynamics (SCFD)

The 1-D solver makes use of a network or Systems Computational Fluid Dynamics (SCFD) solution approach. In SCFD a collection of 1-D elements is used to connect nodes in a random unstructured manner, shown in **Figure 8**. Within **Figure 8** the nodes are denoted by squares and the elements are denoted by circles. The nodes have an associated volume, which can be used to represent a tank or reservoir. The elements can be of any type of thermal-fluid component, including heat exchanger elements, turbines, compressors, pipes etc. (Flownex SE, 2016)

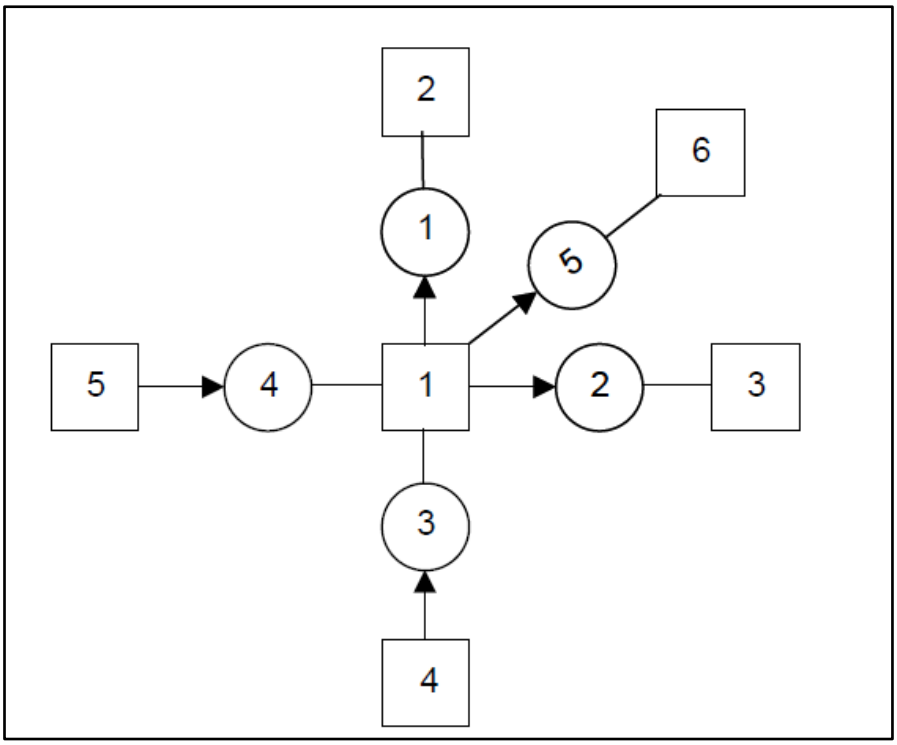

Figure 8: Node-element configuration for SCFD approach

Source: (Rousseau, 2014)

Similar to the CFD approach, the fluid properties in a node are assumed to be represented by a single average value. The conservation of mass and energy is applied at the nodes and the conservation of momentum is applied for the elements as it serves as a connection between the nodes.

3.2 Numerical Modelling

3.2.1 Computational Fluid Dynamics Modelling

The numerical methods and models, governing equations and discretization will be addressed in this section.

3.2.1.1 Governing Equations

Mathematical statements of the conservation laws of mass, momentum and energy are represented in **Table 1**. The different 3-D solvers used in this study solve these equations numerically.

Table 1: Governing equations of a viscous incompressible fluid.

Continuity	$\nabla(\rho\vec{v}) = 0$
x-momentum	$\nabla(\rho u\vec{v}) = -\frac{\partial p}{\partial x} + \nabla\cdot[(\mu+\mu_t)\nabla(u)] + S_{M_x}$
y-momentum	$\nabla(\rho v\vec{v}) = -\frac{\partial p}{\partial y} + \nabla\cdot[(\mu+\mu_t)\nabla(u)] + S_{M_y}$
z-momentum	$\nabla(\rho w\vec{v}) = -\frac{\partial p}{\partial z} + \nabla\cdot[(\mu+\mu_t)\nabla(u)] + S_{M_z}$
Energy	$\nabla(\rho T\vec{v}) = -p\nabla(\vec{v}) + \nabla\cdot[k\nabla(T)] + \Phi + S_E$

Source: (Versteeg & Malalasekera, 2007)

The symbols used in **Table 1** refer to external momentum sources (buoyancy, gravity or flow obstructions etc.) and are defined by the momentum source terms S_{M_x}, S_{M_y} and S_{M_z} respectively, with the energy source term S_E. The pressure is denoted by p and density by ρ.

Note: the turbulent fluid viscosity (μ_t) will be discussed in **3.2.2.1**

The velocity vector ($\vec{v}$) is described in **Equation (1)** (CD-adapco, 2015):

$$\vec{v} = u\vec{\imath} + v\vec{\jmath} + w\vec{k} \tag{1}$$

where $\vec{\imath}$, $\vec{\jmath}$ and $\vec{k}$ are the unit vectors in the *x*, *y*, and *z* directions respectively.

The energy dissipation term Φ is defined in **Equation (2)** (Versteeg & Malalasekera, 2007):

$$\Phi = (\mu + \mu_t)\left\{2\left[\left(\frac{\partial u}{\partial x}\right)^2 + \left(\frac{\partial v}{\partial y}\right)^2 + \left(\frac{\partial w}{\partial z}\right)^2\right] + \left(\frac{\partial u}{\partial y} + \frac{\partial v}{\partial x}\right)^2 + \left(\frac{\partial u}{\partial z} + \frac{\partial w}{\partial x}\right)^2 + \left(\frac{\partial v}{\partial z} + \frac{\partial w}{\partial y}\right)^2\right\} \tag{2}$$

3.2.1.2 Discretization

For convenience the vector approach is considered as the conservation of mass, momentum and energy can be represented in differential equations that do not depend on a coordinate system. For example, let φ be the physical quantity to be observed, then for an Eulerian frame of reference the governing equations listed in **Table 1** can be described as in **Equation (3)** (Versteeg & Malalasekera, 2007):

$$\frac{\partial \rho\varphi}{\partial t} + \nabla(\rho\varphi\vec{u}) = \nabla \cdot \left[\Gamma_\varphi \nabla(\varphi)\right] + S_\varphi \qquad (3)$$

Equation (3) describes the conservation of φ: where t is time, ρ density, Γ a diffusion constant, $\vec{u}$ a velocity vector and S_φ a sink/source of the quantity φ.

Consider the second order non-linear partial differential equation in **Equation (3)** and the closed domain in **Figure 9**. The first term $\frac{\partial \rho\varphi}{\partial t}$ represents the property φ: change over time within the closed domain due to movement over the boundary and the source/sink (S_φ) inside the closed domain. The movement over the boundary is a result of convection, due to the fluid velocity $\boldsymbol{u}$, and diffusion due to differences in concentration.

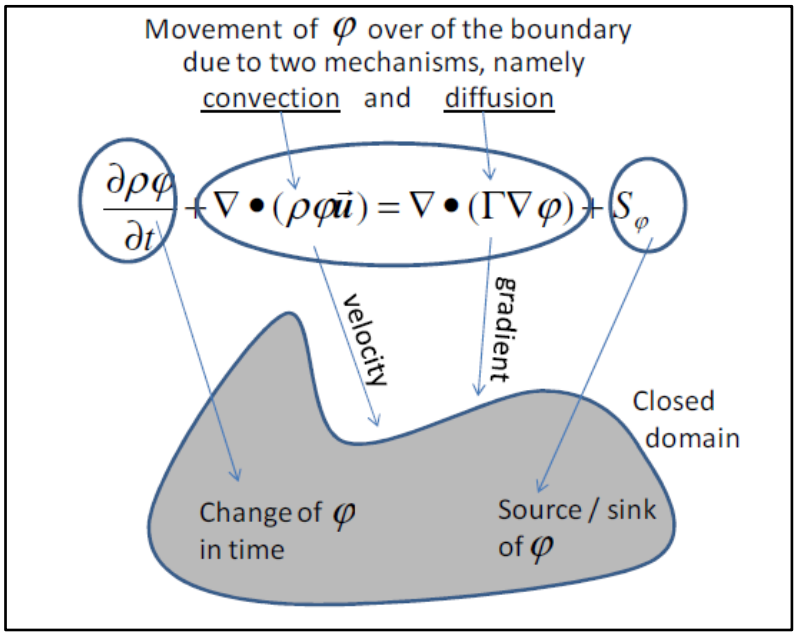

Figure 9: Schematic representation of a closed domain illustrating the meaning of the different terms in Equation (3) (Versteeg & Malalasekera, 2007)

The Finite Volume Method is the method of choice to discretize the conservation equations (transport equations) for fluid flow. This implies that the properties of mass, momentum and energy are conserved locally over each control volume. The Finite Volume Method (FVM) discretizes the flow domain into a finite number of non-overlapping Control Volumes (CV) with flat faces.

Integrating **Equation (3)** yields the integral form of the conservation equation, the property φ over the control volume and the time step δt.

$$\int_{t}^{t+\delta t}\left(\int_{V}\frac{\partial \rho\varphi}{\partial t}dV\right)dt+\int_{t}^{t+\delta t}\left(\int_{V}\nabla\cdot(\rho\varphi\boldsymbol{u})\,dV\right)dt = \int_{t}^{t+\delta t}\left(\int_{V}\nabla\cdot\left[\Gamma_{\varphi}\nabla(\varphi)\right]dV\right)dt + \int_{t}^{t+\delta t}\left(\int_{V}S_{\varphi}\,dV\right)dt \tag{4}$$

Where V is the domain volume and t time.

Gauss's theorem is applied to the convection and diffusion terms in **Equation (4)**. Since the CV consists of a volume surfaced by **n** flat faces, the surface integral can be decomposed as a sum of the integrals over the different faces that surround the control volume (f denotes the control volume face number). The integration midpoint rule is implemented to all the integrals and **Equation (4)** is reduced to:

$$\int_{t}^{t+\delta t}\left(V_P\,\frac{\partial \rho\varphi}{\partial t}\right)dt+\int_{t}^{t+\delta t}\left(\sum_{f=1}^{n}\rho_f\varphi_f\boldsymbol{u}_f\cdot\boldsymbol{A_f}\right)dt = \int_{t}^{t+\delta t}\left(\sum_{f=1}^{n}\Gamma_f(\nabla\varphi)_f\cdot\boldsymbol{A_f}\right)dt+\int_{t}^{t+\delta t}\left(S_{\varphi_P}V_P\right)dt \tag{5}$$

The outward pointing face area vector $A_f = (\hat{n}A)_f$ and the subscript P, the control volume label, as defined in **Equation (5)** is shown in **Figure 10**.

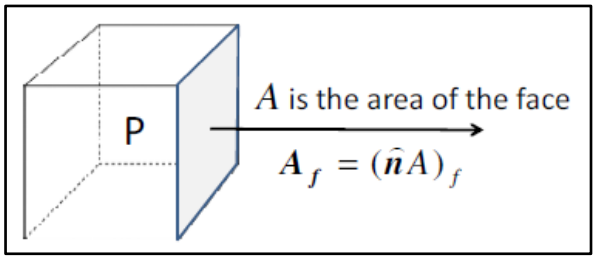

Figure 10: Area vector and Control volume

Eulerian methods have stationary grids where the mass moves through a stationary grid (Versteeg & Malalasekera, 2007) therefore; the volume of the control volume can be considered as a constant as it does not change with respect to time. The first term of **Equation (5)** is reduced to:

$$\int_{t}^{t+\delta t} \left(V_P \frac{\partial \rho \varphi}{\partial t} \right) dt = V_P \left((\rho \varphi)_P^{t+\delta t} - (\rho \varphi)_P^{t} \right) \tag{6}$$

The mid-point integration rule can be applied over the interval δt for the other integrals as it changes continuously over time. This is done by approximating the midpoint value as a linear combination of the values at the two end points $t + \delta t$ and t:

$$
\begin{aligned}
V_P\big(\,(\rho\varphi)_P^{t+\delta t} - (\rho\varphi)_P^{t}\big) \\
&+ \left[\theta_c\left(\sum_{f=1}^{n}\rho_f\varphi_f\boldsymbol{u}_f\cdot\boldsymbol{A_f}\right)^{t}\right. \\
&\left.+ (1-\theta_c)\left(\sum_{f=1}^{n}\rho_f\varphi_f\boldsymbol{u}_f\cdot\boldsymbol{A_f}\right)^{t+\delta t}\right]\delta t \\
&= \left[\theta_d\left(\sum_{f=1}^{n}\Gamma_f(\nabla\varphi)_f\cdot\boldsymbol{A_f}\right)^{t}\right. \\
&\left.+\ (1-\theta_d)\left(\sum_{f=1}^{n}\Gamma_f(\nabla\varphi)_f\cdot\boldsymbol{A_f}\right)^{t+\delta t}\right]\delta t \\
&+ \left[\theta_s(S_{\varphi_P}V_P)^{t} +\ (1-\theta_s)(S_{\varphi_P}V_P)^{t+\delta t}\right]\delta t
\end{aligned}
\tag{7}
$$

Where θ is a weighting parameter between 0 and 1. The subscripts *c, d, s* or φ refer to the different terms, namely convection term, diffusion term and source term as in **Figure 9**.

3.2.1.3 Turbulence model

The realizable k-epsilon or k-ε turbulence model is used, to account for the turbulent flow present in both the coupled flow and heat transfer problem and the full 3D CFD verification thereof. The k- ε turbulence model is appropriate for recirculating flows and has been the most widely used and validated turbulence model for many industrial applications (Envenio, 2017). Wall functions are implemented in the model, which lowers the memory requirements for its use, and the model demonstrates good convergence behaviour (CD-adapco, 2015). This model is regarded as a two-equation model as it contains two extra transport equations to represent the turbulent properties of the flow. The k-ε turbulence model accounts for the convection and diffusion of turbulent energy (Envenio, 2017).

Turbulent kinetic energy, k, determines the energy in the turbulence, whereas the turbulent dissipation, ε, is the rate at which the turbulent energy is dissipated.

For turbulent kinetic energy, k (Ansys, 2010):

$$\frac{\partial}{\partial t}(\rho k) + \frac{\partial}{\partial x_i}(\rho k u_i) = \frac{\partial}{\partial x_j}\left[\left(\mu + \frac{\mu_t}{\sigma_k}\right)\frac{\partial k}{\partial x_j}\right] + P_k + P_b - \rho\varepsilon - Y_M + S_k \quad (8)$$

For dissipation, ε (Ansys, 2010):

$$\frac{\partial}{\partial t}(\rho \varepsilon) + \frac{\partial}{\partial x_i}(\rho \varepsilon u_i) = \frac{\partial}{\partial x_j}\left[\left(\mu + \frac{\mu_t}{\sigma_k}\right)\frac{\partial \varepsilon}{\partial x_j}\right] + \rho C_1 S_\epsilon - C_2 \rho \frac{\varepsilon^2}{k + \sqrt{v\varepsilon}} + C_{1_\varepsilon}\frac{\varepsilon}{k} C_{3_\varepsilon} P_b + S_\varepsilon \quad (9)$$

In **Equation (8)** and **Equation (9)**, the generation of turbulent kinetic energy due to buoyancy and mean velocity gradients is represented by P_b and P_k respectively. The S_k and S_ε terms refer to additional sources of turbulent kinetic energy or dissipation rate. (Versteeg & Malalasekera, 2007). In the same way, the turbulent Prandtl numbers for the turbulent kinetic energy and turbulent dissipation rate is represented by σ_k and σ_ε.

The turbulent viscosity μ_t (Versteeg & Malalasekera, 2007) is modelled as:

$$\mu_t = \rho C_\mu \frac{k^2}{\varepsilon} \quad (10)$$

Furthermore,

$$C_1 = \max\left[0.43, \frac{\eta}{\eta + 5}\right] \tag{11}$$

and

$$\eta = S\,\frac{k}{\epsilon} \tag{12}$$

with S, the modulus of the mean rate-of-strain tensor (Versteeg & Malalasekera, 2007):

The values for the constants associated with the realizable k-ε turbulence model is given in **Table 2**

Table 2: Realizable k- ε turbulence model constants

Constant	$C_{1\varepsilon}$	C_2	σ_k	σ_ε
Value	1.44	1.9	1.0	1.2

Source: (CD-adapco, 2015)

3.2.2 Heat Transfer Modelling

3.2.2.1 Thermal Resistance

Consider the schematic of thermal resistance through a heat exchanger wall as depicted in **Figure 11**.

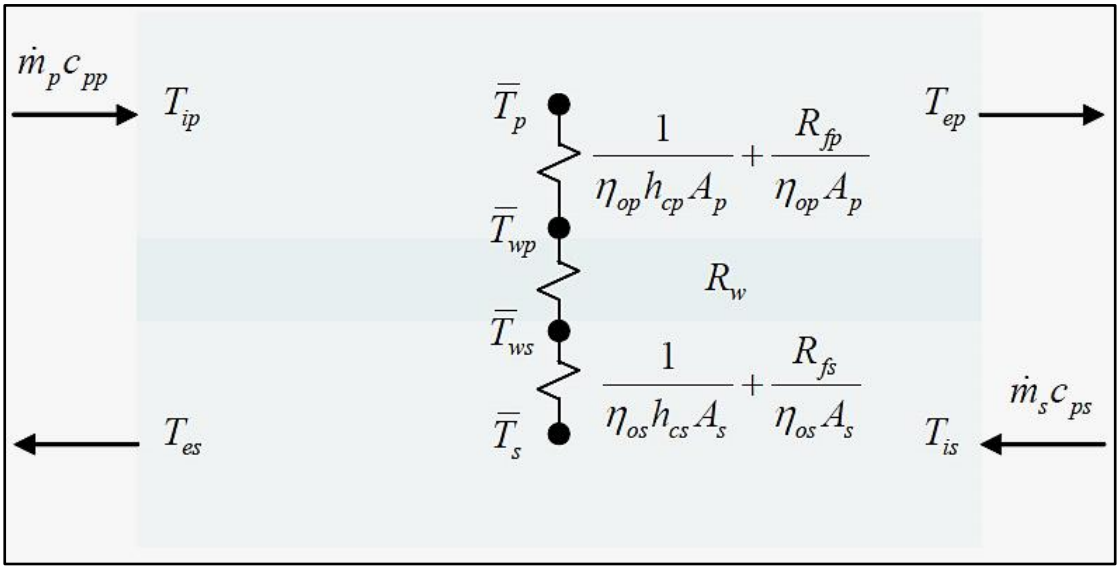

Figure 11: Schematic of thermal resistance through a heat exchanger wall

Source: (Rousseau, 2014)

The inverse of the total thermal resistance between the two fluid streams is defined as the overall heat transfer coefficient, UA (Rousseau, 2014):

$$\frac{1}{UA} = \frac{1}{\eta_{op} h_{cp} A_p} + \frac{R_{fp}}{\eta_{op} A_p} + R_w + \frac{1}{\eta_{os} h_{cs} A_s} + \frac{R_{fs}}{\eta_{os} A_s} \tag{13}$$

The heat transfer rate between the two fluids can be expressed as (Rousseau, 2014):

$$\dot{Q} = UA\Delta\bar{T} \tag{14}$$

With $\Delta\bar{T}$ the difference between the average fluid temperatures of the primary ($\bar{T}_p$) and secondary ($\bar{T}_s$) fluid streams. R refers to the heat transfer resistance in (m^2K/W).
The subscripts i and e refer to inlet and exit, while p and s refer to the primary- and secondary fluid streams.

The expression for the overall surface efficiency, η_o is (Rousseau, 2014):

$$\eta_o = 1 - \frac{A_f}{A}\left(1 - \eta_f\right) \tag{15}$$

With A_f the fin surface area, A the surface area and η_f the efficiency of a single fin.

The LMTD method, which takes into account the variation in temperature between the inlet and outlets, rather than using the average fluid temperatures is a variation on the $\dot{Q} = UA\Delta\bar{T}$ method. For counter flow we have (Incropera, et al. 2013):

$$\dot{Q} = UA \cdot \text{LMTD} \tag{16}$$

with

$$LMTD = \frac{\Delta T_1 - \Delta T_2}{\ln \frac{\Delta T_1}{\Delta T_2}} \quad (17)$$

Where $\Delta T_1 = T_{hi} - T_{ce}$ and $\Delta T_2 = T_{he} - T_{ci}$.

In order to apply either the "$\dot{Q} = UA\Delta\bar{T}$" or "LMTD" approaches, the overall heat transfer coefficient, UA, must be calculated, but this requires the respective convection coefficients as shown in **Equation (13).**

3.2.2.2 Conduction

Conduction heat transfer occurs in a solid material or fluid when a temperature difference is present while no bulk motion is occurring. A schematic representation of conductive heat transfer process is shown in **Figure 12**.

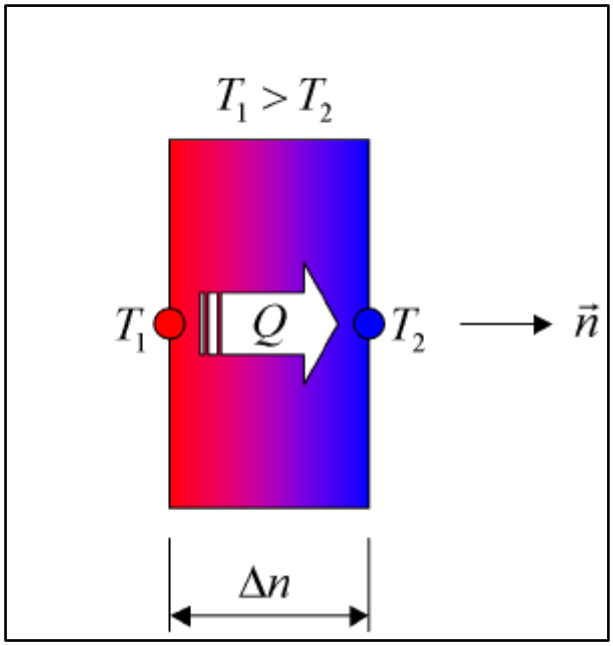

Figure 12: Conduction Heat Transfer

Source: (Flownex SE, 2016)

The conductive heat transfer is a function of the thermal conductivity of the material, k. The rate of heat transfer through the solid material can be expressed by **Equation (18)** (Incropera et al., 2013):

$$\dot{Q}_H = -kA \frac{\partial T}{\partial n} \tag{18}$$

For the problem shown in **Figure 12** the heat transfer can be calculated as follows using **Equation (19)** (Incropera et al., 2013):

$$\dot{Q}_H = kA \frac{T_1 - T_2}{\Delta n} \tag{19}$$

Heat transfer occurs from a higher temperature region to a lower temperature region. Therefore, the heat transfer is in the opposite direction to the temperature gradient.

3.2.2.3 Convection

A schematic representation of the convective heat transfer process is shown in **Figure 13**. Heat is transferred to a fluid (at a bulk temperature) moving across the plate from a surface with a higher temperature than that of the bulk temperature. If the bulk temperature happens to be higher than the surface temperature, the heat transfer will be be transferred from the fluid to the surface. The heat transferred from the surface to the fluid, or vice versa, is determined by the convective heat transfer coefficient, h. The heat transfer rate through convection is determined by **Equation (20)** (Incropera et al., 2013):

$$\dot{Q}_H = hA(T_s - T_\infty) \tag{20}$$

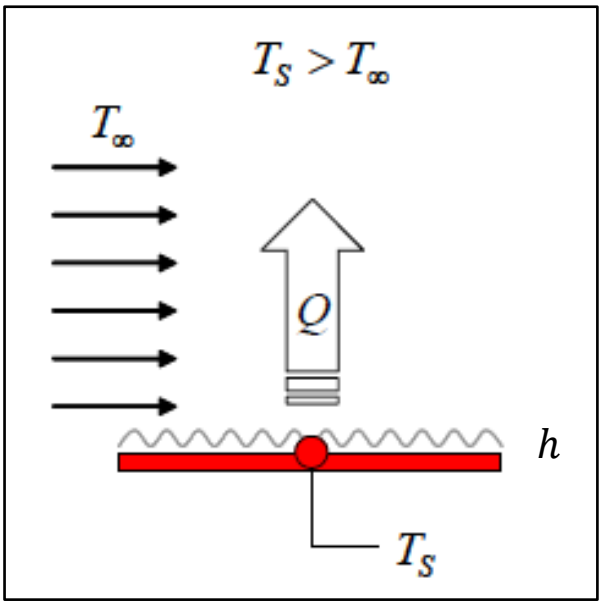

Figure 13: Convection Heat Transfer

Source: (Flownex SE, 2016)

Where T_S is the surface temperature, T_∞ is the bulk temperature and A is the area. The assumption is made that the heat transfer from the fluid to the surface is negative while heat transfer from the surface to the fluid is positive.

3.3 Coupling Strategies

Successful coupling of the 1-D and 3-D solvers will require care in both coding and numerical modelling approaches. A bare tube configuration was used within the air-cooled heat exchanger configuration test cases, to simplify the coupling procedure. This was done, as the main focus of this research study was to test the feasibility of using a 1-D/3-D modelling approach. During the solution process, principles of conservation were preserved at the interface between the two different flow domains. The 1-D solver and 3-D solver networks were explicitly coupled by transferring temperature and heat flux between the two networks. As a result, the following coupling strategies have been identified:

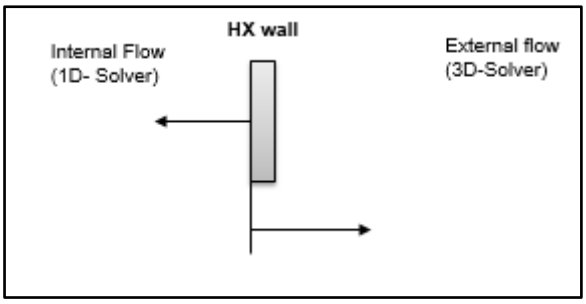

Figure 14: Coupling strategy (a)

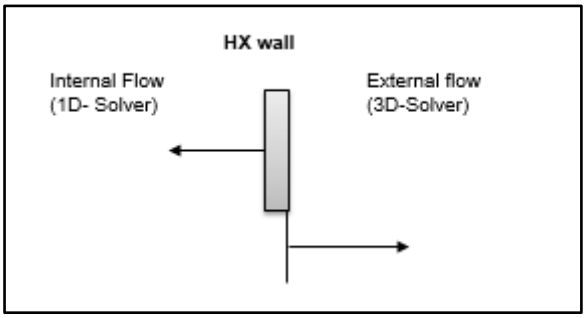

Figure 15: Coupling strategy (b)

The thermal resistance (through the heat exchanger wall) and the inner wall itself can be modelled as either part of the 3-D solver as illustrated in **Figure 14** or as part of the 1-D solver as shown in **Figure 15**.

The air-flow field surrounding the tube or tube bundles would benefit from being modelled in 3-D CFD as this would account for all flow phenomena that were experienced. However, the internal/duct flow does not require the same detail as fewer flow phenomena were present inside the tubes and can be modelled in 1-D, the flow inside the tube bundles was assumed to be uniform.

3.4 Summary

Coupling strategy (b) is implemented in this study where the tube/pipe walls are modelled as part of the 1-D solver. The air flow field is modelled in the 3-D CFD solver and the tube/duct flow is modelled in the 1-D solver. By modelling the tube/pipe walls in 1-D the computational resources required is reduced as no additional cells are required to represent the duct wall.

Chapter 4: Methodology

Overview

This chapter describes the methodology followed to best achieve the objectives as stated in Chapter 1. It includes a description of the solution algorithm, the instruments applied and simulation structure. The reasoning behind the choice of the various methods implemented are also justified in this chapter.

4.1 Introduction

This section describes by means of a demonstration how a 1-D Solver and 3-D CFD solver can be coupled to simulate an air-cooled heat exchanger configuration. This is done by describing a bare tube configuration of an air-cooled heat exchanger test case as used within this study.

The full 3-D CFD analysis of an ACHE can be very resource consuming. To overcome these issues, a combination of 3-D CFD and 1-D analysis is proposed. The area of the simulation that would greatly benefit from the increased detail of CFD, the external/air-flow field surrounding the tube or tube bundles is simulated using the general mixed physics 3-D solver, Fluent. The external air flow field is assumed to be incompressible for all the ACHE configuration test cases. The internal/duct flow is modelled using a 1-D network code, Flownex. The Flownex and Fluent networks are explicitly coupled by transferring temperature and heat flux between the two networks.

4.2 Model description

A geometric representation of the test case used to demonstrate the coupled 1-D/3-D modelling technique is shown in **Figure 16.** The test case consists of a tube bundle assembly being simulated in Flownex. The air-flow field surrounding the tube bundle is represented by the volume surrounding the pipe network as illustrated in **Figure 16**. The volume`s dimensions were chosen to be sufficiently large, such that the boundary effects of the air-volume on the coolant pipes was minimal.

However, in the air flow field meshing operation, the growth rate was set to generate a coarse mesh where fine detail was not critical. This air flow field is simulated within Fluent with the air flow direction as shown in the figure.

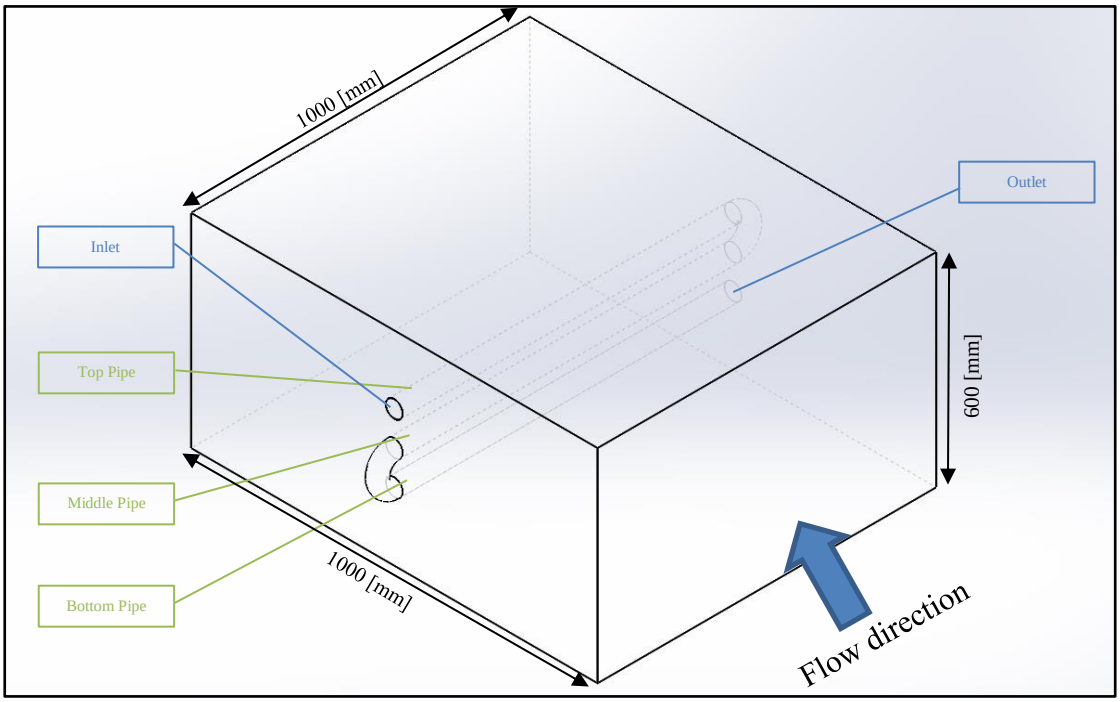

Figure 16: Geometric representation of air-cooled heat exchanger test case

Before coupling the Flownex and Fluent networks, the upstream Flownex network as well as the Fluent air-cooled heat exchanger flow field simulation are setup to run separately with fixed boundary conditions. A short description of each model follows.

4.2.1 Flownex network

The Flownex network simulates the pipe/tube bundle network in the air-cooled heat exchanger configurations. To illustrate the network, refer to the network as depicted in **Figure 17**. The working fluid (water) that needs to be cooled, enters the top pipe-element at a specific pressure and temperature after which a triple pass through the air-flow field is simulated. In the Flownex network the pipe elements and heat transfer elements, are discretised into a number of sub elements. The bends are assumed to be adiabatic, and serve only as a way to reverse the flow direction of the water.

The surface temperature, from Flownex results, for each pipe sub element is transferred to the corresponding "pipe-sub element cavity" in Fluent.

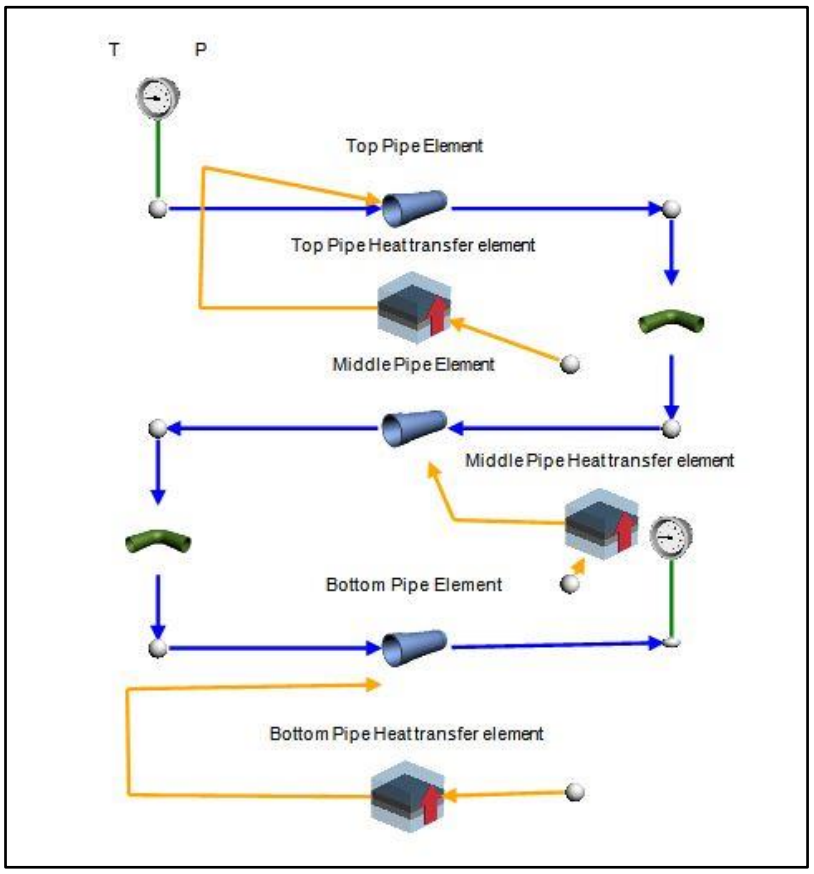

Figure 17: Flownex network for ACHE configuration test case

4.2.2 Fluent ACHE flow field simulation

Since the air flow field surrounding the pipe/tube bundle will benefit the most from the 3-D CFD solver, Fluent is used to perform the air-flow field simulation of the air-cooled heat exchanger configuration. **Figure 18** illustrates the geometrically meshed view of an ACHE flow field as simulated in ANSYS Fluent. As coupling strategy (b) is implemented in this study, the meshed flow field does not contain any cells related to the pipe network. Heat flux and heat transfer coefficients, from Fluent results, for each "pipe sub-element" is transferred to the corresponding pipe heat transfer sub- element in Flownex.

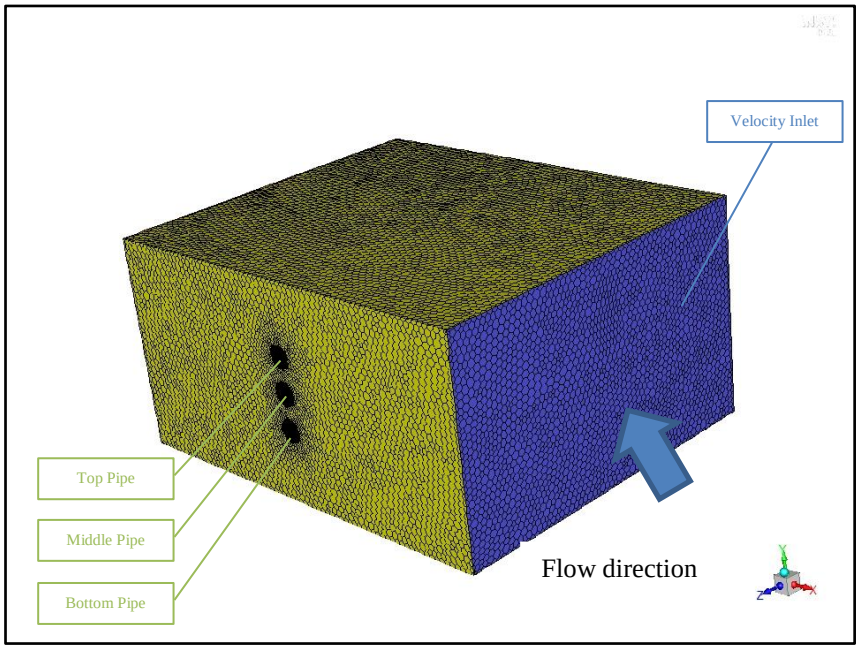

Figure 18: ACHE flow-field as simulated in Fluent

4.2.3 Coupling interfaces

To illustrate the coupled 1-D/3-D modelling approach, refer to the simulation test case as depicted in **Figure 19**. The working fluid (water) that needs to be cooled, enters the top pipe-element at a specific pressure and temperature after which a triple pass through the air-flow field is simulated. During each pass through the 3-D simulated air-flow field, data transfer between the two codes is established and the necessary values are linked to one another. Information transfer between Flownex and Fluent can be accomplished by using an "internal"- or "external"-coupling method. The first method makes use of an "internal"-coupling where a single global matrix system is used and the solving of the generated equations is done as an implicit system. (Kruger & Du Toit, 2006). In this study however, the Flownex and Fluent networks are explicitly coupled by transferring temperature and heat flux between the two networks. The Flownex and Fluent network interface as well as the data transfer links are shown in **Figure 19**.

Both node-averaged and boundary values can be explicitly coupled between Flownex and Fluent. The averaged values are calculated by using the appropriate volume, area or density weighted property depending on the mesh geometry or type of property.

Refer to **Figure 16** and **Figure 18**. For the Flownex network, the pipe elements with their increments are defined and the average surface temperature value for each increment is linked to the corresponding Fluent "pipe sub-element increment" cavity. Fluent then uses this average surface temperature and applies it across the "pipe-sub-element" cavity as a surface temperature. The heat flux is then sent from the individual "pipe sub-element" cavity sections to the corresponding Flownex pipe sub-element increments.

The data transfer links shown in **Figure 19** between Flownex and Fluent will be explained below:

Data Transfer link #1: Input from Excel to the Flownex pipe network

- The working fluid's inlet temperature and pressure are transferred from the Excel workbook as a boundary condition.

Data Transfer link #2: Input from Excel to the Flownex pipe network

- The working fluid's Outlet conditions is transferred from the Excel workbook to the outlet boundary condition in the Flownex pipe network.

Data Transfer link #3: Input from Excel to the Fluent for Start-up Conditions

- The environmental- temperature and pressure as well as the velocity magnitude of the air moved over the tube bundle is transferred from the Excel workbook to Fluent as initial boundary conditions.

Data Transfer link #4: Input from Excel to Top Pipe Heat transfer element

- The environmental temperature is transferred from the Excel workbook to heat transfer element.

Data Transfer link #5: Input from Excel to Middle Pipe Heat transfer element

- The environmental temperature is transferred from the Excel workbook to heat transfer element.

Data Transfer link #6: Input from Excel to Bottom Pipe Heat transfer element

- The environmental temperature is transferred from the Excel workbook to heat transfer element.

Data Transfer link #7: Input & Output from Top Pipe Heat transfer element and Fluent

- Convection coefficients associated with the air side is transferred from Fluent to Flownex.
- Surface temperature associated with the air side is transferred from Flownex to Fluent and assigned as a wall boundary condition.

Data Transfer link #8: Input & Output from Middle Pipe Heat transfer element to Fluent

- Convection coefficients associated with the air side is transferred from Fluent to Flownex.
- Surface temperature associated with the air side is transferred from Flownex to Fluent and assigned as a wall boundary condition.

Data Transfer link #9: Input & Output from Bottom Pipe Heat transfer element to Fluent

- Convection coefficients associated with the air side is transferred from Fluent to Flownex.
- Surface temperature associated with the air side is transferred from Flownex to Fluent and assigned as a wall boundary condition.

Data Transfer link # 10: Input from Fluent to Top Pipe element

- Heat flux is transferred from Fluent to the Flownex pipe element, modelling the heat removal from the pipe surface by the air.

Data Transfer link # 11: Input from Fluent to Middle Pipe element

- Heat flux is transferred from Fluent to the Flownex pipe element, modelling the heat removal from the pipe surface by the air.

Data Transfer link # 12: Input from Fluent to Bottom Pipe element

- Heat flux is transferred from Fluent to the Flownex pipe element, modelling the heat removal from the pipe surface by the air.

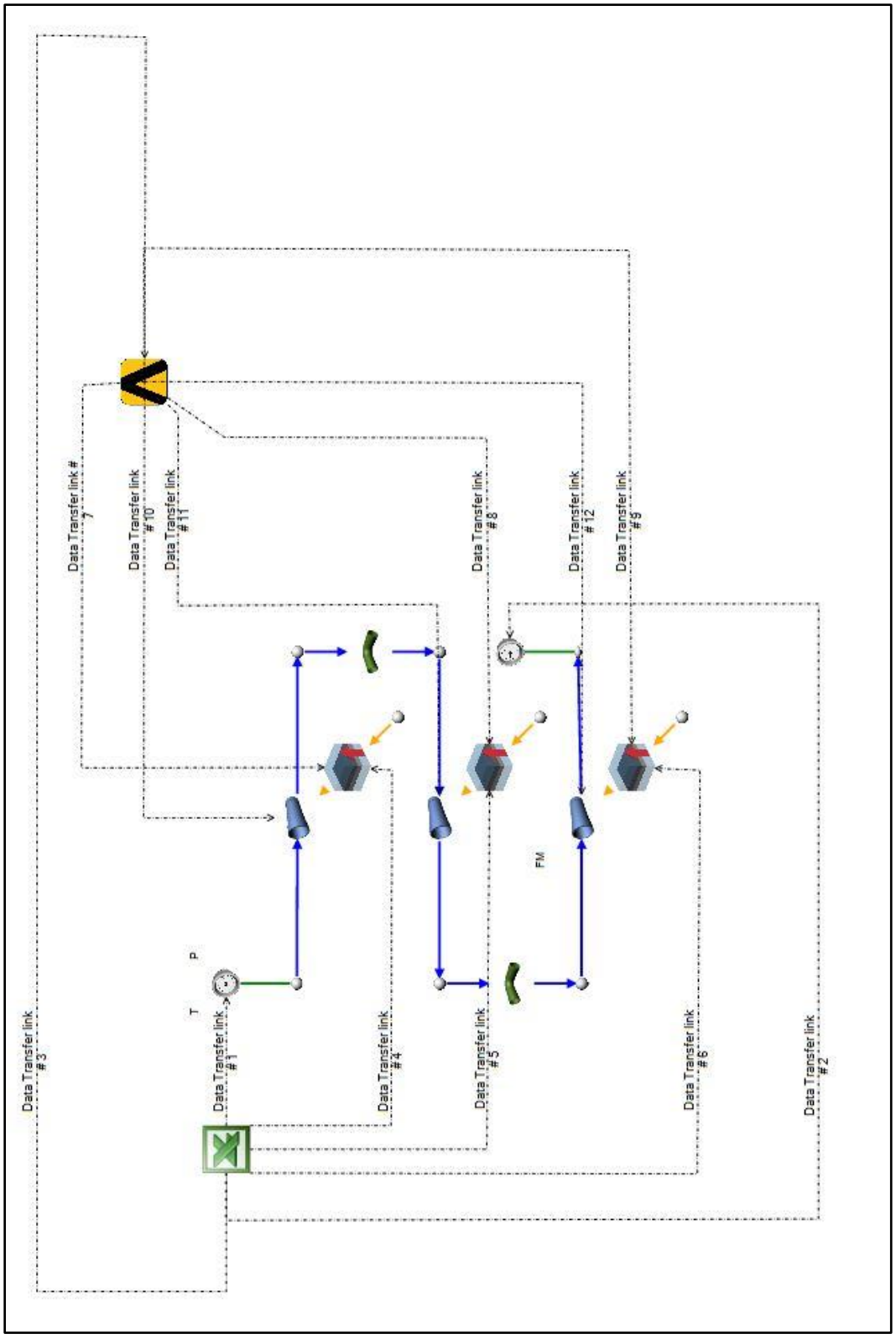

Figure 19: Sample of a Schematic representation of the parameter exchange between Flownex and Fluent

The calculated water outlet temperature from Flownex is linked to Excel, from which appropriate figures are drawn.

4.3 Solution algorithm

It is evident, from the Flownex manuals Flownex SE (2016) that when using a coupled 1-D/3-D modelling process, transient simulations should be assumed to initiate from a steady state condition. This will aid in reducing the time-consuming iterations between the different codes until the 3-D domain solution converged.

The solution algorithm used for coupled 1-D/3-D numerical modelling is illustrated in **Figure 20**. The solution algorithm starts by initializing both the Flownex and Fluent models and ensuring that both cases can run separately in a stable manner by using fixed boundary conditions – i.e. uncoupled. The initial boundary values used as input conditions in both Flownex and Fluent networks should have similar values to ensure any numerical discrepancy between the Flownex and Fluent networks are minimized.

Information transfer is initialized after steady-state solutions for both Flownex and Fluent are achieved. The communication link (Journal File) is established between the two different codes and information transfer between them occurs. An iterative procedure is then followed in which Flownex completes a number of iterations and transfers the necessary values to Fluent. These transferred values from Flownex are then used by Fluent. Corresponding iterations are performed in Fluent and the parameters required by Flownex are then sent back. After the information transfer from Flownex to Fluent and vice versa, is achieved, the global iteration advances.

This process is repeated until some acceptable convergence criteria are reached in both Flownex and Fluent. The same solution algorithm is applied to transient cases, except a time-step iteration loop is added to the solution algorithm.

Note: Refer to **Appendix B** for a sample Journal file created.

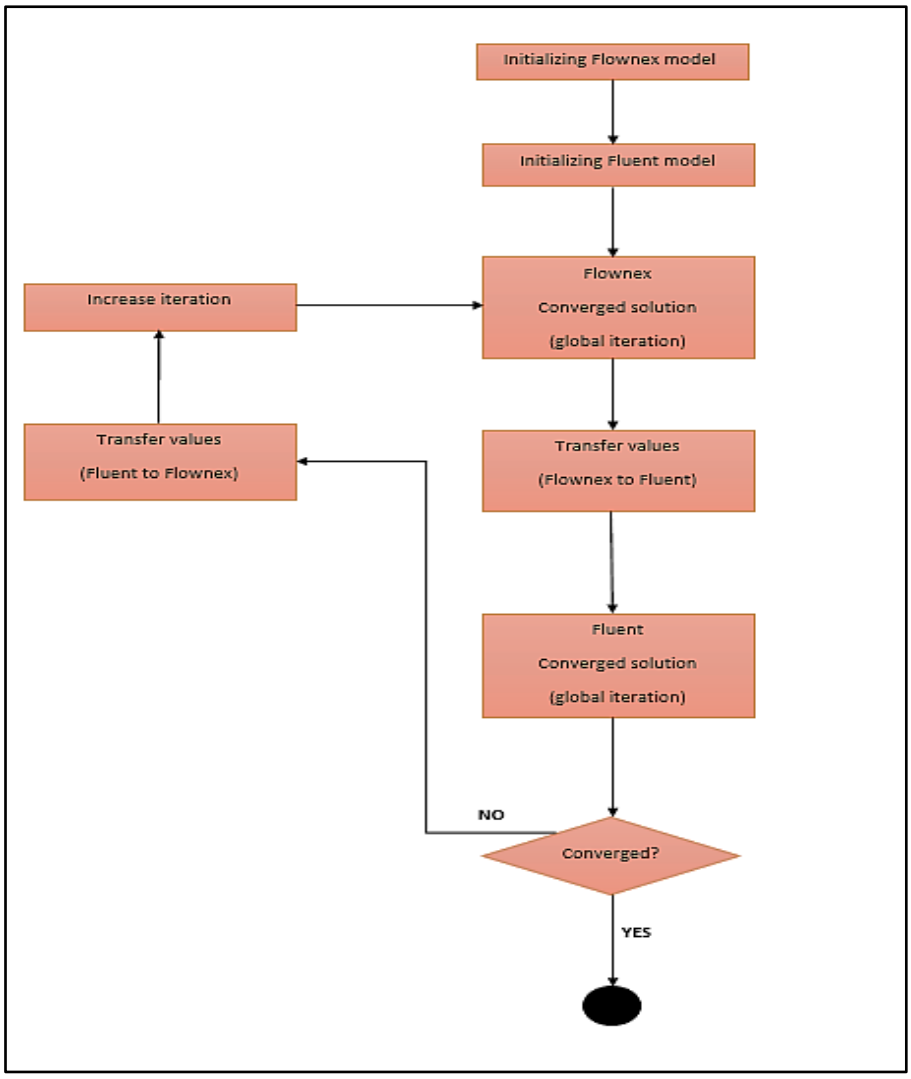

Figure 20: Solutions algorithm for coupling Flownex and Fluent

Adapted from source: (Kruger & Du Toit, 2006)

4.4 Evaluation of ACHE configuration test cases

The nature of the results and the verification thereof, will be the same for all the different simulation test cases as described in **Chapter 5.2**. The coupled 1-D/3-D modelling process will be verified by comparing the results to that of a full 3-D CFD model with the same specifications and input variables. The outlet temperature of the water after the triple pass will be compared between the two different methods. Comparisons regarding the number of iterations, model size, computation time etc. will also be made. The energy balance, heat transfer and water outlet temperature plots from the full 3-D CFD (Star-CCM+) simulations was used to check the accuracy of the coupled 1-D/ 3-D simulation approach.

Chapter 5: Results

Overview

In this chapter of the report the solution algorithm discussed in the previous chapter was applied to the different air-cooled heat exchanger configuration test cases. For each case the air-flow field was modelled using the 3-D solver, Fluent. While the duct/pipe flow containing the process fluid that needs to be cooled was modelled using the 1-D solver, Flownex. The two different solvers were explicitly coupled by transferring temperature and heat flux between them. The combination or coupled 1-D/3-D modelling approach proposed in this study is then verified by testing the results obtained against a full 3-D CFD analysis of the same specifications and setup in Star-CCM+. This chapter concludes with a brief summary of the results obtained.

5.1 Introduction

The proposed coupled 1-D/3-D modelling technique was applied to different air-cooled heat exchanger configuration test cases. In addition to all the test cases being verified to a full 3-D CFD analysis thereof, the input specifications (Refer to **Table 3**), solution strategy (**Table 4**) and overall geometric characteristics were kept the same in the different cases. The mass flow rate of the water within the tube bundle, magnitude of the air velocity flowing over the tubes and the arrangement of these pipes within the airflow field are varied in the different ACHE configuration cases. The use of similar geometric configurations simplifies the modelling process as well as aids in the evaluation of the results.

Star-CCM+ is a widely recognized commercial 3-D CFD tool and has the ability to model heat transfer, turbulence and flow for various industrial application (CD-adapco, 2015). It was therefore used to verify the coupled 1-D/3-D modelling approach.

Table 3 contains the general inputs specifications, applicable to all the different air-cooled heat exchanger configuration test cases. As fins are not included in this study, several steps were taken to increase the temperature difference between the inlet and outlet water temperature of the ACHE configurations. This included increasing the pipe diameter, magnitude of the air velocity and decreasing the mass flow rate of the water inside the tube bundle, as well as, reducing the environmental temperature. The specifications related to the air-cooled heat exchanger configurations are similar to that found in industry as the pitch and pipe diameter both adhere to the standards as stated by TEMA. (Tubular Exchanger Manufactures Association, 2007)

Table 3: General Input Specifications for ACHE configuration test cases

Input Specification	**Value**
Working Fluid (Flownex)	H2O- Water | Liquids
Working Fluid (Fluent)	Air
Inlet boundary conditions (Air)	277.13 [K]
Ambient Pressure (Fluent/Star-CCM+)	101.325 [kPa]
Air Velocity (Fluent/Star-CCM+)	15.86 [m/s]
Inlet water Pressure	140 [kPa]
Inlet water Temperature	50 [°C]
Pipe length for each pipe-element	1000 [mm]
Pipe diameter	50 [mm]
Pitch between pipes	100 [mm]
Surface & Roughness Selection	37.5 [µm] , New drawn Aluminium
Method of Heat Transfer	Fixed Heat transfer
Conduction Area discretization scheme	Standard (Average areas)
Convection option	To ambient
Convection Area discretization scheme	Standard (Average areas)
Bends	Adiabatic

Table 4 contains the solution strategies applied to the ACHE configurations. The strategies chosen are based on the research aims and objectives (the solvers were explicitly coupled by transferring temperature and heat flux between them). The realizable k-ε turbulence model is chosen as it is appropriate for recirculating flows and aids in reducing the computational resources required (see section **3.2.1.3**). In both Star-CCM+ and Fluent the second-order upwind scheme were implemented as it is considered to be the simplest and most stable discretization scheme (Versteeg & Malalasekera, 2007).

Table 4: Solution Strategies applied to ACHE configuration test cases

	Models/Strategies applied
Turbulence model	Realizable k-ε turbulence
Flow modelling strategy	Modelled as Incompressible flow
Coupling Strategy	Coupling Strategy (b) (**Figure 15**)
Information transfer (Flownex to Fluent)	Surface Temperature
Information transfer (Fluent to Flownex)	Heat Flux
Inlet boundary conditions (3D Solvers)	Velocity Inlet Boundary
Outlet boundary conditions (3D Solvers)	Pressure Outlet Boundary
Solution Methods (3D solvers)	Second-order Upwind
	Coupled Implicit

5.2 Air-Cooled Heat Exchanger configuration test cases

The different air-cooled heat exchanger configuration test cases are discussed. The results obtained from the coupled 1-D/3-D solution approach and the verification of these results will be addressed below.

Table 5 contains the parameters or values being transferred between the codes for all the air-cooled heat exchanger test cases.

Table 5: Information Transfer for all ACHE configuration test cases

Parameter	**Transfer medium**
Ambient Temperature	From Excel to Fluent
Ambient Pressure	From Excel to Fluent
Air Velocity (Velocity Input Boundary)	From Excel to Fluent
Surface Temperature as wall Boundary condition (from each pipe sub-element)	From Flownex to Fluent
Heat Flux (To each pipe sub-element)	From Fluent to Flownex
Water Outlet Temperature	From Flownex to Excel
Number of iterations for Steady-state solution	From Flownex to Excel
Number of global iterations	From Flownex to Excel
Model size	From Fluent to Excel
Number of Iterations (3D solver)	From Fluent to Excel
Solution time	From Fluent/Flownex to Excel

For all the air-cooled heat exchanger configuration test cases, the temperature of the water exiting the pipe network, the number of iterations, solution time and model size are the main attributes examined.

These results were compared to the verification test case with the same input specifications and setup. The solution accuracy was deemed acceptable when the residuals were below $1e^{-05}$.

This comparison of results between the two different solution approaches formed the basis on which the coupled 1-D/3-D modelling approach was evaluated.
Table 6 contains the general meshing parameters used in both Fluent and Starr-CCM+.

Table 6: General meshing parameters

Meshing strategy applied	
Meshing scheme (Star-CCM+)	Polyhedral meshing scheme
Meshing scheme (Fluent)	Tetrahedral meshing scheme (Converted to Polyhedral mesh)
Meshing models	Prism Layer mesher Surface remesher
Relevance (Fluent)	100 %
Number of Prism Layers	5
Prism Layer relative size	33% of base size
Surface Growth rate	1.1
Surface Proximity	3
Tet/Poly density	1
Advanced size function (Fluent)	Fine

5.2.1 Case 1: Perpendicular flow (x-Axis) 3 Pipe ACHE configuration

5.2.1.1 Overview

The perpendicular flow 3 pipe ACHE configuration consists of an integrated Flownex and Fluent model representing a triple pass bare tube air-cooled heat exchanger configuration. Within this integrated model, water (as the process fluid) enters the top pipe element at a temperature and pressure of 50 [°C] and 140 [kPa] respectively. During the coupled 1-D/3-D modelling approach, data was transferred between Flownex and Fluent.

In **Figure 21** the meshed geometric representation of the bare tube configuration within the airflow field is shown, it can be seen that for case 1 the pipe network or tube bundle frontal area was subjected to direct airflow. The boundary conditions associated with the airflow field are also shown in the figure.

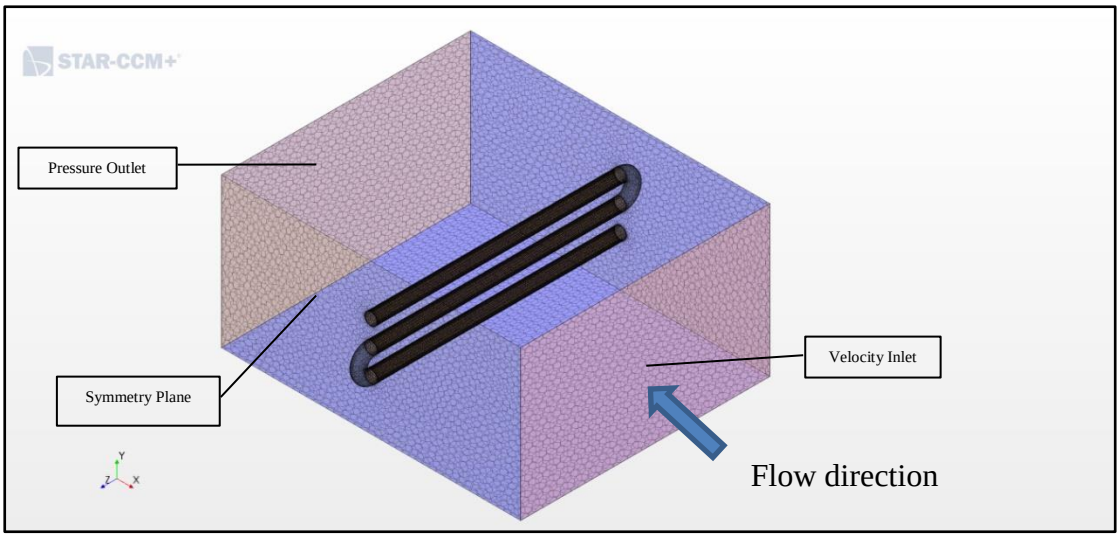

Figure 21: Meshed Geometric representation of the Perpendicular flow (x-Axis) 3 Pipe ACHE configuration

The coupled 1-D/3-D modelling approach associated with case 1 is shown in **Figure 22**, the coupling procedure used and the information transferred between the different solvers was similar to that described in **Table 5** and section **4.2**.

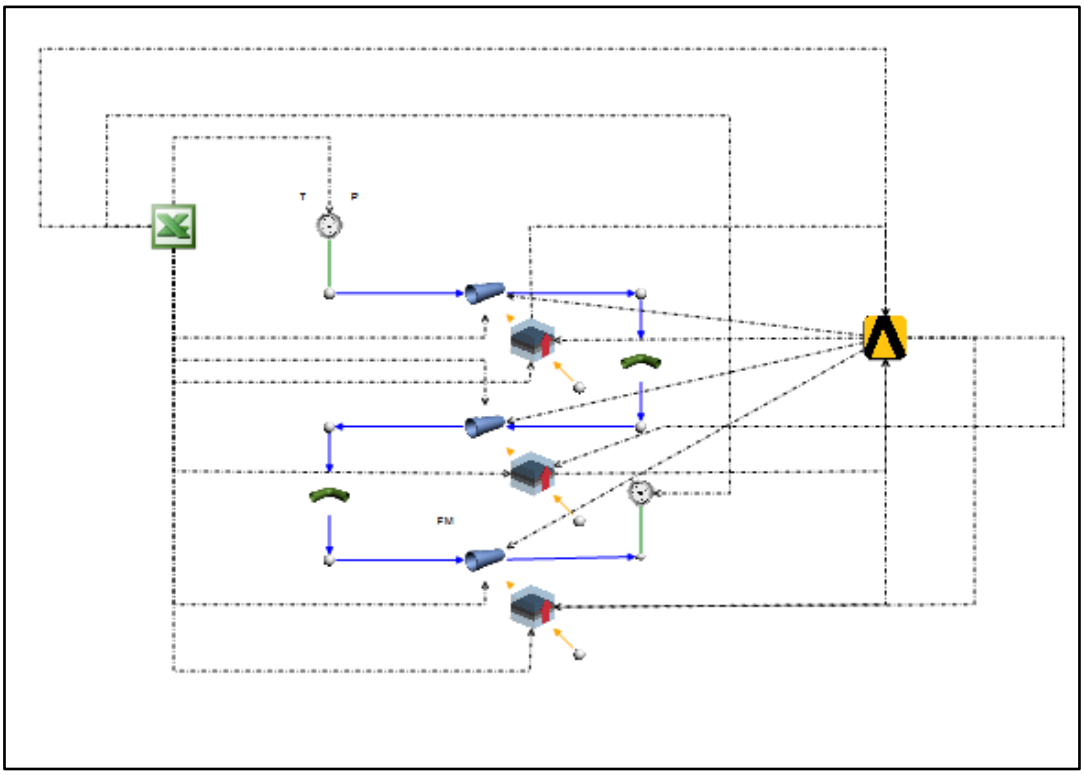

Figure 22: Schematic representation of the data transfer links between Flownex and Fluent for the Perpendicular flow (x-Axis) 3 Pipe ACHE configuration

For every global iteration the temperature of the water exiting the pipe-network was exported to Excel. Information transfer was initialized once both Flownex and Fluent had reached a steady state solution, using the boundary conditions as stated in **Table 3**.

5.2.1.2 Case 1 Investigation

The base test case for the proposed coupled 1-D/3-D numerical modelling approach was simulated using the input specifications as listed in **Table 3**. The mass flow rate of the water entering the top pipe element was 0.05 [kg/s] and the magnitude of the airflow field velocity was 15.86 [m/s]. The meshing- and solutions strategies was applied as specified in section **5.1.**

The results obtained from the coupled 1-D/3-D modelling approach and full 3-D modelling approach are shown in **Table 7** and **Table 8** respectively.

Table 7: Coupled 1-D/3-D modelling approach results for the test base case (x-Axis) 3 Pipe ACHE configuration

Outputs	**Value**
Number of Iterations (Global)	771
Number of Iterations for convergence	783
Number of cells (model size)	85 052
Computational Time	2 349 [s]
Water Outlet Temperature	47.13 [°C]

The global number of iterations refers to the number of iterations/times data transfer between the two solvers occurred until convergence was achieved. The number of iterations for convergence is therefore the global number of iterations plus the number of iterations needed by the Flownex network to achieve steady state conditions. These additional iterations are necessary for the coupling of the 1-D solver and he 3-D solver (refer to section **4.2**).

Table 8: Full 3-D modelling results for the test base case (x-Axis) 3 Pipe ACHE configuration

Outputs	**Value**
Number of Iterations (Global)	N.A.
Number of Iterations for convergence	1053
Number of cells (model size)	118 123
Computational Time	3 386 [s]
Water Outlet Temperature	46.49 [°C]

The outlet water temperature for the coupled 1-D/3-D modelling approach shows a 2% difference in temperature to that of the full 3-D CFD analysis. In addition, the coupled 1-D/3-D modelling technique is less resource intensive as a reduction in solution time of 30% and model size of 28% was achieved.

Mesh Independence:

Following the test base case, hereafter refer to as case 1A a mesh independence study was conducted. The same input specifications were used, with different mesh sizes to perform the mesh independence study. The base sizes used in the mesh independence study is shown in **Table 9**. As Fluent and Star-CCM+ use different meshing schemes, the Fluent-meshes were converted from the tetrahedral cells to polyhedral cells. This was done so that the mesh sizes between the two simulation codes can be directly compared. Refinement and cell relevance changes were made in the Fluent-mesher to ensure the two meshes could be compared. The reduction in model size seen in the coupled 1-D/3-D numerical model is due to the omission of the cells associated with the meshing of the pipe-network. It was found that the Flownex pipe network's discretization also needed refinement to achieve mesh independence.

Table 9: Mesh sizes for independence study case 1

	Case 1 A	**Case 1 B**	**Case 1 C**	**Case 1 D**
Air flow field base size	27.8 [mm]	13.9 [mm]	7.00 [mm]	5.00 [mm]
Pipe network base size	4.36 [mm]	2.18 [mm]	1.09 [mm]	1.09 [mm]
Number of increments (discretized per Pipe/Heat transfer element)	5	10	20	20

The results obtained from the coupled 1-D/3-D approach and the full 3-D modelling approach for case 1A to case 1D after convergence criteria (residuals < $1e^{-05}$) were achieved, are shown in **Table 10** and **Table 11** respectively.

Table 10: Coupled 1-D/3-D modelling approach results for Case 1A – Case 1-D

	Case 1A	**Case 1B**	**Case 1C**	**Case 1D**
Outputs	**Value**	**Value**	**Value**	**Value**
Number of Iterations (Global)	771	982	1290	1608
Number of Iterations for convergence	783	995	1302	1624
Number of cells (model size)	85 052	399 174	1 255 896	3 727 026
Computational Time	2 349 [s]	2 985 [s]	4 167 [s]	5 968 [s]
Water Outlet Temperature	47.13 [°C]	46.48 [°C]	45.25 [°C]	45.25 [°C]
Temperature Difference (Water inlet and outlet)	2.87 [°C]	3.52 [°C]	4.75 [°C]	4.75 [°C]

A maximum 5 % temperature difference was shown in the coupled 1-D/3-D modelling approach compared to that of the full 3-D CFD analysis. In addition, the coupled 1-D/3-D modelling technique is less resource intensive as a reduction in solution time of 36.5% and model size of 26% was achieved.

Table 11: Full 3-D modelling results for Case 1A- Case 1-D

	Case 1A	**Case 1B**	**Case 1C**	**Case 1D**
Outputs	**Value**	**Value**	**Value**	**Value**
Number of Iterations (Global)	N.A.	N.A.	N.A.	N.A.
Number of Iterations for convergence	1053	1705	1874	2030
Number of cells (model size)	118 123	538 067	1 744 312	4 827 302
Computational Time	3 686 [s]	5 660	6 559 [s]	7 126 [s]
Water Outlet Temperature	46.49 [°C]	45.26 [°C]	45.01 [°C]	44.92 [°C]
Temperature Difference (Water inlet and outlet)	2.87 [°C]	4.74 [°C]	4.99 [°C]	5.08 [°C]

Figure 23 illustrates the outlet water temperature as a function against the number of iterations to convergence for the coupled 1-D/3-D modelling approach. As soon as the information transfer between the different solvers (Flownex and Fluent) initialized, (in which a heat flux from Fluent is transferred to the Flownex pipe sub elements) the outlet water temperature decreases. The coupled 1-D/3-D modelling approach quickly resolves the numerical discrepancy.

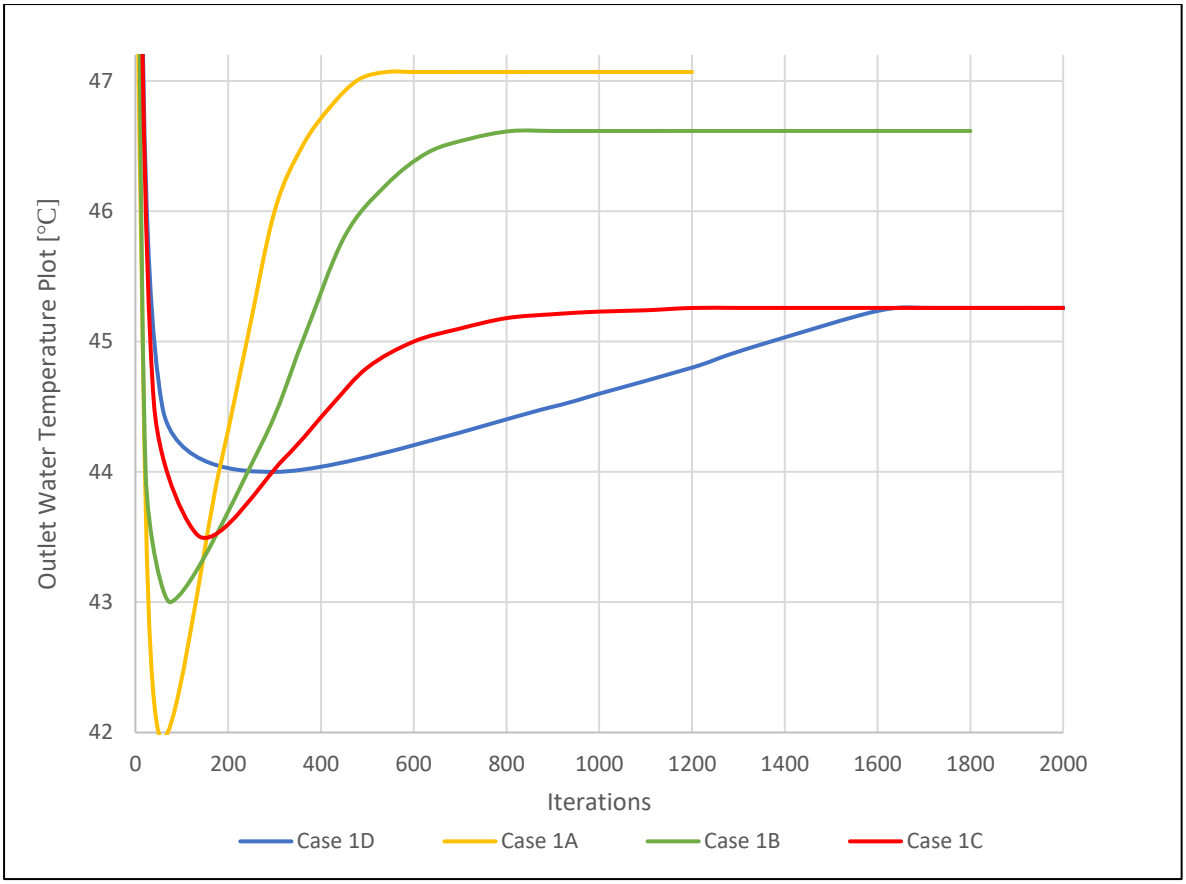

Figure 23: Outlet water temperature plot for the Coupled 1-D/3-D modelling approach (Case 1A – Case 1-D)

Figure 24 illustrates the water outlet temperature for the full 3D modelling approach for the test case 1A to 1D. A cross sectional area-averaged temperature was monitored at the outlet of the tube bundle.

Note this temperature boundary condition could be increased to reduce the solving time, but since this boundary condition of 300 [K] was patched in the coupled 1-D/3-D modelling approach the same principle and modelling procedure should be implemented in the full 3-D simulation.

The temperature decreases and then increases as the flow field develops through the pipe network until acceptable convergence criteria (residuals < $1e^{-05}$) is reached.

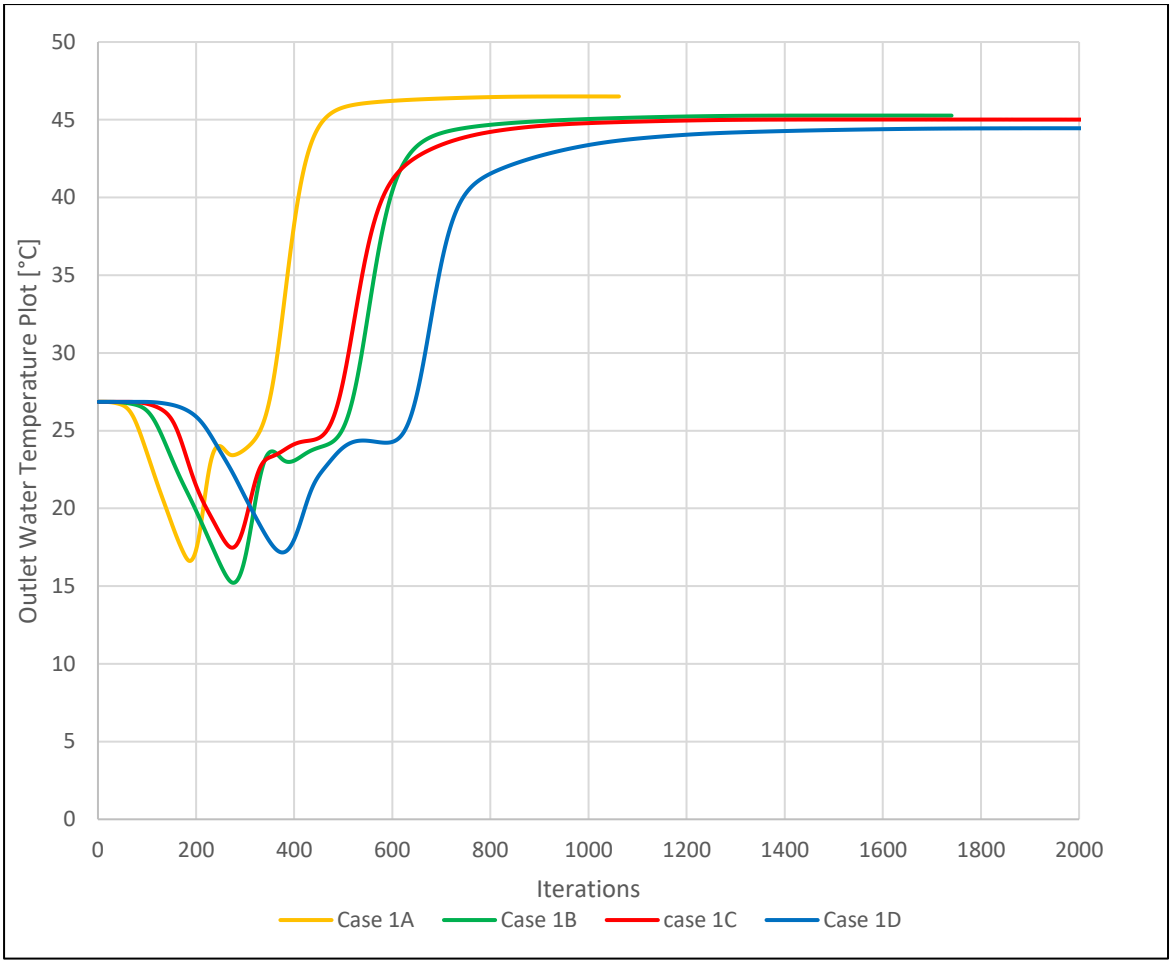

Figure 24: Outlet water temperature plot for the full 3D modelling approach (Case 1A – Case 1-D)

The energy balance was defined and programmed as the net energy available after heat transfer between the air and the water inside the pipe-network had occurred.

Note: Refer to **Appendix A** for an illustration of the flow field development

Figure 25 illustrates the energy balance for Case 1A. Up to the point where the temperature front had propagated through the entire pipe network, the temperature and consequently the heat transfer from the water to air was out of balance. This resulted in the fluctuations seen in the energy plot. At around 520 iterations the flow field stabilized, there after the heat transfer and temperature gradient started to achieve steady state conditions. At around 700 iterations energy exchange stabilized and therefore the outlet water temperature can start to converge.

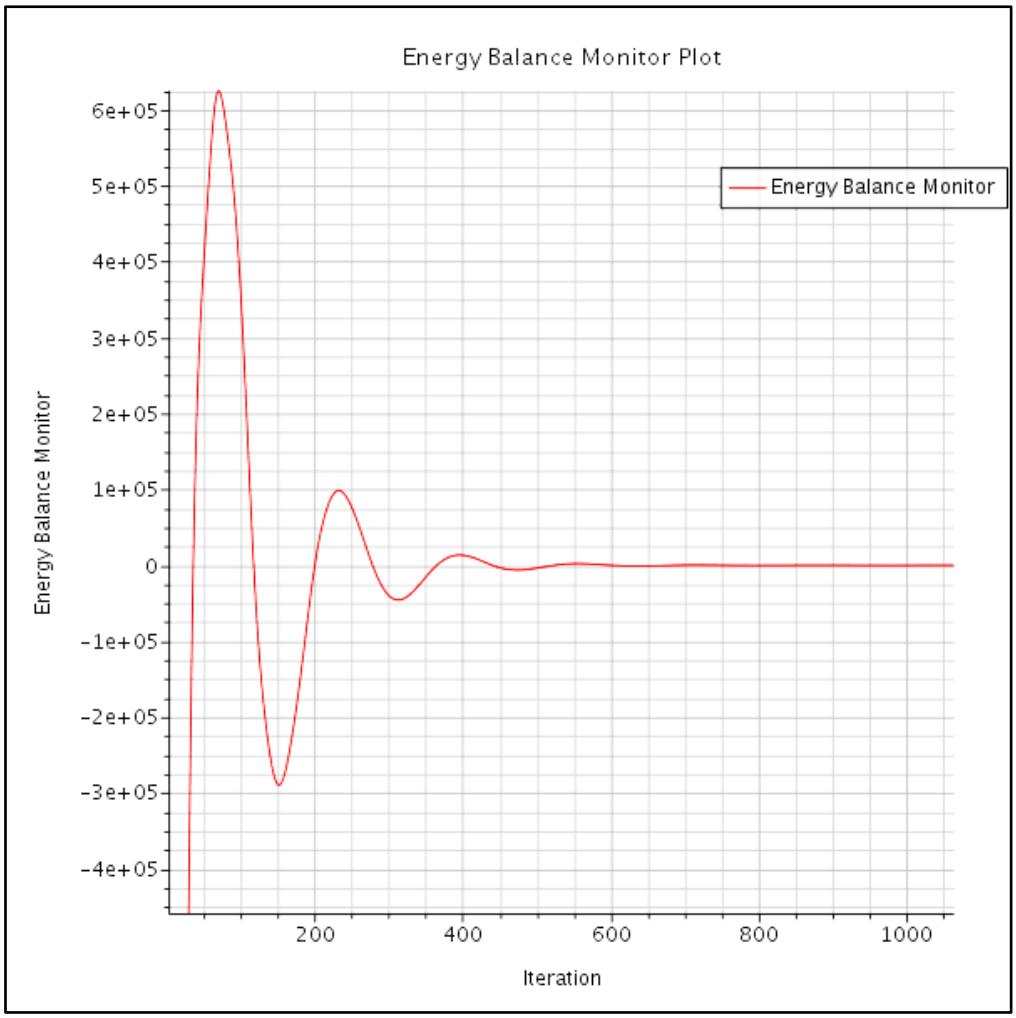

Figure 25: Energy Balance for Case 1A as a function of the iteration number for the full 3-D modelling approach

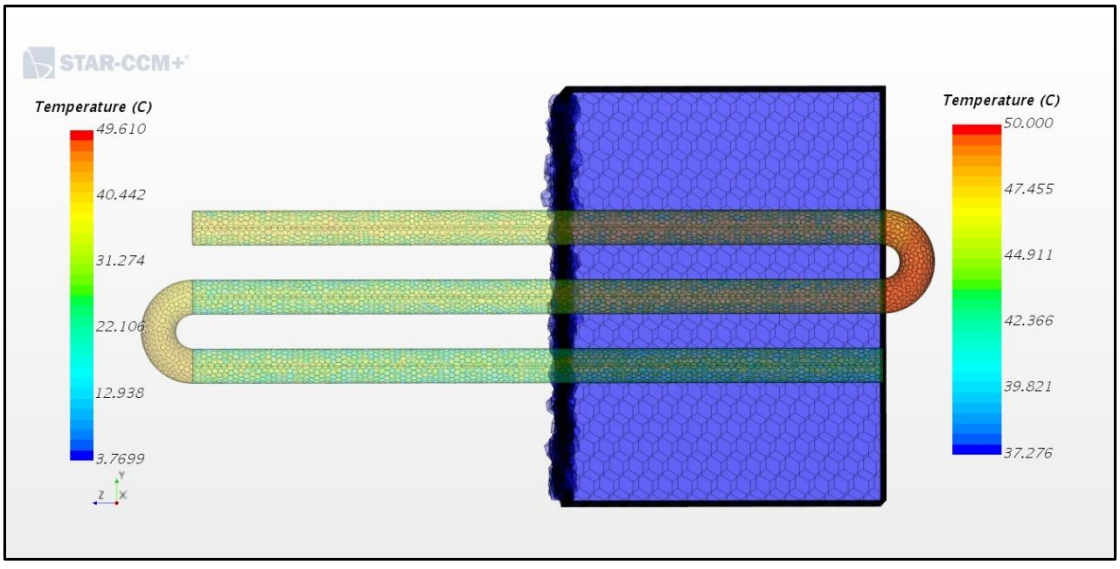

Figure 26: Temperature distribution for the full 3-D modelling for case 1A after convergence

Figure 26 illustrates the temperature distribution after convergence was achieved. The right axis represents the temperature distribution within the pipe bundle and the left axis represent the temperature distribution across the outer air-flow field.

It is evident from **Figure 23** that the mesh utilized in case 1C provides accurate and mesh independent results while achieving steady state conditions in fewer iterations than the mesh utilized in case 1D (finest mesh explored in the study). Therefor Case 1C was used in the input variation sensitivity analyses.

Input variation sensitivity analyses:

Case 1C was used as the base test case for the input variation sensitivity analyses. The input specifications as listed in **Table 3** as well as the meshing- and solutions strategies stated in section **5.1** applies to Case 1E through to Case 1G. However, the mass flow rates, and air flow velocity was altered.

The effect of these changed specifications was examined in the coupled 1-D/3-D modelling approach as well as the full 3-D CFD approach.

The changed input specifications for case 1E to case 1G are shown in **Table 12** below.

Table 12: Input specification variation for case 1

	Case 1E	**Case 1F**	**Case 1G**
Air flow field base size	7.00 [mm]	7.00 [mm]	7.00 [mm]
Pipe network base size	1.09 [mm]	1.09 [mm]	1.09 [mm]
Number of increments (Pipe/Heat transfer Element)	20	20	20
Air flow velocity	15.86 [m/s]	15.86 [m/s]	20 [m/s]
Water mass flow rate	0.025 [kg/s]	0.01 [kg/s]	0.01 [kg/s]

The results obtained for the full 3-D CFD modelling approach and the coupled 1-D/3-D modelling approach is listed in **Table 14** and **Table 13** respectively.

Table 13: Coupled 1-D/3-D modelling approach results for Case 1E – Case 1-G

	Case 1E	**Case 1F**	**Case 1G**
Outputs	**Value**	**Value**	**Value**
Number of Iterations (Global)	1698	2070	2089
Number of Iterations for convergence	1720	2093	2109
Number of cells (model size)	1 255 896	1 255 896	1 255 896
Computational Time	5 332 [s]	6 489 [s]	6 538 [s]
Water Outlet Temperature	40.49 [°C]	30.90 [°C]	29.35 [°C]
Temperature Difference (Water inlet and outlet)	9.51 [°C]	19.1 [°C]	20.65 [°C]

The water outlet temperature plots for the coupled 1-D/3-D modelling approach for case 1E and Case 1F (water mass flow rate was altered) are illustrated in **Figure 27** while the results for Case 1G (air flow velocity was altered) are shown in **Figure 28**. From **Figure 27** it can be seen that by reducing the mass flow rate of the water in the pipe network, the heat transfer capability of the bare tube configuration is increased, resulting in an increased temperature difference between the inlet and outlet water temperatures.

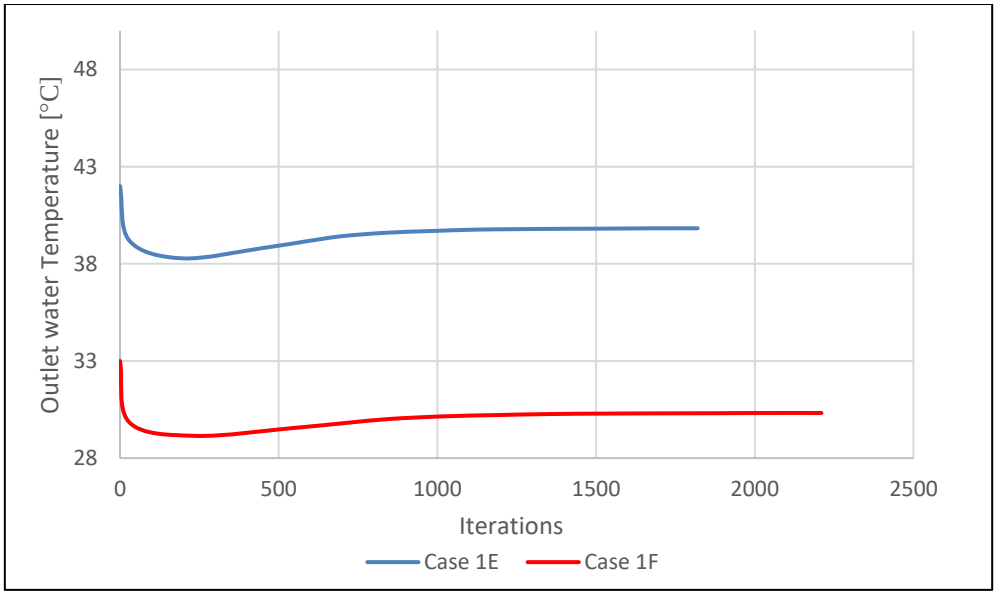

Figure 27: Outlet water temperature plot for the Coupled 1-D/3-D modelling approach (Case 1E – Case 1-F)

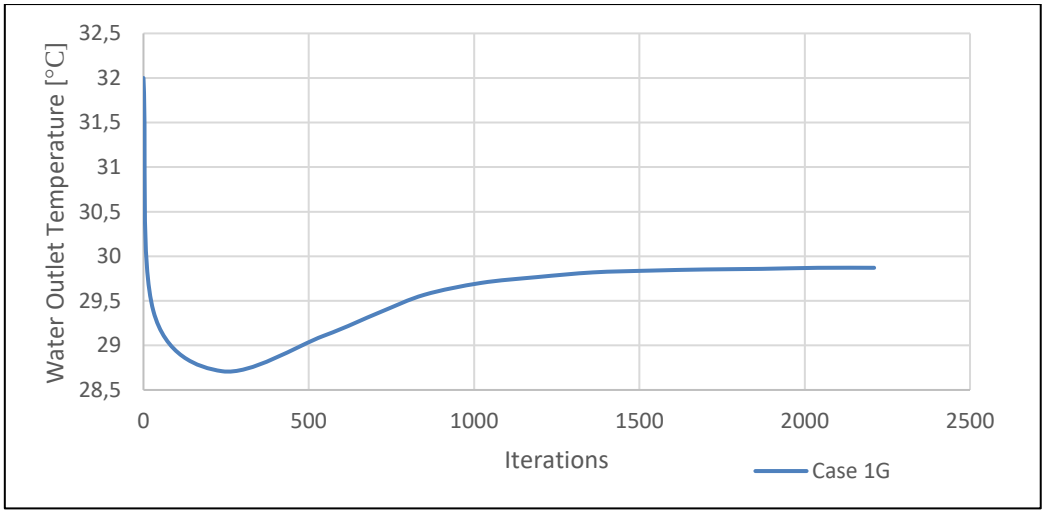

Figure 28: Outlet water temperature plot for the Coupled 1-D/3-D modelling approach (Case 1F)

It can be seen from **Figure 27** and **Figure 28**, that the nature of the coupled 1-D/3-D simulated water temperatures follows the same transient trend as that observed in the mesh independence study. The same claims regarding information transfer can thus be made (refer to **Figure 23**).

Table 14 represent the results obtained for the full 3-D CFD modelling of the input specifications sensitivity analyses.

Table 14: Full 3-D modelling results for Case 1E- Case 1-G

	Case 1E	**Case 1F**	**Case 1G**
Outputs	**Value**	**Value**	**Value**
Number of Iterations (Global)	N.A.	N.A.	N.A.
Number of Iterations for convergence	2346	2771	2775
Number of cells (model size)	1 744 312	1 744 312	1 744 312
Computational Time	8 211 [s]	9 699 [s]	9 680 [s]
Water Outlet Temperature	40.79 [°C]	31.20 [°C]	29.66 [°C]
Temperature Difference (Water inlet and outlet)	9.21 [°C]	18.8 [°C]	20.34 [°C]

Figure 29 and **Figure 30** illustrates the outlet water temperature plot for the full 3-D CFD modelling approach for the cases 1E – 1G. A cross sectional area-average temperature was taken at the exit of the pipe network, resulting in the values seen in the figures. The before mentioned solution strategy was applied to these cases and similar conclusions regarding the temperature boundary conditions (300 [K]), can be made to explain the outlet water temperature stabilization phase.

The temperature decreases as the flow field develops through the pipe network until acceptable convergence criteria (residuals < $1e^{-05}$) were reached. Additional convergence criteria involved monitoring the energy balance and ensuring values close to zero were reached.

Note: Plots illustrating energy balance and water temperature distribution for the input specification analyses can be found in **Appendix B**.

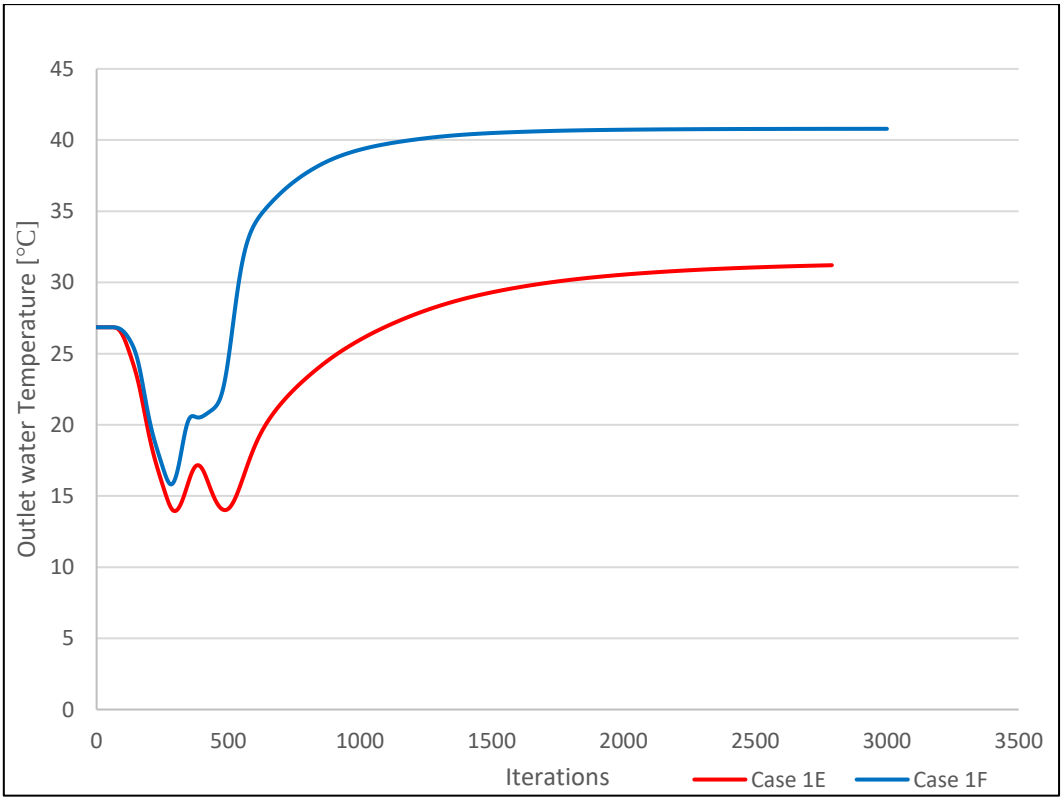

Figure 29: Outlet water temperature plot for the full 3D modelling approach (Case 1E– Case 1-F)

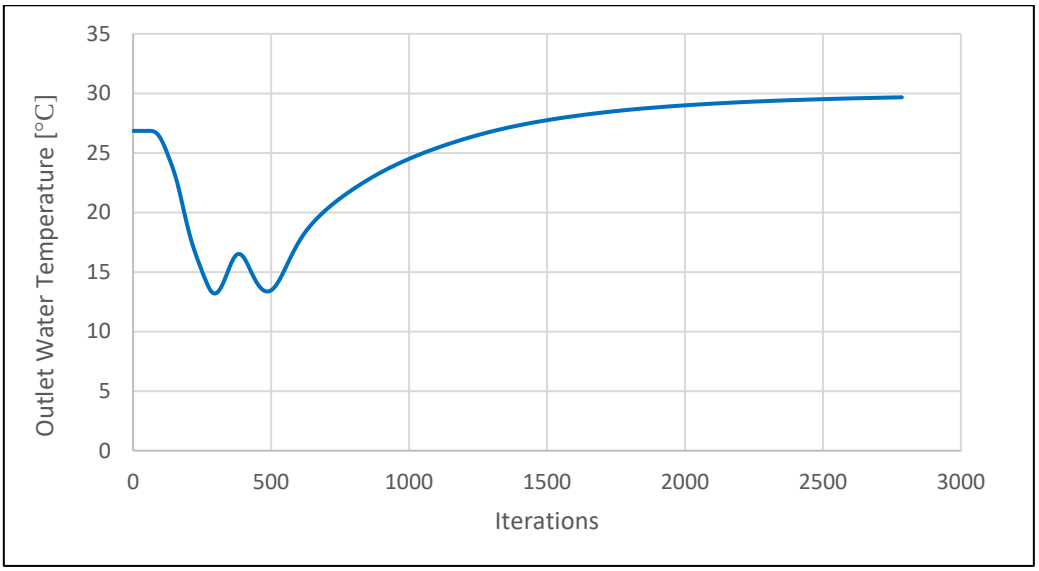

Figure 30: Outlet water temperature plot for the full 3D modelling approach (Case 1G)

5.2.1.3 Results

A results comparison between the coupled 1-D/3-D and a full 3-D modelling approach for the perpendicular flow (x-Axis) 3 Pipe ACHE configuration will be discussed below.

Mesh Independence:

As case 1C provides accurate and mesh independent results a comparison between the results obtained for the coupled 1-D/3-D and full 3-D modelling approach is made in regards to case 1C and is shown in **Table 15**.

The coupled 1-D/3-D modelling approach shows a 5 % temperature difference compared to that of the full 3-D CFD analysis for Case 1C. In addition, the coupled 1-D/3-D modelling technique is less resource intensive as a reduction in solution time of 36.5% and model size of 26% was achieved.

Table 15: Results comparison for Case 1C

Outputs	**Coupled 1-D/3-D**	**Full 3 D CFD**	**Difference in reference to the full 3D CFD model**
Number of Iterations (Global)	1290	N.A.	N.A.
Number of Iterations for convergence	1302	1874	30 %
Number of cells (model size)	1 255 896	1 744 312	26 %
Computational Time	4 167 [s]	6 559 [s]	36.5 %
Water Outlet Temperature	45.25 [°C]	45.01 [°C]	0.24 [°C]
Temperature Difference (Water inlet and outlet)	4.75 [°C]	4.99 [°C]	5%

Input variation sensitivity analyses:

A Result comparison for the input variation sensitivity analyses is shown in **Table 16** to**Table 18**.

Table 16: Results comparison for Case 1E

Outputs	**Coupled 1-D/3-D**	**Full 3 D CFD**	**Difference in reference to the full 3D CFD model**
Number of Iterations (Global)	1698	N.A.	N.A.
Number of Iterations for convergence	1720	2346	27%
Number of cells (model size)	1 255 896	1 744 312	26%
Computational Time	5 332 [s]	8 211 [s]	35%
Water Outlet Temperature	40.49 [°C]	40.79 [°C]	0.3[°C]
Temperature Difference (Water inlet and outlet)	9.51 [°C]	9.21 [°C]	3%

Table 17: Results comparison for Case 1F

Outputs	**Coupled 1-D/3-D**	**Full 3 D CFD**	**Difference in reference to the full 3D CFD model**
Number of Iterations (Global)	2070	N.A.	N.A.
Number of Iterations for convergence	2093	2771	24.5%
Number of cells (model size)	1 255 896	1 744 312	26%
Computational Time	6 489 [s]	9 699 [s]	33%
Water Outlet Temperature	30.90 [°C]	31.20 [°C]	0.3[°C]
Temperature Difference (Water inlet and outlet)	19.1 [°C]	18.8 [°C]	1.5%

Table 18 Results comparison for Case 1G

Outputs	**Coupled 1-D/3-D**	**Full 3 D CFD**	**Difference in reference to the full 3D CFD model**
Number of Iterations (Global)	2089	N.A.	N.A.
Number of Iterations for convergence	2109	2775	24%
Number of cells (model size)	1 255 896	1 744 312	26%
Computational Time	6 538 [s]	9 680 [s]	32%
Water Outlet Temperature	29.35 [°C]	29.66 [°C]	0.31[°C]
Temperature Difference (Water inlet and outlet)	20.65 [°C]	20.34 [°C]	1.5%

In all these cases (Case 1E to Case 1G) the same meshing principles and mesh sizing was implemented, therefor the model size reduction of 26 % can be noted across these case variations. A maximum temperature difference of 3 % was observed when comparing the two different solving techniques to each other.

For the variation of input specifications, the coupled 1-D/3-D numerical modelling approach was found to reduce the solution time by around 33 %.

5.2.2 Case 2: Parallel flow (y-Axis) 3 Pipe ACHE configuration

5.2.2.1 Overview

Case 2 is similar to case 1 as described in section **5.2.1.** Water enters the top pipe element at a temperature of 50 [°C] and a pressure of 140 [kPa]. In **Figure 31** the meshed geometric representation of the bare tube configuration within the airflow field is shown. It can be seen that the origin of the air moved over the pipe network or tube bundle differs from that in case 1. In case 2, the origin of the air being "forced" over the tubes is parallel to the pipes (y-axis) i.e. from the top into the control volume. The boundary conditions associated with the airflow field are also shown in the figure. The outlet pressure boundary was at the bottom of the control volume and the velocity inlet boundary was at the top plane (Flow direction).

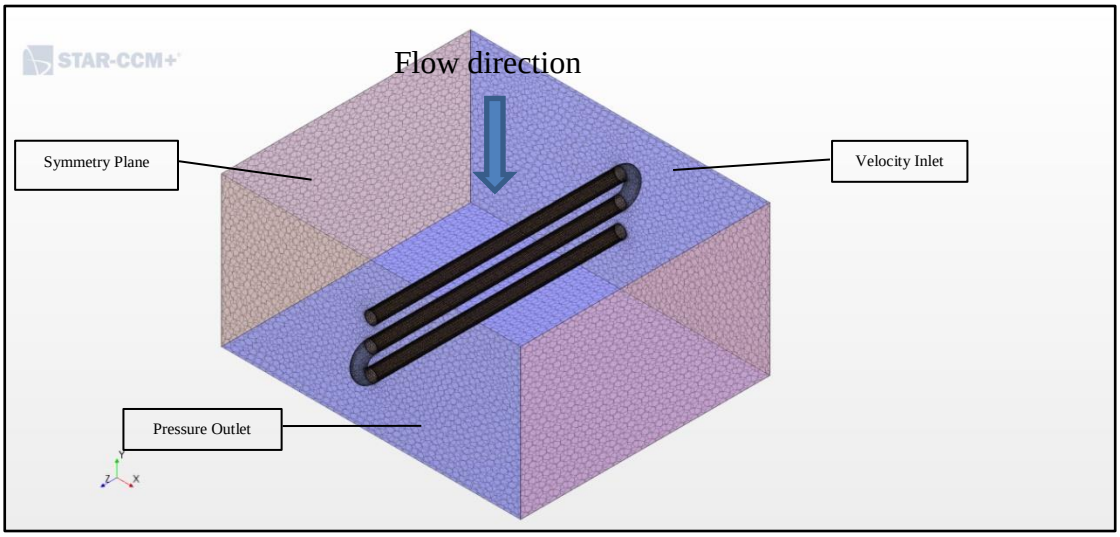

Figure 31: Meshed Geometric representation of the Parallel flow (y-Axis) 3 Pipe ACHE configuration

The coupled 1-D/3-D modelling approach associated with case 2 is shown in **Figure 32**, the coupling procedure used and the information transferred between the different solvers was similar to that described in **Table 5** and section **4.2**.

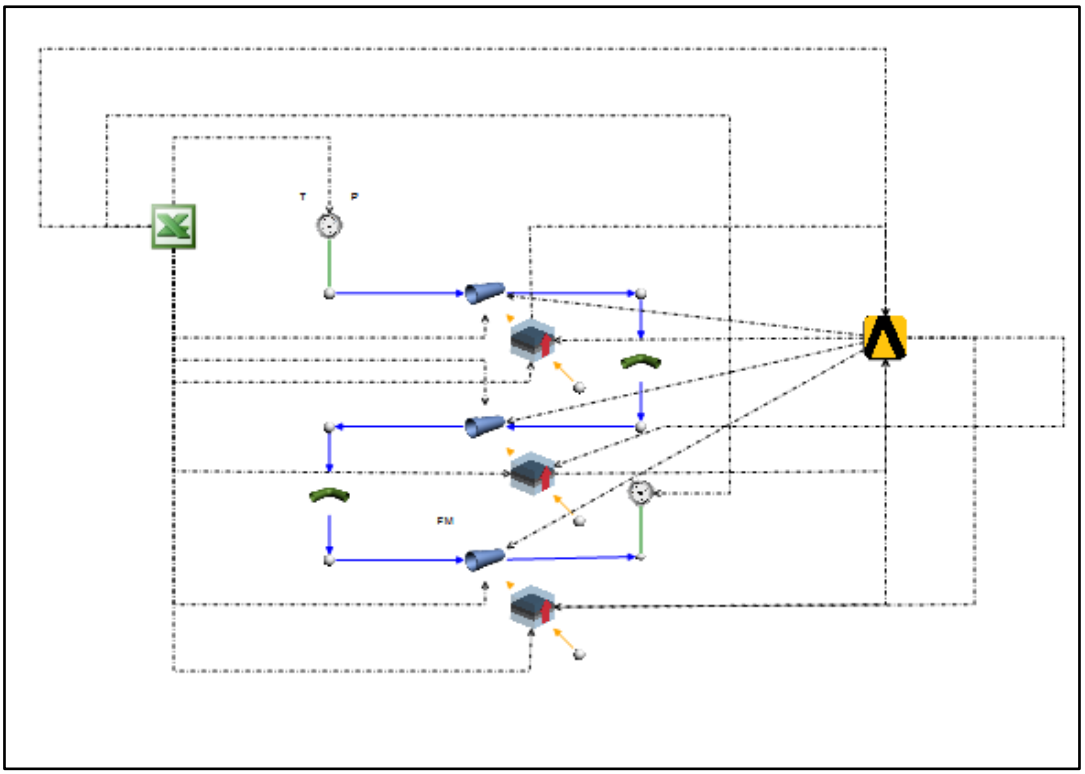

Figure 32: Schematic representation of the data transfer links between Flownex and Fluent for the Perpendicular flow (x-Axis) 3 Pipe ACHE configuration

5.2.2.2 Results

Case 2 was a variation from Case 1G (The origin of the air flowing over the tube bundle was along the y-axis in case 2 instead of the x-axis as in case 1). Case 2 was simulated using the input specifications as listed in **Table 3**. The mass flow rate of the water entering the top pipe element is 0.01 [kg/s] and the magnitude of the airflow field velocity is 20 [m/s]. The meshing- and solutions strategies were applied as specified in section **5.1.** The mesh size associated with case 1C was also implemented in case 2.

A comparison between the results obtained for the coupled 1-D/3-D and full 3-D modelling approach is made with regards to Case 2 and is shown in **Table 19**.

Table 19: Results comparison for Case 2

Outputs	**Coupled 1-D/3-D**	**Full 3 D CFD**	**% Difference in reference to the full 3D CFD model**
Number of Iterations (Global)	2089	N.A.	N.A.
Number of Iterations for convergence	2109	2875	27 %
Number of cells (model size)	1 368 896	1 845 892	26 %
Computational Time	7 538 [s]	10 680 [s]	30 %
Water Outlet Temperature	29.38 [°C]	29.69 [°C]	0.31 [°C]
Temperature Difference (Water inlet and outlet)	20.62 [°C]	20.31 [°C]	1.5 %

For Case 2 the full 3-D CFD analysis showed an outlet water temperature difference of 1.5% when compared to the coupled 1-D/3-D numerical modelling approach. The same mesh sizing scheme was implemented in terms of base size for the pipe-network and air-flow as stated in **Table 9**. A reduction in model size of about 26 % was observed. A reduction in the computational time and number of iterations needed to achieve acceptable convergence criteria was also noted. The water temperature difference between the inlet and outlet of the pipe-network was computed to be 1.5 %, similar to that of case 1G. This is due to the fact that Case 2 is modelled around Case 1G.

Figure 33 shows the Outlet water temperature plot for the coupled 1-D/3-D modelling approach. The solution neared convergence at around 1790 iterations and eventually meeting the convergence criteria (residuals < $1e^{-05}$) at 2109 iterations. The converged solution yielded an outlet water temperature of 29.38 [°C].

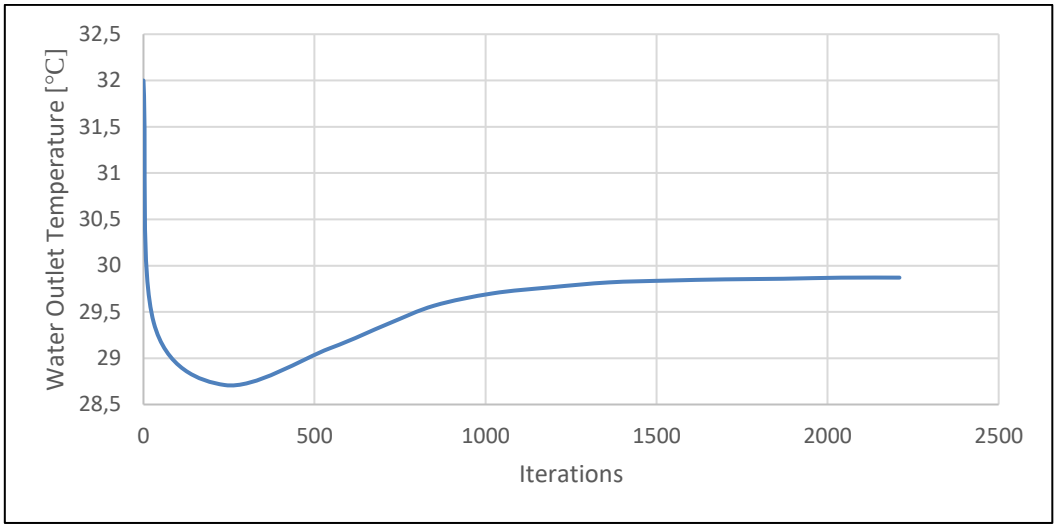

Figure 33: Outlet water temperature plot for the Coupled 1-D/3-D modelling approach (Case 2)

For the full 3-D CFD modelling of case 2, an outlet water temperature of 29.69 [°C] is recorded at 2875 iterations (see **Figure 34**). A scalar representation of the outlet water temperature (**Figure 34**) is depicted in **Figure 36**. The right axis represents the temperature distribution within the pipe bundle and the left axis represents the temperature distribution across the outer air-flow field.

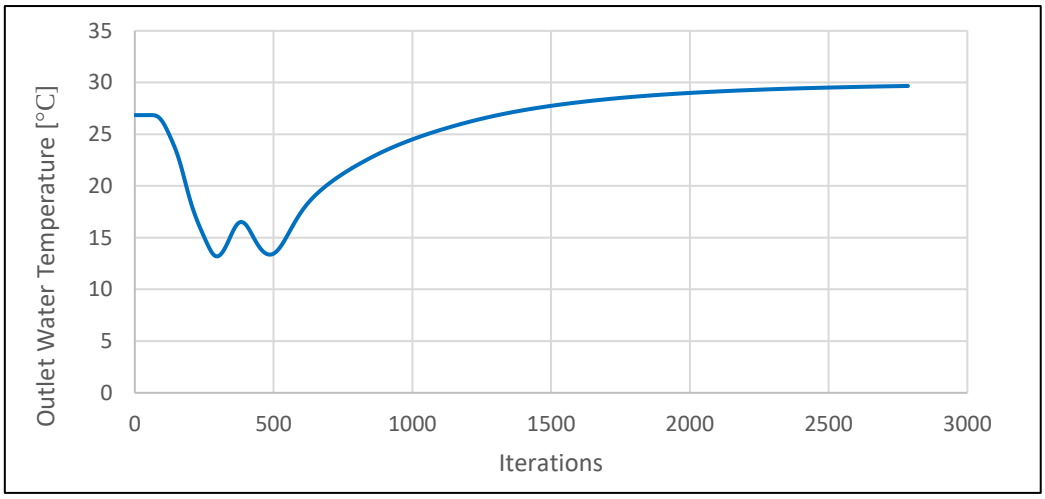

Figure 34: Outlet water temperature plot for the full 3D modelling approach (Case 2)

Figure 35 illustrates the energy balance as a function of iteration for Case 2. The fluctuations seen in the energy plot was due to the temperature front still numerically propagating throughout the pipe network. The temperature and consequently the heat transfer from the water to air were out of balance as a result. The flow field stabilized, at around 1200 iterations where after the heat transfer and temperature gradient started to achieve steady state conditions.

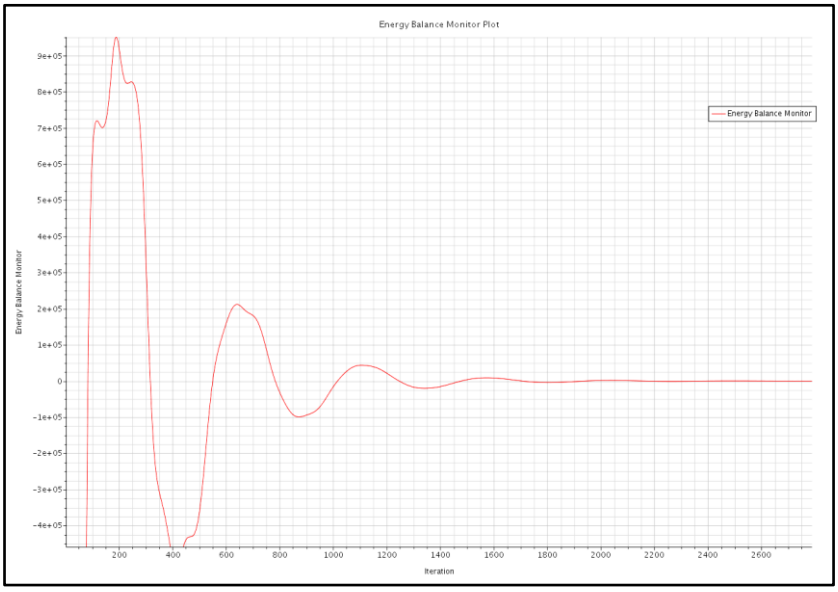

Figure 35: Energy Balance for Case 2 as a function of the iteration number for the full 3-D modelling approach

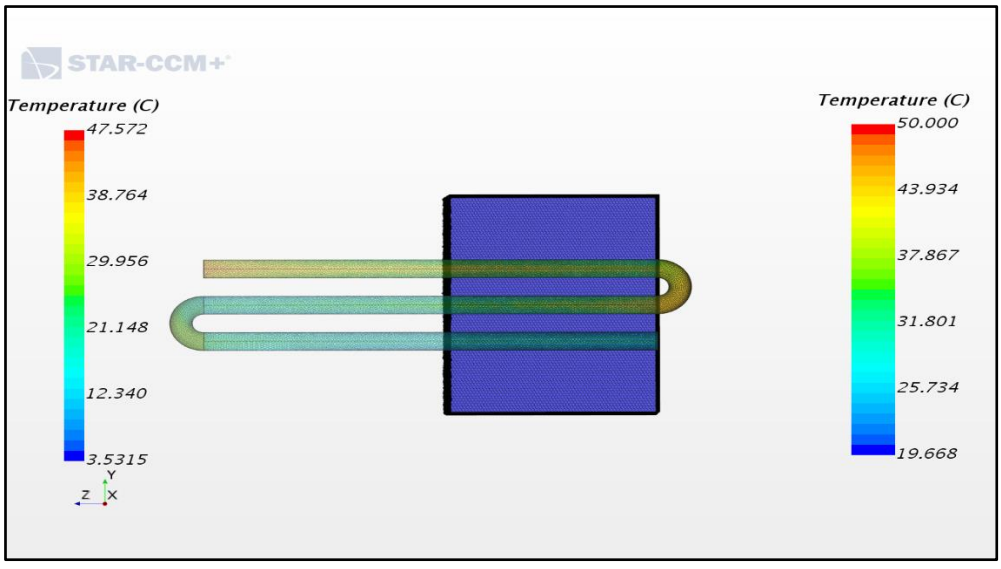

Figure 36: Temperature distribution for the full 3-D modelling for case 2 after convergence

5.2.3 Case 3: Perpendicular flow (x-Axis) 6 Pipe ACHE configuration

5.2.3.1 Overview

The perpendicular flow 6 pipe ACHE configuration consists of an integrated Flownex and Fluent model. The configuration consists of 2 triple pass bare tube/pipe- networks immersed in an air flow domain. Water (as the process fluid) enters both the front- and back- top pipe element at a temperature and pressure of 50 [°C] and 140 [kPa] respectively.

Figure 37 illustrates a geometric representation of the 6-pipe air-cooled heat exchanger configuration.

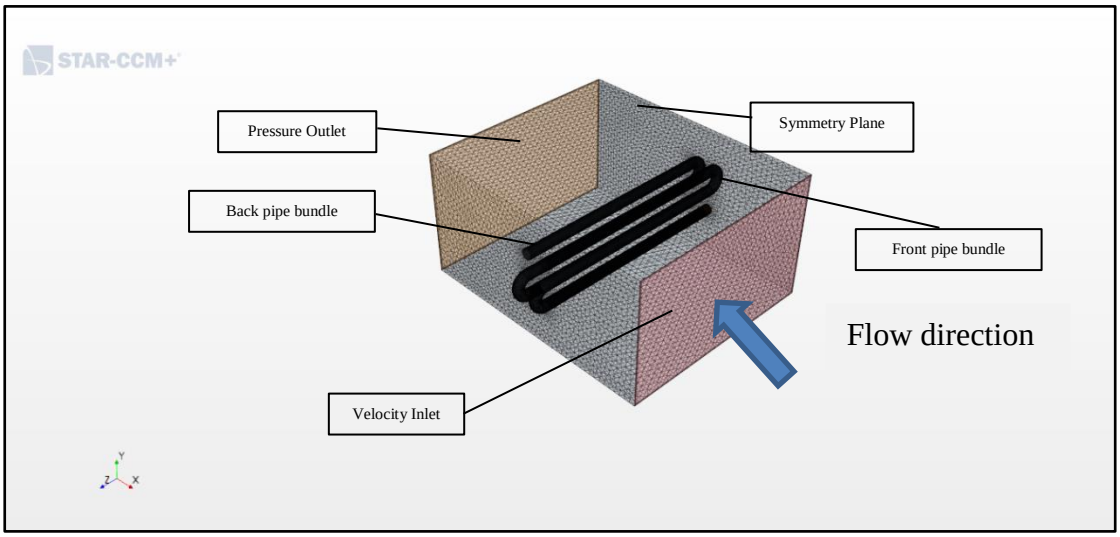

Figure 37: Meshed Geometric representation of the Perpendicular flow (x-Axis) 6 Pipe ACHE configuration.

Figure 38, is a schematic representation of the coupled 1-D/3-D modelling approach associated with case 3 and the data transfer links between the different solvers are shown. Information transfer is done in a similar manner to that to that described in **Table 5** and section **4.2**.

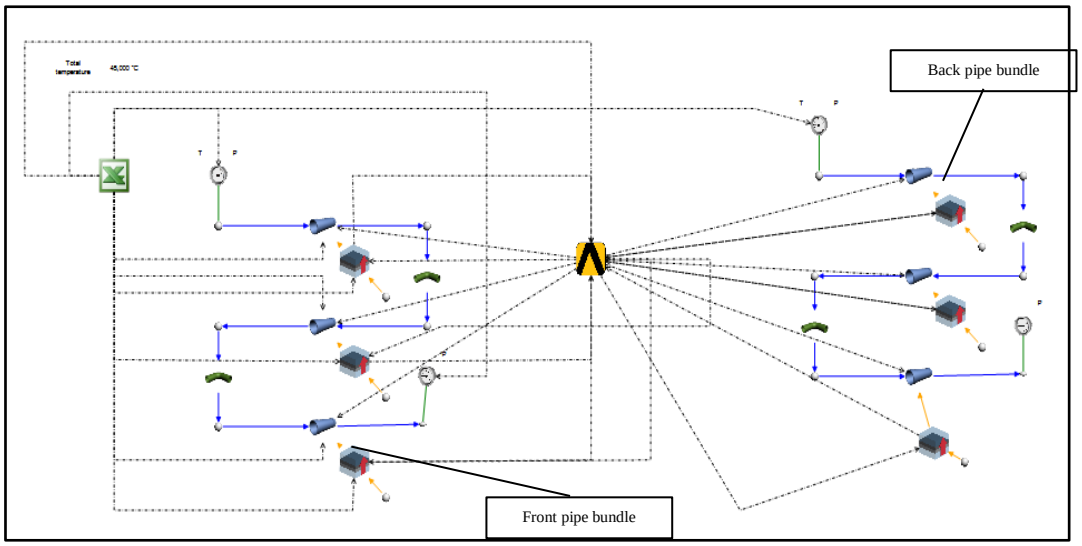

Figure 38: Schematic representation of the data transfer links between Flownex and Fluent for the Perpendicular flow (x-Axis) 6 Pipe ACHE configuration

5.2.3.2 Case 3 Investigation

Case 3 was handled in the same way as Case 1. A base test case was simulated using the input specifications as listed in **Table 3**. The mass flow rates of the water entering both the front- and back- top pipe element is 0.05 [kg/s] and the magnitude of the airflow field velocity is assumed to be 15.86 [m/s]. The meshing- and solutions strategies were applied as specified in section **5.1.**

The following results were obtained from the coupled 1-D/3-D modelling approach and full 3-D modelling approach are shown in **Table 20** and **Table 21** respectively.

Table 20: Coupled 1-D/3-D modelling approach results for the test base case (x-Axis) 6 Pipe ACHE configuration

Outputs	**Value**
Number of Iterations (Global)	2002
Number of Iterations for convergence	2016
Number of cells (model size)	155 974
Computational Time	6 451[s]
Water Outlet Temperature (Front Pipe Bundle)	42.80[°C]
Water Outlet Temperature (Back Pipe Bundle)	45.32 [°C]

Table 21: Full 3-D modelling results for the test base case (x-Axis) 6 Pipe ACHE configuration

Outputs	**Value**
Number of Iterations (Global)	N.A.
Number of Iterations for convergence	2957
Number of cells (model size)	227 544
Computational Time	9 462 [s]
Water Outlet Temperature (Front Pipe Bundle)	44.58 [°C]
Water Outlet Temperature (Back Pipe Bundle)	46.43[°C]

Mesh Independence:

Case 3 A was a test base case. The same input specifications were used, with different mesh sizes in order to perform a mesh independence study. The base sizes used in the mesh independence study are shown in **Table 22**. Refinement and cell relevance changes were made in the Fluent-mesher to ensure the Star-CCM+ and Fluent meshes can be directly compared. The reduction in model size seen in the coupled 1-D/3-D numerical model is due to the omission of the cells associated with the meshing of the pipe-networks. The same level of discretization used in Case 1C was applied to Case 3.

Table 22: Mesh sizes for independence study case 3

	Case 3 A	**Case 3 B**	**Case 3 C**
Air flow field base size	27.8 [mm]	13.9 [mm]	7.00 [mm]
Pipe network base size	4.36 [mm]	2.18 [mm]	1.09 [mm]
Number of increments (discretized per Pipe/Heat transfer element)	20	20	20

Table 23 and **Table 24** contain the results for the coupled 1-D/3-D and full 3-D modelling approach, for the test cases 3A to 3C respectively.

Table 23: Coupled 1-D/3-D modelling approach results for Case 3A – Case 3C

	Case 3A	**Case 3B**	**Case 3C**
Outputs	**Value**	**Value**	**Value**
Number of Iterations (Global)	2002	2348	3362
Number of Iterations for convergence	2016	2359	3373
Number of cells (model size)	155 974	847 689	3 597 532
Computational Time	6 451[s]	7 325[s]	8 593[s]
Water Outlet Temperature (Front Pipe Bundle)	42.80[°C]	41.65[°C]	41.77[°C]
Temperature Difference (Front Pipe Water inlet and outlet)	7.20 [°C]	8.35 [°C]	8.23 [°C]
Water Outlet Temperature (Back Pipe Bundle)	45.32 [°C]	43.52[°C]	43.43[°C]
Temperature Difference (Back Pipe Water inlet and outlet)	4.68 [°C]	6.48 [°C]	6.57 [°C]

Table 24: Full 3D modelling results for Case 3A – Case 3C

	Case 3A	**Case 3B**	**Case 3C**
Outputs	**Value**	**Value**	**Value**
Number of Iterations (Global)	N.A.	N.A.	N.A.
Number of Iterations for convergence	2957	3312	4339
Number of cells (model size)	227 544	1 177 338	4 861 475
Computational Time	9 462 [s]	10 965[s]	11 472[s]
Water Outlet Temperature (Front Pipe Bundle)	44.58 [°C]	42.94[°C]	42.28[°C]
Temperature Difference (Front Pipe Water inlet and outlet)	5.42 [°C]	7.06 [°C]	7.72 [°C]
Water Outlet Temperature (Back Pipe Bundle)	46.43[°C]	44.86[°C]	44.18[°C]
Temperature Difference (Back Pipe Water inlet and outlet)	3.57 [°C]	5.14 [°C]	5.82 [°C]

Figure 39 and **Figure 40** illustrates the outlet water temperature for the front and back pipe bundles respectively, as a function of the number of iterations to convergence for the coupled 1-D/3-D modelling approach.

Note: Case 3C nears mesh independent results. Mesh independence can be obtained by increasing the mesh size, however this was not possible due to computational restrictions.

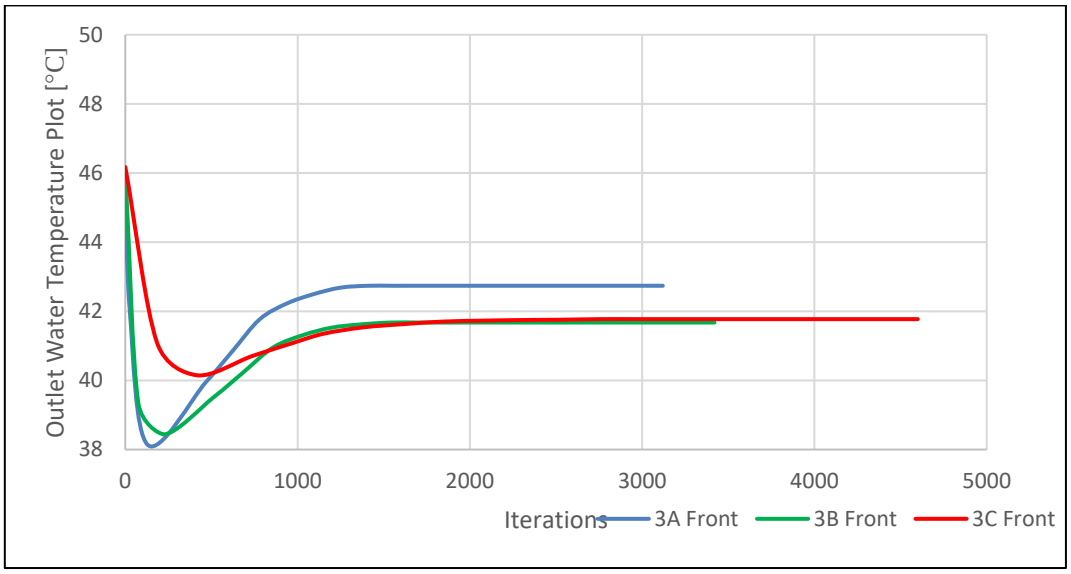

Figure 39: Front tube-bundle outlet water temperature plot for the coupled 1-D/3-D modelling approach (Case 3A-3C)

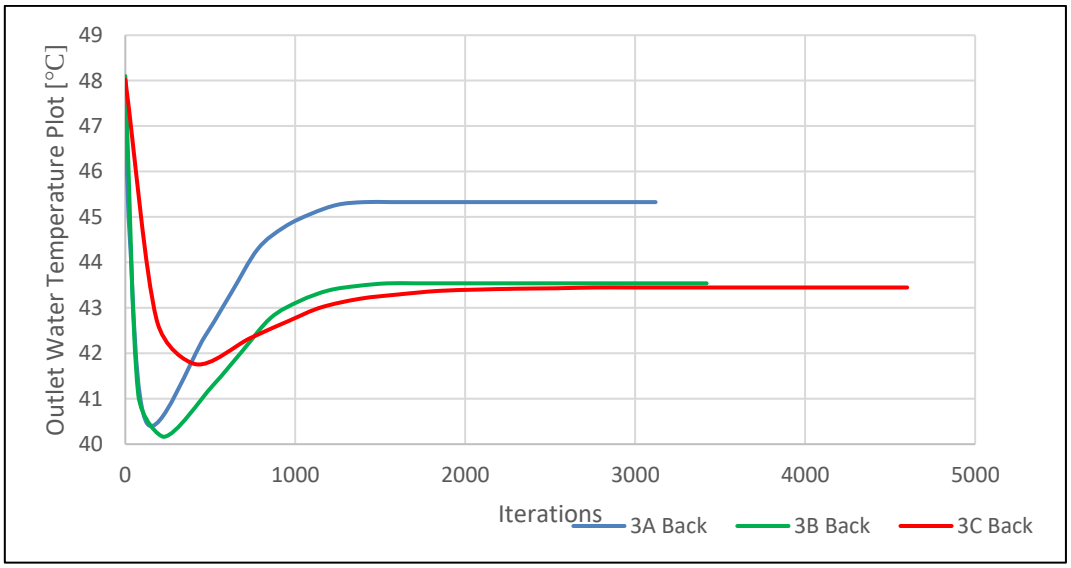

Figure 40: Back tube-bundle outlet water temperature plot for the coupled 1-D/3-D modelling approach (Case 3A-3C)

The full 3-D CFD outlet water temperature plot for the front- and back tube-bundles are shown in **Figure 41** and **Figure 42** respectively.

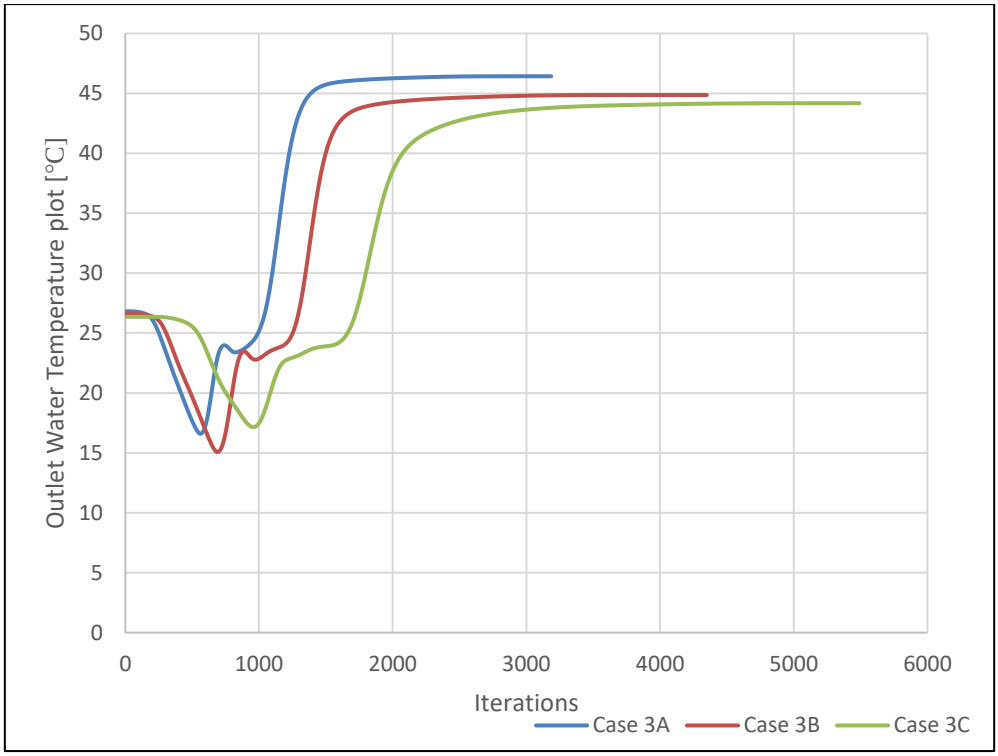

Figure 41: Front tube-bundle outlet water temperature plot for the full 3D modelling approach (Case 3A – Case 3C)

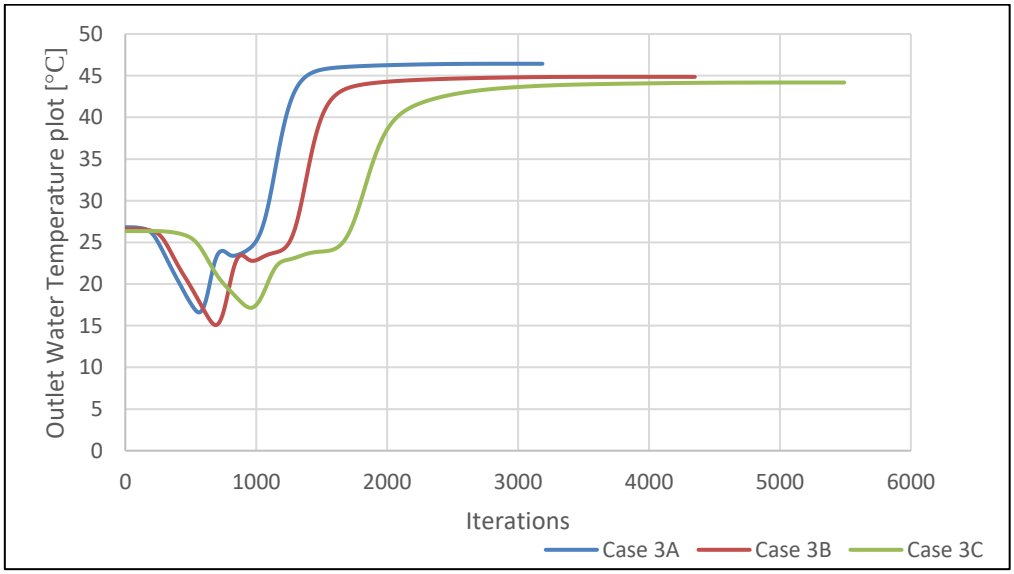

Figure 42: Back tube-bundle outlet water temperature plot for the full 3D modelling approach (Case 3A – Case 3C)

Input variation sensitivity analyses:

Case 3C was used as the base test case for the input variation sensitivity analyses.
For Case 3D and Case 3E, the mass flow rate of the water in both the front and back tube bundles were changed. The same meshing scheme and meshing size was implemented in these test cases. The effects of changing the mass flow rates were examined in both the full 3-D CFD approach as well as the coupled 1-D/3-D modelling approach. The properties of the water entering the respective tube bundles were kept at the same temperature and pressure as stated in **Table 3**.

The changed input specifications for Case 3D and Case 3E is shown in **Table 25**.

Table 25: Input specification variation for case 3

	Case 3D	**Case 3E**
Air flow field base size	7.00 [mm]	7.00 [mm]
Pipe network base size	1.09 [mm]	1.09 [mm]
Number of increments (pipe/heat transfer element)	20	20
Air flow velocity	15.86 [m/s]	15.86 [m/s]
Water mass flow rate	0.025 [kg/s]	0.01 [kg/s]

The coupled 1-D/3-D modelling approach for Case 3D and Case 3E yield the following results as shown in **Table 26**.

Table 26: Coupled 1-D/3-D modelling approach results for Case 3D and Case 3E

	Case 3D	**Case 3E**
Outputs	**Value**	**Value**
Number of Iterations (Global)	3382	3418
Number of Iterations for convergence	3399	3427
Number of cells (model size)	3 597 532	3 597 532
Computational Time	11 226 [s]	11 426 [s]
Water Outlet Temperature (Front Pipe Bundle)	35.93 [°C]	36.62 [°C]
Temperature Difference (Front Pipe Water inlet and outlet)	14.07 [°C]	13.38 [°C]
Water Outlet Temperature (Back Pipe Bundle)	28.84 [°C]	29.25 [°C]
Temperature Difference (Back Pipe Water inlet and outlet)	21.16 [°C]	20.75 [°C]

Figure 43 illustrate the outlet water temperature plot for the coupled 1-D/3-D modelling approach for Case 3D and Case 3E. As the mass flow rate decreases, the heat transfer capability increases, resulting in a higher temperature difference between the inlet and outlet water temperatures.

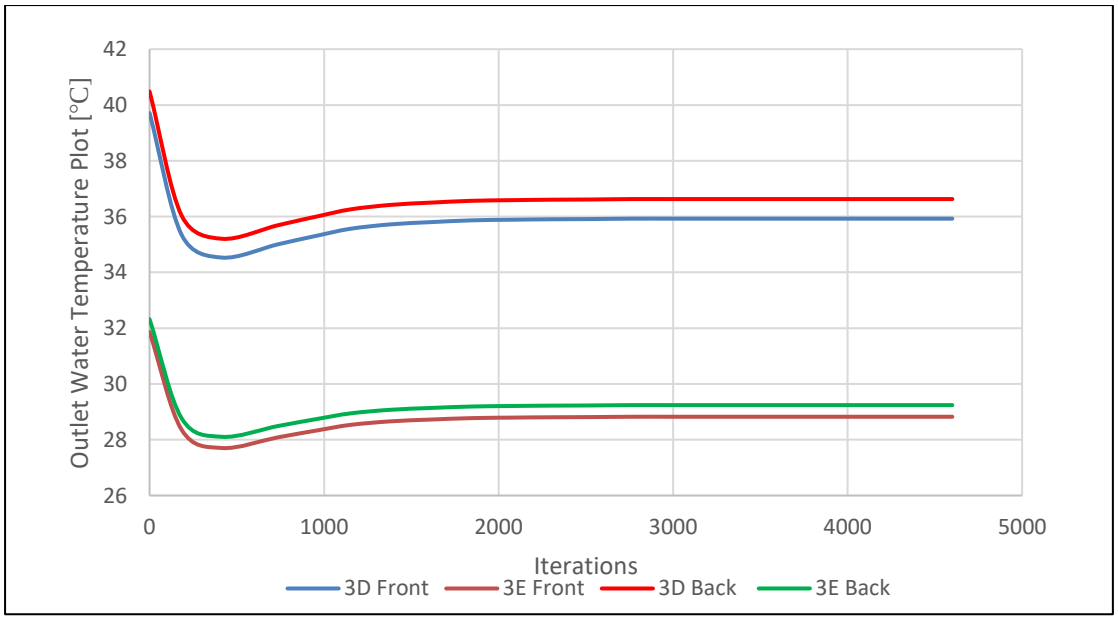

Figure 43: Outlet water temperature plot for the coupled 1-D/ 3-D modelling approach (Case 3D and Case 3E)

Table 27 represents the results obtained from the full 3-D CFD modelling approach for Case 3D and Case 3E.

Table 27: Full 3-D modelling results for Case 3D and Case 3E

	Case 3D	**Case 3E**
Outputs	**Value**	**Value**
Number of Iterations (Global)	N.A.	N.A.
Number of Iterations for convergence	4472	4497
Number of cells (model size)	4 861 475	4 861 475
Computational Time	15 657 [s]	15 836 [s]
Water Outlet Temperature (Front Pipe Bundle)	37.99 [°C]	36.36 [°C]
Temperature Difference (Front Pipe Water inlet and outlet)	12.01 [°C]	13.64 [°C]
Water Outlet Temperature (Back Pipe Bundle)	30.16 [°C]	29.17 [°C]
Temperature Difference (Back Pipe Water inlet and outlet)	19.84 [°C]	20.83 [°C]

For Case 3D and Case 3E the outlet water temperature as a function of iteration is illustrated in **Figure 44**.

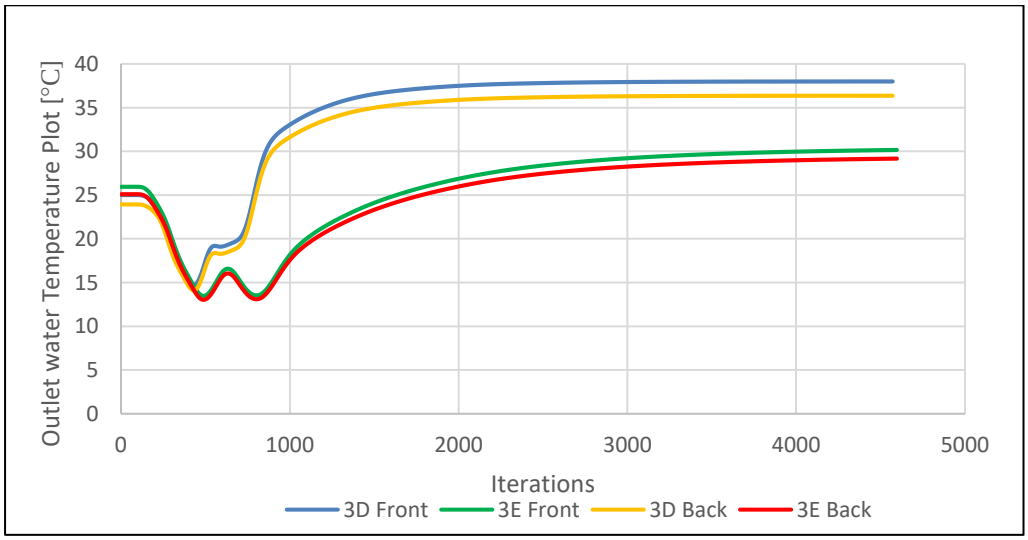

Figure 44: Outlet water temperature plot for the full 3-D CFD modelling approach (Case 3D and Case 3E)

5.2.3.3 Results

A results comparison between the coupled 1-D/3-D and a full 3-D modelling approach for the perpendicular flow (x-Axis) 6 Pipe ACHE configuration will be discussed below.

Table 28: Results comparison for Case 3C

Outputs	***Coupled 1-D/3-D***	***Full 3-D CFD***	***Difference in reference to the full 3D CFD model***
Number of Iterations (Global)	3362	N.A.	N.A.
Number of Iterations for convergence	3373	4339	32%
Number of cells (model size)	3 597 532	4 861 475	36%
Computational Time	8 593[s]	11 472[s]	25%
Water Outlet Temperature (Front Pipe Bundle)	41.77[°C]	42.28[°C]	0.51[°C]
Temperature Difference (Front Pipe Water inlet and outlet)	8.23 [°C]	7.72 [°C]	6%
Water Outlet Temperature (Back Pipe Bundle)	43.43[°C]	44.18[°C]	0.75[°C]
Temperature Difference (Back Pipe Water inlet and outlet)	6.57 [°C]	5.82 [°C]	11%

The outlet water temperature for the coupled 1-D/3-D modelling approach shows a 6% difference in temperature for the front tube bundle and an 11% temperature difference when compared to the full 3-D CFD analysis. In addition, the coupled 1-D/3-D modelling technique is less resource intensive as a reduction in solution time of 26% and model size of 36% was achieved.

Table 29: Results comparison for Case 3D

Outputs	***Coupled 1-D/3-D***	***Full 3-D CFD***	***Difference in reference to the full 3D CFD model***
Number of Iterations (Global)	3382	N.A.	N.A.
Number of Iterations for convergence	3399	4472	24%
Number of cells (model size)	3 597 532	4 861 475	36%
Computational Time	11 226 [s]	15 657 [s]	29%
Water Outlet Temperature (Front Pipe Bundle)	35.93 [°C]	37.99 [°C]	2.06[°C]
Temperature Difference (Front Pipe Water inlet and outlet)	14.07 [°C]	12.01 [°C]	14%
Water Outlet Temperature (Back Pipe Bundle)	28.84 [°C]	30.16 [°C]	1.32 [°C]
Temperature Difference (Back Pipe Water inlet and outlet)	21.16 [°C]	19.84 [°C]	6%

It is clear that the coupled 1-D/3-D numerical modelling approach is less resource intensive than the full 3-D CFD approach. A sizable difference in model size and computational time can be seen. A maximum temperature difference (ΔT) of 14% was recorded in the front tube bundle.

Table 30: Results comparison for Case 3E

Outputs	***Coupled 1-D/3-D***	***Full 3-D CFD***	***Difference in reference to the full 3D CFD model***
Number of Iterations (Global)	3418	N.A.	N.A.
Number of Iterations for convergence	3427	4497	24%
Number of cells (model size)	3 597 532	4 861 475	36%
Computational Time	11 426 [s]	15 836 [s]	28%
Water Outlet Temperature (Front Pipe Bundle)	36.62 [°C]	36.36 [°C]	0.26[°C]
Temperature Difference (Front Pipe Water inlet and outlet)	13.38 [°C]	13.64 [°C]	1.9%
Water Outlet Temperature (Back Pipe Bundle)	29.25 [°C]	29.17 [°C]	0.18[°C]
Temperature Difference (Back Pipe Water inlet and outlet)	20.75 [°C]	20.83 [°C]	0.8%

The outlet water temperature for the coupled 1-D/3-D modelling approach shows a 1.9% difference in temperature for the front tube bundle and an 0.8% temperature difference when compared to the full 3-D CFD analysis.

5.2.4 Case 4: Perpendicular flow (x-Axis) 5 Pipe Staggered ACHE configuration

5.2.4.1 Overview

The configuration used in the perpendicular 5 pipe staggered ACHE configuration consists of a double and triple pass bare tube/pipe- network immersed in an air flow domain. For both tube bundles (see **Figure 45**) water enters the respective top pipe element at a temperature of 45 [°C] and pressure of 140 [kPa]. The water entering the front tube bundle makes a triple pass through the air flow field, while the back tube-bundle makes a double pass through the air flow field.

The meshed geometric representation of case 4 is shown in **Figure 45**. The boundary conditions, flow directions and tube layouts are displayed.

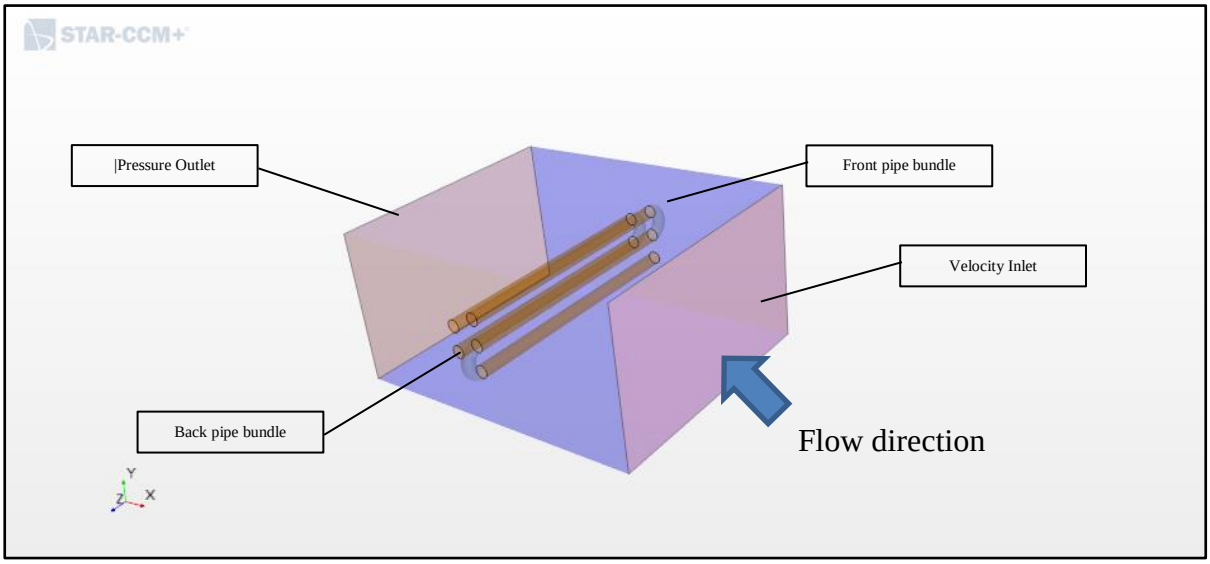

Figure 45: Geometric representation of the Perpendicular flow (x-Axis) 5 Pipe Staggered ACHE configuration

The coupled 1-D/3-D modelling approach associated with the 5-pipe staggered grid is shown in **Figure 46**.

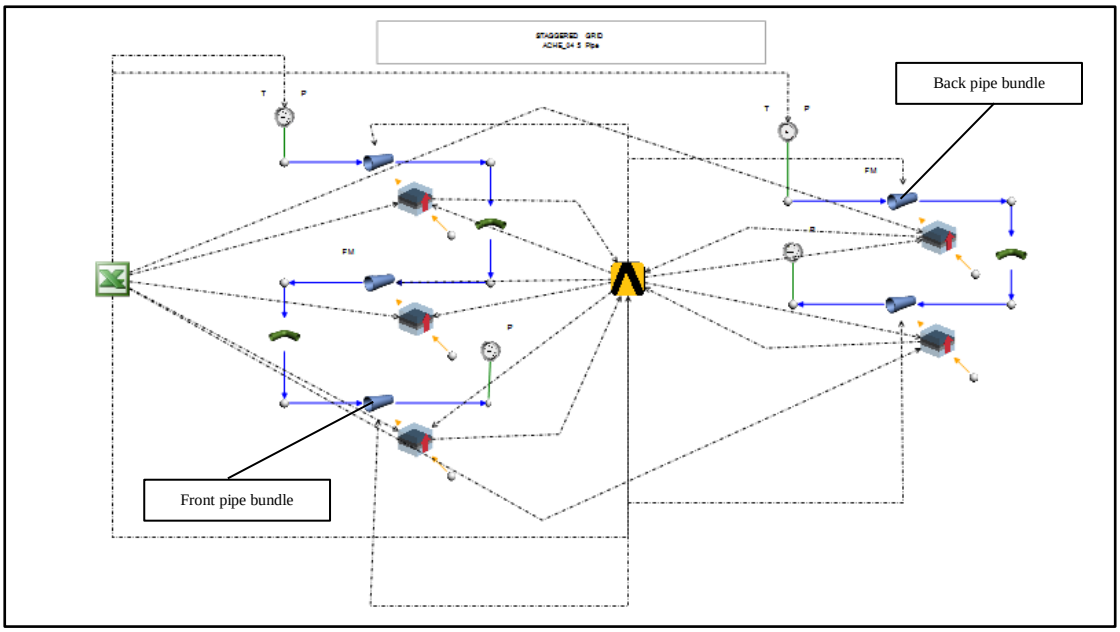

Figure 46: Schematic representation of the integrated Perpendicular flow (x-Axis) 5 Pipe Staggered ACHE configuration

5.2.4.2 Results

Case 4 was simulated using the input specifications as described in the model overview. The meshing and solution strategies explained in section **5.1** as well as the mesh size associated with Case 3C were implemented in Case 4. A results comparison for the coupled 1-D/3-D and full 3D modelling approach is illustrated in **Table 31**.

Table 31: Result Comparison for Perpendicular flow (x-Axis) 6 Pipe ACHE configuration

	Coupled 1-D/3-D	**Full 3D CFD**	**difference in reference to the full 3D CFD model**
Number of Iterations (Global)	968	N.A.	N.A.
Number of Iterations for convergence	980	1652	40%
Number of cells (model size)	2 130 765	2 730 710	26.5 %
Computational Time	4460 [s]	6608 [s]	32 %
Water Outlet Temperature (Front tube Bundle)	43.09[°C]	42.42 [°C]	1.5 %
Water Outlet Temperature (Back tube Bundle)	43.95 [°C]	42.83 [°C]	2.5 %

The outlet water temperature (refer to**Figure 47**) for the coupled 1-D/3-D modelling approach shows a 1.1 % difference in temperature to that of the full 3-D CFD analysis for the front tube bundle and a 2.5% difference in temperature for the back tube-bundle. In addition, the coupled 1-D/3-D modelling technique is less resource intensive as a reduction in solution time of 32% and model size of 26.5% was achieved.

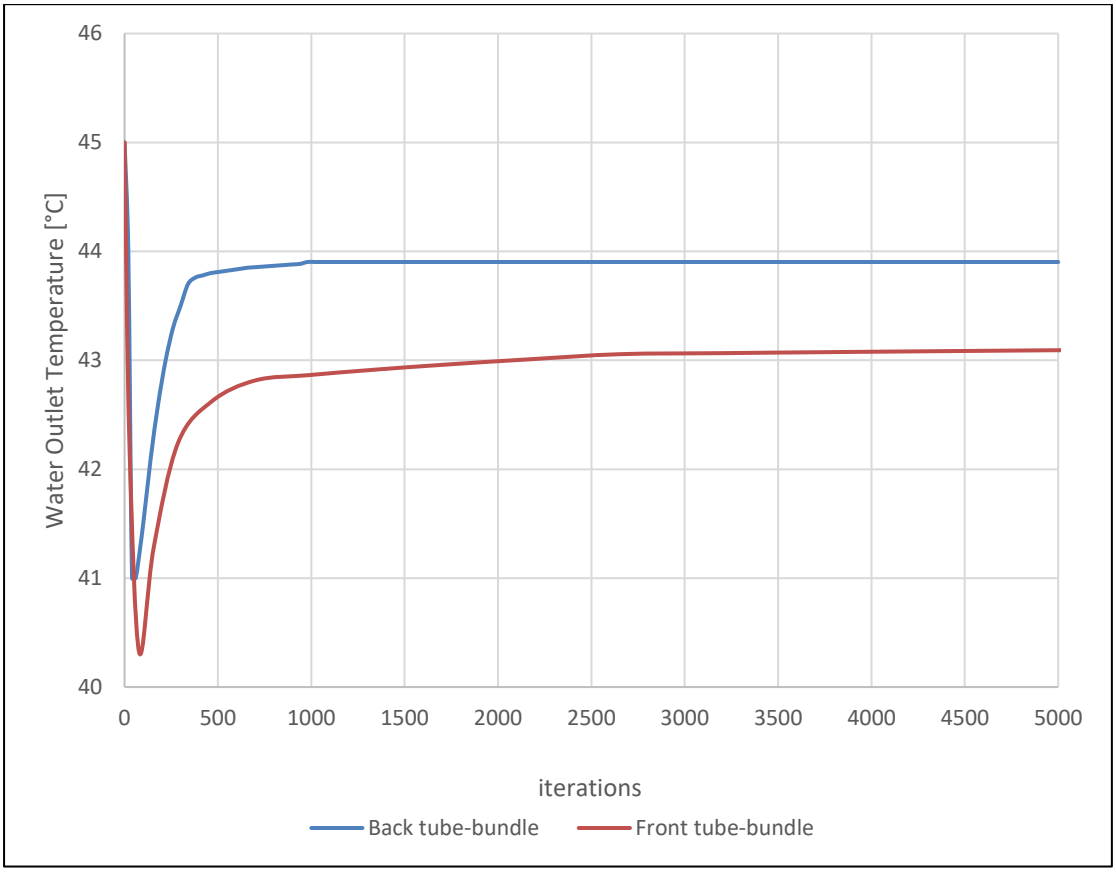

Figure 47: Outlet water Temperature plot for the coupled 1-D/3-D modelling approach (Case 4)

For the full 3D CFD modelling of Case 4, water outlet temperatures of 42.42[°C] and 42.83[°C] were recorded for the front tube bundle and back tube bundle respectively. The water outlet temperatures are shown in **Figure 48**. A Scalar representation of the full 3-D CFD water outlet temperature is depicted in **Figure 49**. The vertical axis denotes the temperature distribution within the pipe bundle and the horizontal axis represents the temperature distribution across the outer air-flow field.

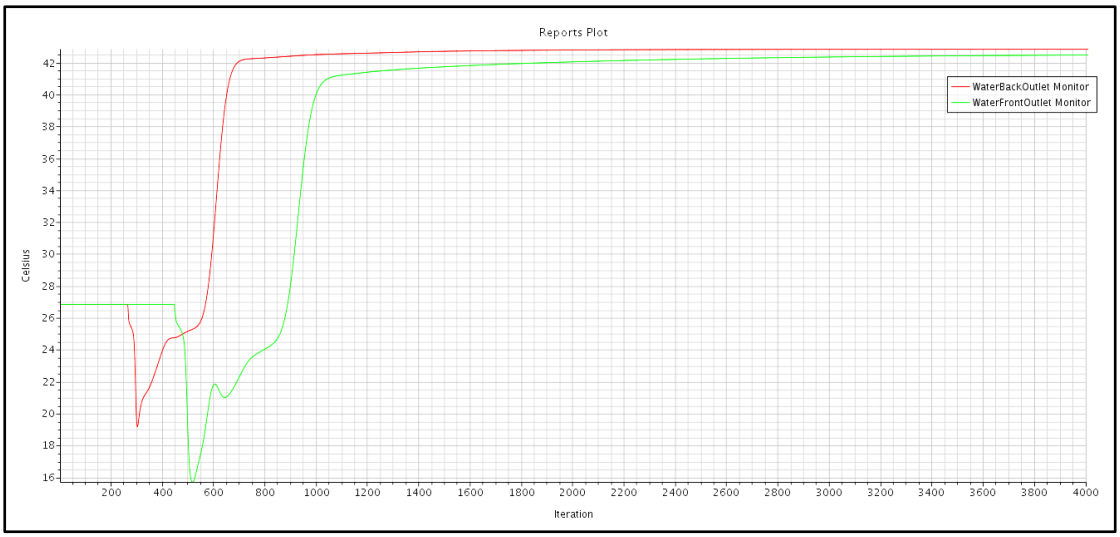

Figure 48: Outlet Water Temperature Monitor Plot for the full 3-D modelling for the Perpendicular flow (x-Axis) 5 Pipe Staggered ACHE configuration

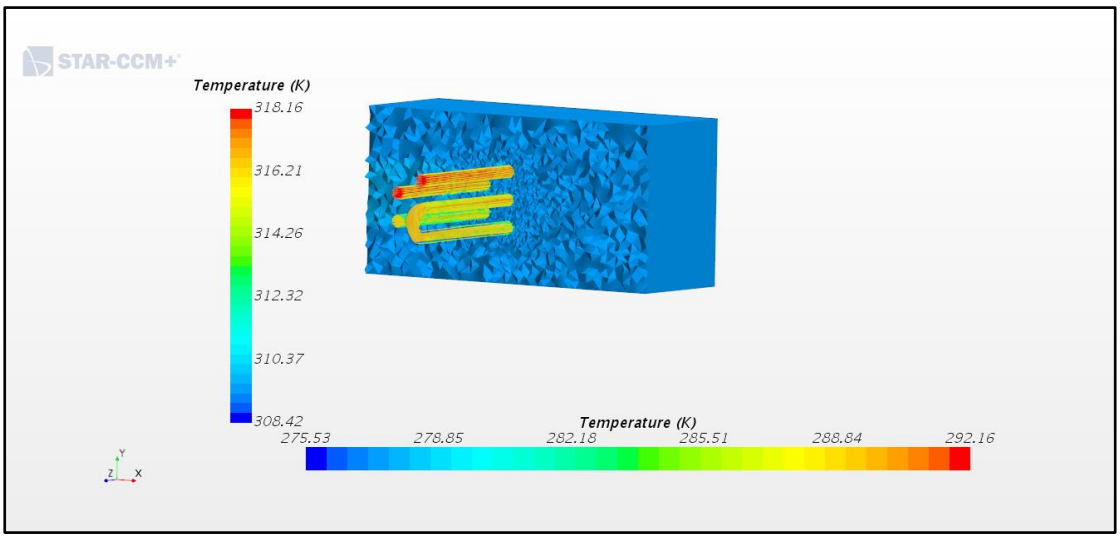

Figure 49: Temperature distribution for the full 3-D modelling for the Perpendicular flow (x-Axis) 6 Pipe ACHE configuration after convergence

Figure 49 shows the internal flow field streamline temperatures. It can be seen that the temperature decreases as more heat is transferred to the surrounding air flow field. This in effect causes the temperature of the air to increase as it passes over the pipe-bundle. The vertical axis denotes the temperature distribution within the pipe bundle and the horizontal axis represents the temperature distribution across the outer air-flow field.

5.3 Summary

The coupled 1-D/3-D modelling technique was applied to four different air-cooled heat exchanger configuration test cases. These test cases were setup to be representative of typical air-cooled heat exchanger tube layout configurations found in industry. The mass flow rates of the water within the tube bundle/s, velocity magnitude of the air moved over the tube bundles as well as the arrangement of these pipes within the airflow field are varied for the test cases.

These couple 1-D/3-D test cases were compared with the relevant verification test cases (full 3-D CFD) having the same input specifications and set up. The comparison of results between the two different solution approaches formed the basis on which the coupled 1-D/3-D modelling approach was evaluated.

Chapter 6: Discussion, Conclusions and Recommendations

Overview

Chapter 6 analyses the results obtained for the different air-cooled heat exchanger configuration test cases and discusses them from a general viewpoint. The results are interpreted and presented in a summarized format. Recommendations stem from the results obtained and are made based on the insights gathered from the literature survey. The research question is answered and recommendations are made for future research.

6.1 The research question revisited

As mentioned in Chapter 1, the objective of this study was to investigate the feasibility of using a coupled 1-D/3-D numerical modelling approach, as an alternative to the more traditional detailed 3-D CFD approach, for the solution of a coupled flow and heat transfer problem. The objective was based on the analysis of different air-cooled heat exchanger configuration test cases and the analysis aims to answer the question*: Can a coupled 1-D/3-D numerical modelling approach aid in reducing model size and computation time for an air-cooled heat exchanger configuration within an acceptable range of accuracy?*

6.2 Discussion of results

For all the air-cooled heat exchanger configuration test cases, the temperature of the water exiting the pipe network(s), the number of iterations, solution time and model size are the main attributes being examined. These results were compared to a verification test case with the same input specifications and setup. A summary of the results is illustrated in **Table 32** below.

Table 32: Summarized result comparison for the different ACHE configuration cases

	Case 1C	**Case 1E**	**Case 1F**	**Case 1G**	**Case 2**
Number of iterations for convergence	30%	27%	25%	24%	27%
Number of cells (Model size)	26%	26%	26%	26%	26%
Computational Time	37%	35%	33%	32%	30%
Water Temperature difference (ΔT)	5%	3%	2%	2%	2%

(Table 32: continued)

	Case 3C	**Case 3D**	**Case 3E**	**Case 4**
Number of iterations for convergence	32%	24%	24%	40%
Number of cells (Model size)	36%	36%	36%	27%
Computational Time	25%	29%	28	32%
Water Temperature difference (ΔT) for Front Pipe bundle	6%	14%	2%	4%
Water Temperature difference (ΔT) for Back Pipe bundle	11%	6%	1%	1%

From the results of the ACHE configuration test cases, an average reduction in model size of around 30% and approximately 30% in computational time is achieved when applying the coupled 1-D/3-D modelling technique. In the results considered for the ACHE configurations the percentage difference between the temperatures of the coupled 1-D/3-D models and that of the equivalent full 3-D CFD models did not exceed a difference larger than 14 %.

6.3 Conclusion

Full 3-D CFD analysis of an ACHE configuration can be very resource intensive (time and computational). The use of experimental setups may prove difficult, expensive and time consuming in many ACHE configurations.

By using the coupled 1-D/3-D modelling approach implemented in this study, many of the above-mentioned problems can be overcome. This is achieved by reducing the computational time required to numerically model an ACHE configuration when compared to a full 3-D CFD model within an acceptable range of accuracy. Therefore, a coupled 1-D/3-D model can be set up to determine whether an experimental setup would be required for a specific design/configuration. The results may also show important areas of interest when an experimental setup is approved. The coupled 1-D/3-D model allows the user the freedom to manipulate environmental conditions that may be difficult to control when performing experimental measurements.

Even though 1-D analysis is an efficient approach to simulate flow and heat transfer in ducts, it has limited applications in complex geometries. When the flow is not constrained to a primary direction, as in the case of complex geometries, a 3-D CFD analysis is the method of choice to obtain realistic performance predictions. The coupled 1-D/3-D modelling approach provides the best of both worlds by producing accurate results within a relatively short amount of time.

The coupled 1-D/3-D numerical modelling approach aided in reducing model size and computation time for all the air-cooled heat exchanger configurations, and still provided results with an acceptable accuracy.

6.4 Recommendations

Due to the complexity of this study the air-cooled heat exchanger configurations were simplified to a large extent. This leaves room for improvement through expansion of the following modelling parameters:

- The next step would be to expand the model by considering a two-pass configuration with more pipes in parallel and header boxes, where air is flowing vertically through the system.
- Bends can be modelled not to be adiabatic.
- Fins can be included in the study as this form a critical part of the air side area.
- The effect of the properties of the tube side fluid (liquid) on the performance of the model can be studied.

- In this study the air was assumed to be incompressible. This constraint should be relaxed and the air should be taken as compressible.

Coupled 1-D/3-D modelling is worth developing for more industrial applications.

Bibliography

Amercool, 2003. *Basics of Air Cooled Heat Exchnagers,* Tulsa, Oklahoma: Amercool Manfacturing Inc..

Ansys, I., 2010. *Fluent User manual,* s.l.: Ansys.

Calgavin, 2017. *Calgavin Heat Exchangers.* [Online] Available at: https://www.calgavin.com/heat-exchanger-problems/7304/heat-exchanger-problems-part-3 [Accessed 16 November 2017].

CD-adapco, 2015. *Star-CCM+ User guide,* Melville NY: CD-adapco.

De Henau, V. & Ahmed, I., 2005. Heat exchanger analysis combing 1-D and 3-D flow modelling. *Proceedings of the ASME Heat Transfer Division--2005; presented at 2005 ASME International Mechanical Engneering Congress and Exposition,* pp. 79-85.

Envenio,2017.E*nvenio.*[Online] Available at: ε turbulence model

Flownex SE, 2016. *Flownex Simulation Environment Theory Manual,* s.l.: M-Tech Industrial (Pty) Ltd.

Flownex Simulation Software, 2015. *Flownex Library Manual,* s.l.: M-Tech Industrial (Pty) Ltd..

Galindo, J., Tiseira, A., Fajardo, P. & Navarro, R., 2011. Coupling methodology of 1D finite difference and 3D finite volume CFD. *Mathematical and Computer Modelling,* Issue 54, pp. 1738-1746.

GEA Rainey Corporation, 2007. *P.C. Mckenzie Company.* [Online] Available at: http://www.mckenziecorp.com/naturalgas.htm[Accessed 04 April 2015].

Guyer, E. C. & Bartz, J. A., 1991. Dry cooling moves into the main stream. *Power Engineering,* pp. 29-32.

Heaslip, B., 2008. *Heat Exchangers,* s.l.: Queens University.

Hu, H., 2014. Cross scale simulation on transport phenomena of direct air-cooling systems of power regenerating units based on reduced order modeling. *International Journal of Heat and Mass Transfer,* pp. 156-164.

Incropera, F.P., Dewitt, D.P., Bergman, T.L. & Lavine, A.S. 2013. Principles of heat and mass transfer. 7th ed. Hoboken, NJ: Wiley.

Kröger, D. G., 1998. *Air-cooled heat exchangers and cooling towers: Thermal-flow performance evaluation and design.* University of Stellenbosch: South Africa.

Kruger, J.-H. & Du Toit, C., 2006. *Integrated systems CFD analysis applied to Boiler simulation,* Potchefstroom: School of Mechanical Engineering.

Masjuki, H. H., 2011. Integration of 1D and 3D simulation of engine cooling system. *International Symposium on Distributed Computing and Applications to Business, Engineering and Science,* pp. 46-50.

Mentor Graphics, C. M., 2012. *Mentor Graphics Corporation.*. [Online] Available at: www.mentor.com/mechanical [Accessed 2017].

Meyer, C. J., 2005. Numerical investigation of the effect of inflow distortions on forced draft aircooled. *Applied Thermal Engineering,* Volume 25, pp. 1634-1649.

MIT, 2018. *Massachusetts Institute of Technology.* [Online] Available at: http://web.mit.edu/16.unified/www/FALL/thermodynamics/notes/node116.html

Park, I., Lee, J., Yoon, H. & Jeong, J., 2013. An implicit code coupling of 1-D system code and 3-D in-house CFD code. *Annals of Nuclear Energy,* Issue 59, pp. 80-91.

Rohsenow, W. M., 1973. *Handbook of Heat Tranfer.* New York: McGraw-Hill Book Co..

Rousseau, P., 2014. *Thermal-Fluid Systems Modelling II,* Potchefstroom: s.n.

Summers, C., 2011. *Thermopedia/Air cooled Heat Exchangers.* [Online] Available at: www.thermopedia.com [Accessed March 2018].

TUBETECH, n.d. *Tubetech Air cooled heat exchanger.* [Online] Available at: www.tubetech.de/site_en/expert_aircooledhea_en.html [Accessed 20 May 2018].

Tubular Exchanger Manufactures Association, I., 2007. *Tema.* [Online] Available at: www.tema.org [Accessed April 2018].

Versteeg, H. & Malalasekera, W., 2007. *An introduction to computational fluid dynamics: The finite volume method.* 2nd ed. s.l.:Pearson Education Limited.

Wang, H., Wang, S., Wang, X. & Li, E., 2015. Numerical modeling of heat transfer through casting–mould with 3D/1D. *International Journal of Heat and Mass Transfer,* Issue 81, pp. 81-89.

Wang, Q., Zhang, D. & Zeng, M., 2008. CFD simulation on a thermal power plant with air-cooled heat exchanger system in north China. *Engineering Computations: International Journal for Computer-Aided Engineering and Software,* 25(4), pp. 342-365.

Appendix A: Flow Field Development for Case 1

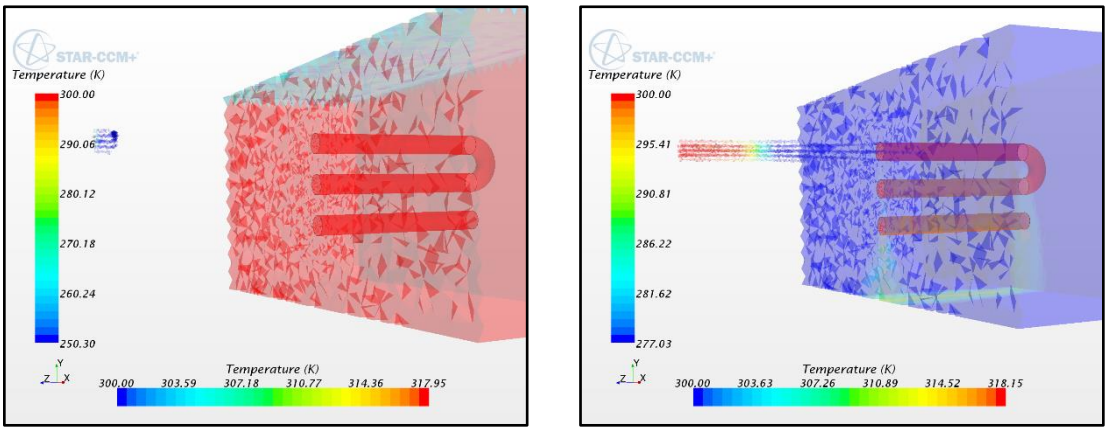

Figure 50: Temperature distribution of an ACHE configuration at iteration 0001 (left) and 0100 (right)

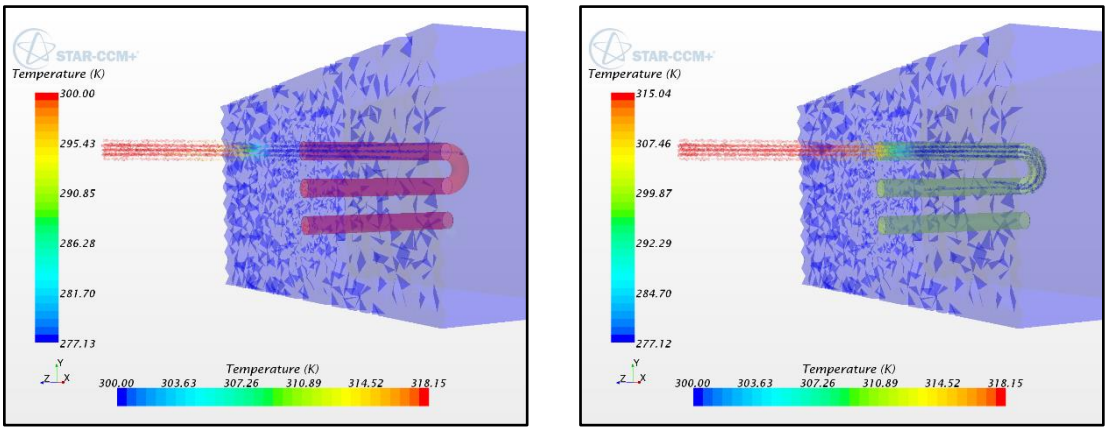

Figure 51: Temperature distribution of an ACHE configuration at iteration 0200 (left) and 0300 (right)

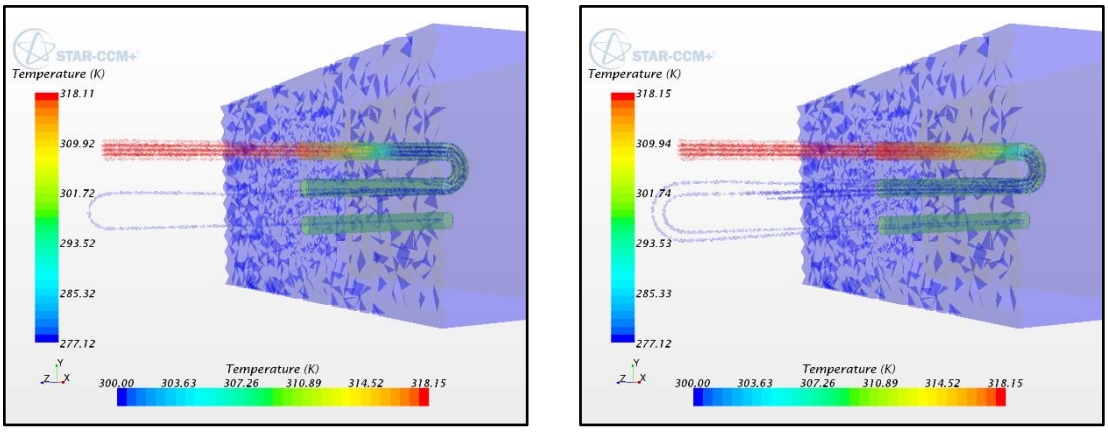

Figure 52:Temperature distribution of an ACHE configuration at iteration 0400 (left) and 0500 (right)

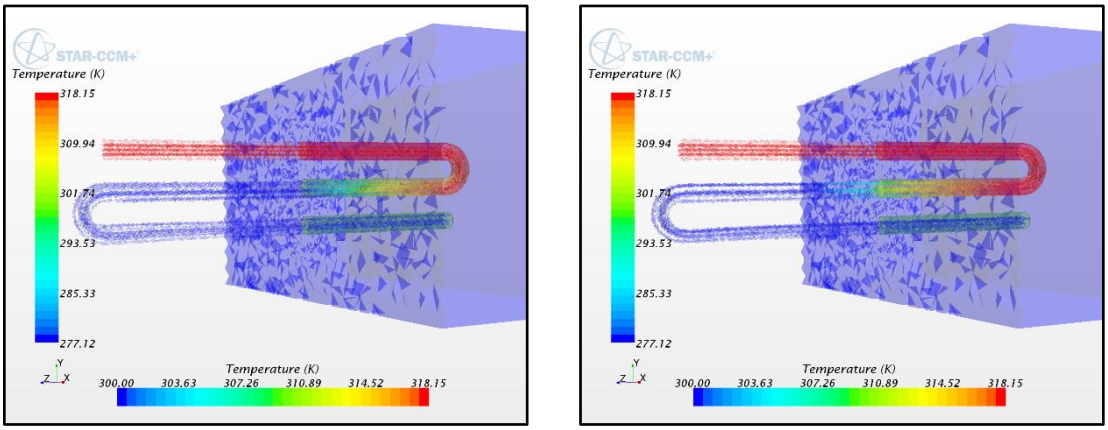

Figure 53: Temperature distribution of an ACHE configuration at iteration 0800 (left) and 0900 (right)

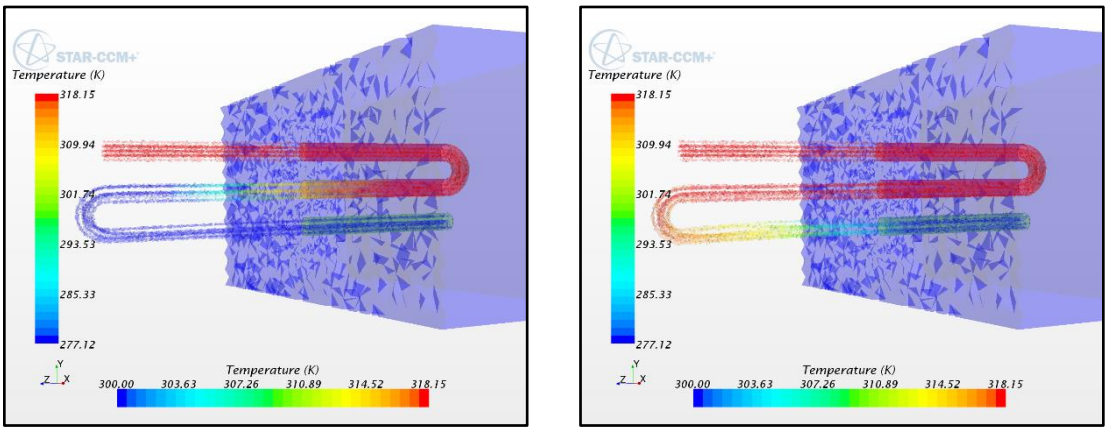

Figure 54: Temperature distribution of an ACHE configuration at iteration 1000 (left) and 1500 (right)

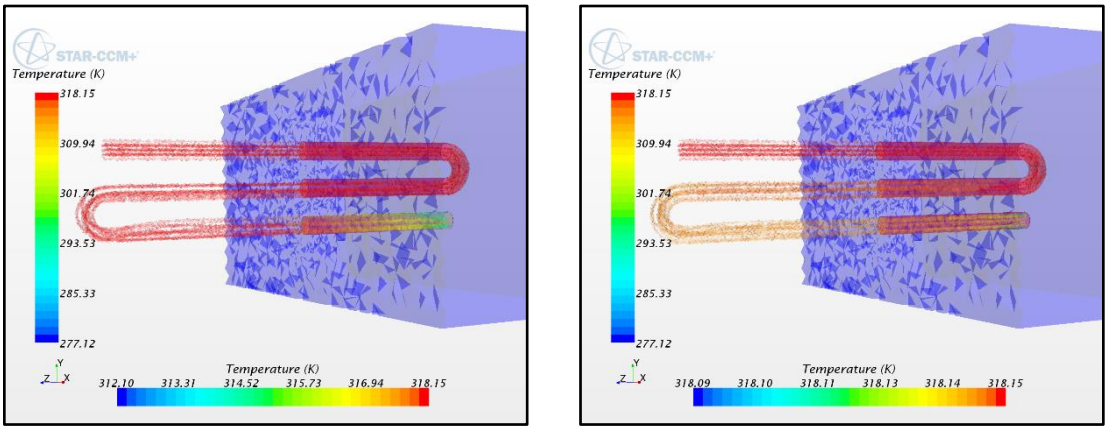

Figure 55: Temperature distribution of an ACHE configuration at iteration 2000 (left) and 2500 (right)

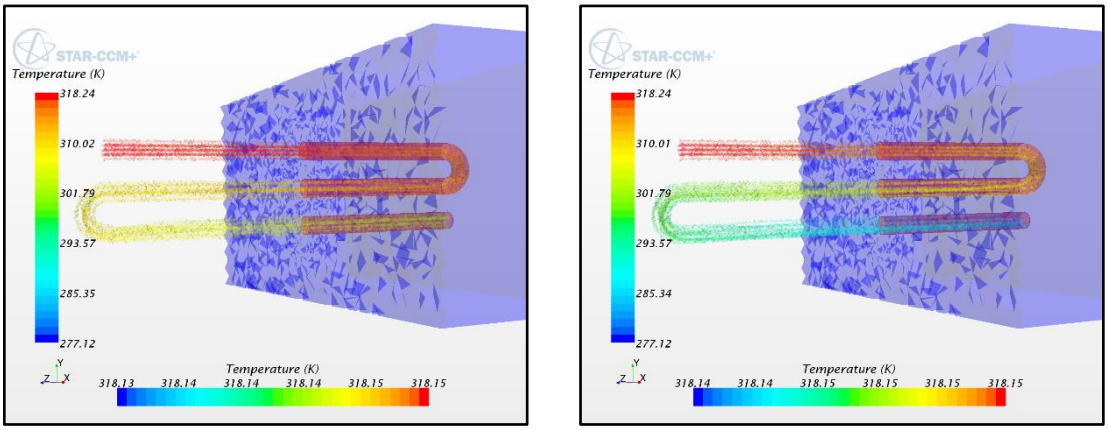

Figure 56: Temperature distribution of an ACHE configuration at iteration 3000 (left) and 3500 (right)

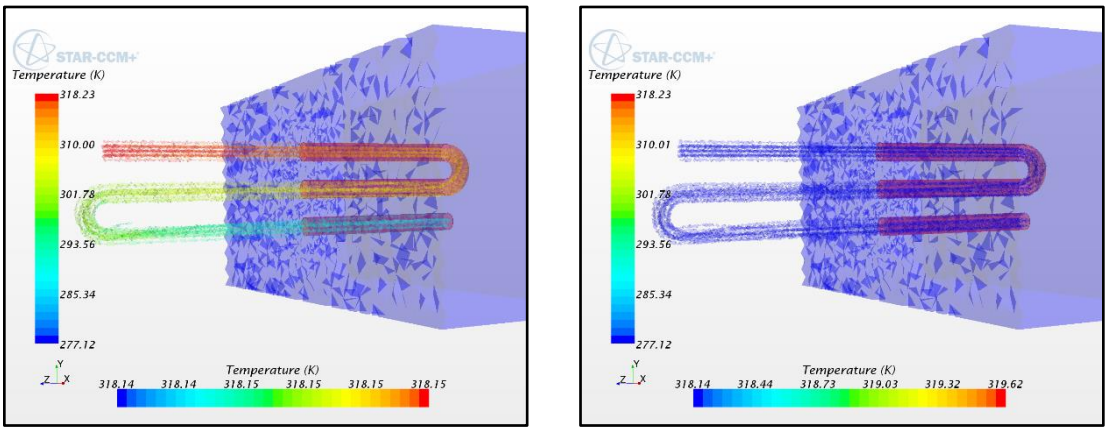

Figure 57: Temperature distribution of an ACHE configuration at iteration 3900 (left) and 4000 (right)

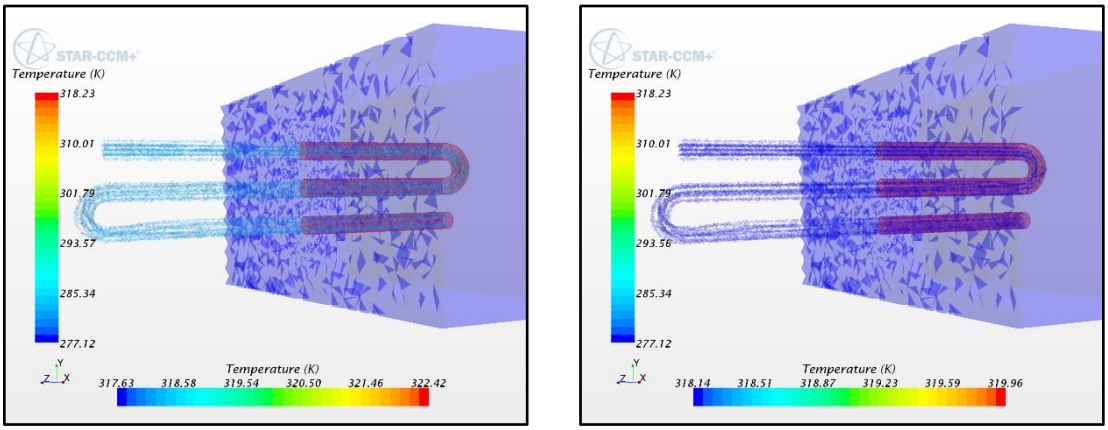

Figure 58: Temperature distribution of an ACHE configuration at iteration 4100 (left) and 4500 (right)

Appendix B: Sample Journal File

Sample Journal file created, for information transfer between Flownex and Fluent:

```
/file/read-case-data "H:\Co-Simulations\ACHE-02\ACHE-02(Y-Axis).cas"
(cx-gui-do cx-activate-item "NavigationPane*Frame1*PushButton9(Boundary
Conditions)")
(cx-gui-do cx-set-list-selections "Boundary
Conditions*Frame1*Table1*Frame1*List1(Zone)" '( 3))
(cx-gui-do cx-activate-item "Boundary
Conditions*Frame1*Table1*Frame1*List1(Zone)")
(cx-gui-do cx-activate-item "Boundary
Conditions*Frame1*Table1*Frame2*Table2*Frame4*Table4*ButtonBox1*PushButt
on1(Edit)")
(cx-gui-do cx-set-real-entry-list "Temperature-inlet-6-
1*Frame4*Frame1(Momentum)*Frame1*Table1*Frame6*Table6*RealEntry2(Total
Temperature)" '( 12345))
(cx-gui-do cx-set-real-entry-list " Temperature e-inlet-6-
1*Frame4*Frame3(Thermal)*Frame1*Table1*Frame1*Table1*RealEntry2(Total
Temperature)" '( 298.15))
(cx-gui-do cx-activate-item " Temperature -inlet-6-
1*PanelButtons*PushButton1(OK)")
(cx-gui-do cx-activate-item "NavigationPane*Frame1*PushButton9(Boundary
Conditions)")
(cx-gui-do cx-set-list-selections "Boundary
Conditions*Frame1*Table1*Frame1*List1(Zone)" '( 1))
(cx-gui-do cx-activate-item "Boundary
Conditions*Frame1*Table1*Frame1*List1(Zone)")
(cx-gui-do cx-activate-item "Boundary
Conditions*Frame1*Table1*Frame2*Table2*Frame4*Table4*ButtonBox1*PushButt
on1(Edit)")
(cx-gui-do cx-set-real-entry-list "pressure-outlet-8-
1*Frame4*Frame1(Momentum)*Frame1*Table1*Frame4*Table4*RealEntry2(Gauge
Pressure)" '( 1590.1))
(cx-gui-do cx-set-real-entry-list "pressure-outlet-8-
1*Frame4*Frame3(Thermal)*Frame1*Table1*Frame1*Table1*RealEntry2(Backflow
Total Temperature)" '( 298.15))
(cx-gui-do cx-activate-item "pressure-outlet-8-1*PanelButtons*PushButton1(OK)")
(cx-gui-do cx-activate-item "MenuBar*WriteSubMenu*Stop Journal")
(cx-gui-do cx-activate-item "NavigationPane*Frame1*PushButton17(Solution
Initialization)")
(cx-gui-do cx-activate-item "Solution
Initialization*Frame1*Table1*ButtonBox8*PushButton1(Initialize)")
(cx-gui-do cx-activate-item "NavigationPane*Frame1*PushButton19(Run
Calculation)")
(cx-gui-do cx-set-integer-entry "Run
Calculation*Frame1*Table1*IntegerEntry9(Number of Iterations)" 40)
```

```
(cx-gui-do cx-activate-item "Run
Calculation*Frame1*Table1*IntegerEntry9(Number of Iterations)")
(cx-gui-do cx-activate-item "NavigationPane*Frame1*PushButton16(Monitors)")
(cx-gui-do cx-set-list-selections "Monitors*Frame1*Table1*Frame3*List3(Surface
Monitors)" '( 0))
(cx-gui-do cx-activate-item "Monitors*Frame1*Table1*Frame3*List3(Surface
Monitors)")
(cx-gui-do cx-activate-item
"Monitors*Frame1*Table1*Frame4*Table4*PushButton3(Delete)")
(cx-gui-do cx-activate-item "NavigationPane*Frame1*PushButton19(Run
Calculation)")
(cx-gui-do cx-activate-item "Run
Calculation*Frame1*Table1*PushButton21(Calculate)")
(cx-gui-do cx-activate-item "Information*OK")
(cx-gui-do cx-activate-item "NavigationPane*Frame1*PushButton23(Reports)")
(cx-gui-do cx-set-list-selections "Reports*Frame1*Table1*Frame1*List1(Reports)" '(
3))
(cx-gui-do cx-activate-item "Reports*Frame1*Table1*Frame1*List1(Reports)")
(cx-gui-do cx-activate-item
"Reports*Frame1*Table1*Frame2*Table2*PushButton1(Set Up)")
(cx-gui-do cx-set-list-selections "Surface Integrals*Frame1*DropDownList1(Report
Type)" '( 7))
(cx-gui-do cx-activate-item "Surface Integrals*Frame1*DropDownList1(Report
Type)")
(cx-gui-do cx-set-list-selections "Surface Integrals*Frame3*List3(Surfaces)" '( 9))
(cx-gui-do cx-activate-item "Surface Integrals*Frame3*List3(Surfaces)")
(cx-gui-do cx-activate-item "Surface Integrals*PanelButtons*PushButton1(Write)")
(cx-gui-do cx-set-text-entry "Select File*Text" "FluentTemperature2.txt")
(cx-gui-do cx-activate-item "Select File*OK")
(cx-gui-do cx-activate-item "Question*Cancel")
(cx-gui-do cx-activate-item "Question*OK")
(cx-gui-do cx-set-list-selections "Surface Integrals*Frame1*DropDownList1(Report
Type)" '( 8))
(cx-gui-do cx-activate-item "Surface Integrals*Frame1*DropDownList1(Report
Type)")
(cx-gui-do cx-set-list-selections "Surface Integrals*Frame3*List3(Surfaces)" '())
(cx-gui-do cx-activate-item "Surface Integrals*Frame3*List3(Surfaces)")
(cx-gui-do cx-set-list-selections "Surface Integrals*Frame3*List3(Surfaces)" '( 9))
(cx-gui-do cx-activate-item "Surface Integrals*Frame3*List3(Surfaces)")
(cx-gui-do cx-set-list-selections "Surface
Integrals*Frame2*Table2*DropDownList1(Field Variable)" '( 1))
(cx-gui-do cx-activate-item "Surface
Integrals*Frame2*Table2*DropDownList1(Field Variable)")
(cx-gui-do cx-set-list-selections "Surface Integrals*Frame2*Table2*DropDownList2"
'( 4))
(cx-gui-do cx-activate-item "Surface Integrals*Frame2*Table2*DropDownList2")
(cx-gui-do cx-activate-item "Surface Integrals*PanelButtons*PushButton1(Write)")
(cx-gui-do cx-set-text-entry "Select File*Text" "FluentHeatFlux2.txt")
(cx-gui-do cx-activate-item "Select File*OK")
(cx-gui-do cx-activate-item "Question*Cancel")
```

```
(cx-gui-do cx-activate-item "Question*OK")
(cx-gui-do cx-set-list-selections "Surface
Integrals*Frame2*Table2*DropDownList1(Field Variable)" '( 4))
(cx-gui-do cx-activate-item "Surface
Integrals*Frame2*Table2*DropDownList1(Field Variable)")
(cx-gui-do cx-set-list-selections "Surface Integrals*Frame2*Table2*DropDownList2"
'( 1))
(cx-gui-do cx-activate-item "Surface Integrals*Frame2*Table2*DropDownList2")
(cx-gui-do cx-set-list-selections "Surface Integrals*Frame3*List3(Surfaces)" '())
(cx-gui-do cx-activate-item "Surface Integrals*Frame3*List3(Surfaces)")
(cx-gui-do cx-set-list-selections "Surface Integrals*Frame3*List3(Surfaces)" '( 9))
(cx-gui-do cx-activate-item "Surface Integrals*Frame3*List3(Surfaces)")
(cx-gui-do cx-activate-item "Surface Integrals*PanelButtons*PushButton1(Write)")
(cx-gui-do cx-set-text-entry "Select File*Text" "FluentTemperature2.txt")
(cx-gui-do cx-set-text-entry "Select File*Text" "FluentTemperature2.txt")
(cx-gui-do cx-activate-item "Select File*OK")
(cx-gui-do cx-activate-item "Question*Cancel")
(cx-gui-do cx-activate-item "Question*OK")
(cx-gui-do cx-activate-item "Surface Integrals*PanelButtons*PushButton2(Cancel)")
(cx-gui-do cx-activate-item "NavigationPane*Frame1*PushButton23(Reports)")
(cx-gui-do cx-set-list-selections "Reports*Frame1*Table1*Frame1*List1(Reports)" '(
3))
(cx-gui-do cx-activate-item "Reports*Frame1*Table1*Frame1*List1(Reports)")
(cx-gui-do cx-activate-item
"Reports*Frame1*Table1*Frame2*Table2*PushButton1(Set Up)")
(cx-gui-do cx-set-list-selections "Surface Integrals*Frame1*DropDownList1(Report
Type)" '( 7))
(cx-gui-do cx-activate-item "Surface Integrals*Frame1*DropDownList1(Report
Type)")
(cx-gui-do cx-activate-item "Surface Integrals*Frame3*List3(Surfaces)")
(cx-gui-do cx-set-list-selections "Surface Integrals*Frame3*List3(Surfaces)" '( 13))
(cx-gui-do cx-activate-item "Surface Integrals*Frame3*List3(Surfaces)")
(cx-gui-do cx-activate-item "Surface Integrals*PanelButtons*PushButton1(Write)")
(cx-gui-do cx-set-text-entry "Select File*Text" "FluentTemperature1.txt")
(cx-gui-do cx-activate-item "Select File*OK")
(cx-gui-do cx-activate-item "Question*Cancel")
(cx-gui-do cx-activate-item "Question*OK")
(cx-gui-do cx-set-list-selections "Surface Integrals*Frame1*DropDownList1(Report
Type)" '( 8))
(cx-gui-do cx-activate-item "Surface Integrals*Frame1*DropDownList1(Report
Type)")
(cx-gui-do cx-set-list-selections "Surface Integrals*Frame3*List3(Surfaces)" '())
(cx-gui-do cx-activate-item "Surface Integrals*Frame3*List3(Surfaces)")
(cx-gui-do cx-set-list-selections "Surface Integrals*Frame3*List3(Surfaces)" '( 13))
(cx-gui-do cx-activate-item "Surface Integrals*Frame3*List3(Surfaces)")
(cx-gui-do cx-set-list-selections "Surface
Integrals*Frame2*Table2*DropDownList1(Field Variable)" '( 1))
(cx-gui-do cx-activate-item "Surface
Integrals*Frame2*Table2*DropDownList1(Field Variable)")
```

```
(cx-gui-do cx-set-list-selections "Surface Integrals*Frame2*Table2*DropDownList2"
'( 4))
(cx-gui-do cx-activate-item "Surface Integrals*Frame2*Table2*DropDownList2")
(cx-gui-do cx-activate-item "Surface Integrals*PanelButtons*PushButton1(Write)")
(cx-gui-do cx-set-text-entry "Select File*Text" "FluentHeatFlux1.txt")
(cx-gui-do cx-activate-item "Select File*OK")
(cx-gui-do cx-activate-item "Question*Cancel")
(cx-gui-do cx-activate-item "Question*OK")
exit
ok
```

Sample Journal Output file created by Flownex, for information transfer between Flownex and Fluent:

"Total Temperature"

Total Temperature	(K)
Temperature Front PipeTOP	300
Temperature Front PipeMID	300
Temperature Front PipeBOT	300
Temperature Back PipeTOP	300
Temperature Back PipeMID	300
Temperature Back PipeBOT	300